ADDIS ABABA UNIVERSITY

ADDIS ABABA INSTITUTE OF TECHNOLOGY

SCHOOL OF CIVIL AND ENVIRONMENTAL ENGINEERING

GEODESY AND GEOMATICS PROGRAM

Accuracy assessment and bias correction for open sources Digital elevation model (DEM): a case study in and around Diredawa city, Ethiopia

A SUBMITTED TO THE SCHOOL OF CIVIL AND ENVIRONMENTAL ENGINEERING IN PARTIAL FULFILLMENT OF THE REQUIREMENT FOR THE DEGREES OF THE MASTERS IN GEODESY AND GEOMATICS PROGRAM

By:

Mesfin Delelegn

ID: GSR/1345/12

Advisor: Dr. Tulu Besha

February, 2022

Approval sheet

Accuracy assessment and bias correction for open sources Digital elevation model (DEM): a case study in and around Diredawa city, Ethiopia

By:
Mesfin Delelegn Dea
ID: GSR/1345/12
Email: delelegnmesfin@gmail.com

Approved by Board of examiners

Dr. Tulu Besha Bedada	_____	_____
Advisor	Signature	Date
Dr. Andenet Ashagrie	_____	_____
Internal Examiner	Signature	Date
Dr. K. V. Suryabhagavan	_____	_____
External Examiner	Signature	Date
Dr. Ing. Mebruk Mohammed	_____	_____
Chairperson	Signature	Date

Declaration

I certify that this thesis work entitled, "**Accuracy assessment and bias correction for open sources Digital elevation model (DEM): a case study in and around Diredawa city**" under the supervision of **Dr. Tulu Besha** is my work. It has not been submitted previously in any person and all sources of material used for the thesis have been appropriately acknowledged.

Mesfin Delelegn _____ _____

Name of the Candidate Signature Date

As Master research advisor, I hereby certify that I have read and evaluated this MSc thesis prepared under my guidance

Dr. Tulu Besha Bedada _____ _____

Advisor Signature Date

Acknowledgments

First of all, thanks to compassionate and merciful God, his aid gave me the power to complete this study. Next, I would like to thank my Advisor **Dr. Tulu Besha Bedada** for his advice to accomplish this study. I would like to express my gratitude to **Dr. Andenet Ashagrie** for his inspiring guidance, support, kind attitude and co-operation thought my study. His guidance greatly encourages me in my study. I am grateful to Abdi Ibrahim, Landholding registration and Information Agency director at Dire Dawa Land Administration and management bureau. His support and permission are greatly appreciated during data collection. I thank also my colleagues, Ethiopia Geospatial information Agency (EGIA), and Dire Dawa University for their cooperation and other kinds of help during data collection.

Finally, my parents and friends are thanks for your encouragement and support.

Accuracy assessment and bias correction for open sources Digital elevation model (DEM): a case study in and around Diredawa city, Ethiopia

Name: Mesfin Delelegn Dea, MSc Thesis
Addis Ababa University, February 2022

Abstract

Digital elevation model (DEM) is a digital and mathematical representation of the real-world topographic surface by using elevation data. The global open-access DEM data contain errors and are not suitable for engineering and other high accuracy requiring applications. The main aims of this study are vertical accuracy assessment and bias correction for open-source global DEM data. Conventional global DEM data; SRTM DEM 1-arc second and ASTER-GDEM 1-arc second, and new global DEM data ALOS-PALSAR both 12.5 m and 30 m spatial resolution DEM data were applied for this study. Ground control point GCP, RTK-GPS data, and photogrammetric DEM reference data were used to evaluate the accuracy of the selected open-source global DEM data. Accuracy assessment was applied in different approaches, one is a point-based approach using statistical measurement. The computed Root mean square (RMSE) for SRTM is 3.68 m, 4.24m, and 3.41m in GCP, RTK-GPS, and Photogrammetric DEM reference data, for ASTER-GDEM the RMSE value is 8.87 m, 7.08 m, and 7.05 m, for ALOS-PALSAR12.5 m it is 4.58 m, 4.46 m and 4.58 m and for ALOS- PALSAR30 m the value is 5.79 m, 5.10 m and 5.34 m, respectively. The accuracy of SRTM showed better in three reference data and ALOS-PALSAR12.5 m is followed the SRTM in the accuracy. Whereas the accuracy of ASTER-GDEM showed less accuracy among the selected global DEM data. The second approach is based on land use land cover data using RTK-GPS reference data; bare land, road line, drainage pattern, rock area, and tree areas point data are collected using TRIMBLE R8 GNSS/R6/5800 instrument, the accuracy of rock area showed less accuracy in all DEM data except SRTM DEM and the accuracy of the bare land area showed better in all DEM averagely. And the third approach of vertical accuracy assessment is terrain classification; the terrain of this study area is segmented into three classes (flat area, moderate slope, and steep slope), the accuracy of the flat area showed high and the accuracy of the steep slope is less for all DEM data. Finally, bias correction was applied using linear transformation parameters to reduce the residual of the global DEM data, the accuracy of ASTER-GDEM was improved by 22.9 % after the bias correction, while the accuracy of SRTM is improved by 6.7 % and the accuracy of PALSAR12.5m and PALSAR30 m was improved by 5.1 % and 2.2 % after the bias correction.

Keywords: Digital Elevation Model, Linear transformation, Reference Data, Vertical accuracy

List of Abbreviations

ALOS Advanced Land Observing Satellite

ASF Alaska satellite Facility

ASPRS American Society for Photogrammetry and Remote Sensing

ASTER-GDEM Advanced Spaceborne Thermal Emission and Reflection Radiometer Global Digital Elevation Model

DEM Digital elevation model

DGPS Differential Global Positioning System

DSM Digital Surface Model

DTM Digital Terrain Model

EDM Electronic distance measurement

EGIA Ethiopia Geospatial Information Agency

EGM Earth Gravity Model

GCP Ground control point

GDEM Global Digital Elevation Model

GDOP Geometric dilution of precision

GeoTIFF Geo-referenced Tagged Image File Format

GIS- Geographic Information System

GNSS Global Navigation Satellite Systems

GPS Global Positioning System

IMU Inertial Measuring Units

InSAR Interferometry Synthetic Aperture Radar

ISPRS International Society for Photogrammetry and Remote Sensing

JAXA	Japan Aerospace Exploration Agency
KMZ	Keyhole Markup Language
LE	Linear Error
LiDAR	Light Detection and Ranging
ME	Mean error
METI	Ministry of economy, trade, and industry of Japan
MSL	Mean Sea Level
NASA	National Aeronautics and Space Administration
NED	National Elevation dataset
NDEP	National Digital Elevation Program
NGA	National Geospatial-Intelligence Agency
NMAS	National Map Accuracy Standard
OTF	On-the-fly
PALSAR	Phased Array type L-band Synthetic Aperture Radar
PDL	Positioning Data Link
PDOP	Precision dilution of position
PPS	Precise positioning service
QGIS	Quantum GIS
RADAR	Radio Detection and Ranging
RMSE	Root Mean square error
RS	Remote sensing
RTC	Radiometric Terrain Correction

RTK	Real Time Kinematic
SAR	Synthetic Aperture Radar
SPS	Standard positioning Service
SRTM	Shuttle Radar Topographic Mission
TIFF	Tagged Image File Format
TIN	Triangulated Irregular Networks
UAV	Unmanned Aerial Vehicle
UHF	Ultra High Frequency
USGS	United States Geological Survey
WGS84	World Geodetic system 84

Table of Contents

Declaration II
Acknowledgments III
Abstract IV
List of Abbreviations V
List of Figures XI
List of Tables XIII
Chapter One 1
1. Introduction 1
1.1 Background 1
1.2 Statement of the problem 3
1.3 Objective of the study 4
1.3.1 Main objective 4
1.3.2 Specific objective 4
1.4 Research questions 5
1.5 Scope of the study 5
1.6 Significance of the study 5
1.7 Organization of the thesis 5
Chapter Two 6
2. Literature Review 6
2.1 Introduction 6
2.2 Digital elevation data 6
2.2.1 Ground survey techniques 6
2.2.2 Existing topographic map 7
2.2.3 Remote sensing data 7
2.3 Global Digital elevation model (DEM) data 9
2.4 Vertical and horizontal datum 10
2.4.1 Types of vertical height 12
2.5 Global positioning system (GPS) 13
2.6 Accuracy Assessment 17
2.6.1 Sample size for accuracy assessment 19
2.6.2 Terrain classification for Accuracy Assessment 19
2.6.3 Mathematical Models for accuracy assessment 19

2.6.4 Functional quality for accuracy assessment 19
2.7 Bias correction 20
2.8 Accuracy standards 21
Chapter Three 24
3. Materials and Methods 24
3.1 Study area 24
3.2 Used software's and Instruments 25
3.3 Data source and its description 25
3.3.1 Global DEM data 25
3.3.2 Reference data 27
3.4 Data Processing, methods, and Analysis 29
3.4.1 Transforming different horizontal datum to the same datum 29
3.4.2 Extracting point elevation data from DEM data 29
3.4.3 Transforming different vertical datum to the same datum 29
3.4.4 Checking the reference control point data and DEM data accuracy 30
3.4.5 RTK GPS data 30
3.4.6 Vertical accuracy assessment (using point-wise measurement) 31
3.4.7 Vertical accuracy assessment (using pixel-based measurement) 33
Chapter Four 35
4. Results and Discussion 35
4.1 Reference data 35
4.1.1 GCP (Ground control point) data 35
4.1.2 RTK GPS data 36
4.1.3 Photogrammetric DEM data 39
4.2 Vertical Accuracy assessment (using point measurement) 40
4.2.1 Statistical measurement for four global DEM 40
4.2.2 Statistical measurement for four global DEM in equal pixel size 41
4.2.3 Accuracy assessment using scatter plot diagram and histogram errors 41
4.2.4 Accuracy assessment by using different land use and land cover 46
4.2.5 Accuracy Assessment in classified elevation data 47
4.3 Vertical accuracy assessment using pixel-based 49
4.3.1 Accuracy assessment using photogrammetric DEM data 49

4.3.2 Accuracy assessment using profile graph 51
4.3.3 Accuracy assessment using slope classes 52
4.4 Bias correction 53
4.5 Discussion 57
Chapter Five 60
5. Conclusion and Recommendations 60
5.1 Conclusion 60
5.2 Recommendations 61
References 62
Appendix: 69

List of Figures

Figure 2.1 The difference between Orthometric height, ellipsoidal height, and geoid height 12

Figure 2.2 Instruments used for RTK data collection 17

Figure 3.1 Location map of the study area 24

Figure 3.2 Connecting radio link with base and rover receiver 31

Figure 3.3 The flow charts of the methodology 34

Figure 4.1 GCP reference data in the study area 36

Figure 4.2 RTK GNSS reference point data of BL-bare land, RD-road line, DR-drainage pattern, TR-tree, and RC- rock area 38

Figure 4.3 Photogrammetric DEM 39

Figure 4.4 Scatter plots of GCP elevation data and a) SRTM DEM b) ASTER-GDEM c) ALOS-PALSAR (12.5 m) D) ALOS-PALSAR (30 m) DEM elevation data 42

Figure 4.5 Scatter plots of RTK elevation data and a) SRTM DEM b) ASTER-GDEM c) ALOS-PALSAR (12.5 m) D) ALOS-PALSAR (30 m) DEM elevation data 43

Figure 4.6 Histograms with normality curve between GCP and a) SRTM-DEM b) ALOS-PALSAR (12.5 m) c) ASTER-GDEM d) ALOS-PALSAR (30 m) 44

Figure 4.7 Histograms with normality curve between RTK-GPS and **a**) SRTM-DEM **b**) ALOS-PALSAR (12.5 m) **c**) ASTER-GDEM **d**) ALOS-PALSAR (30 m) 45

Figure 4.8 RMSE value for classified elevation data using GCP reference data 48

Figure 4.9 RMSE value for classified elevation data using RTK-GPS reference data 49

Figure 4.10 : Deviation map of photogrammetric DEM and A) SRTM B) ASTER-GDEM c) ALOS-PALSAR (1) D) ALOS-PALSAR (2) 50

Figure 4.11 Profile graph of Photogrammetric DEM and global DEM 51

Figure 4.12 Slope classification of global DEM data in photogrammetric DEM reference data . 53

Figure 4.13 RMSE value before and after bias correction a) GCP reference and b) RTK-GPS reference..... 55

Figure 4.14 Histograms of elevation errors and normal distribution curve after bias correction in GCP reference data 56

List of Tables

Table 2.1 Recommended checkpoints in ASPRS accuracy standards 22
Table 3.1 List of software's and its specifications 25
Table 3.2 Sources of the data and its description 28
Table 4.1 Transforming vertical datum GCP data EGM96 geoid model to EGM2008 35
Table 4.2 RTK GPS Sample data which collected from the study area 37
Table 4.3 Statistical analysis for the photogrammetric DEM using GCP reference data 39
Table 4.4 Statistical analysis for four global DEM using GCP data reference 40
Table 4.5 Statistical analysis for four global DEM using RTK GPS reference data 40
Table 4.6 Statistical measurement for resampled ALOS-PALSAR DEM in GCP and RTK reference data 41
Table 4.7 Statistical measurement of different land use and land covers between RTK-GPS and global DEM data, unit is (m) 46
Table 4.8 Statistical measurement for classified elevation data 47
Table 4.9 Statistical measurement for classified elevation data (RTK-GPS reference data) 48
Table 4.10 Random point data statistics measurement by using photogrammetric DEM reference (m) 50
Table 4.11 Statistical measurement for classified slope data 52
Table 4.12 Linear transformation parameters for bias correction in different DEM based on multiple linear regression 54
Table 4.13 Statistical measurement value of DEM value before and after bias correction (in GCP reference data) 54
Table 4.14 Statistical measurement value for improved global DEM (in RTK-GPS reference data) 55

Chapter One

1. Introduction

1.1 Background

Digital elevation model (DEM): -is a digital and mathematical representation of real-world topographic surface by using regularly or irregularly spaced point elevation values (Joachim et al., 2011). There is no clear and universally agreed distinction among digital surface model (DSM), digital elevation model (DEM), and digital terrain model (DTM) (Zhou Qiming, 2017). Nevertheless, some common tenets are described in the following ways. DEM is classified into two types, DTM and DSM. DSM includes elevation data of man-made or natural features height (building height, forest, or whatever) (Li Zhilin et al.,, 2007). And DTM does not include man-made and natural features height, it only shows the bare earth of ground surface. Sometimes DTM and DEM are used as synonyms (Joachim et al., 1986). On the other hand, some literature explains DTM includes break lines, mass points, and significant topographic features elevation to improve the accuracy of the data (Joachim et al., 2011). In this study, DEM is considered a synonym with DTM. The recent DEM acquiring techniques like photogrammetry, InSAR, LiDAR, and other techniques are the main source for the DEM data. And some of them like RADAR can penetrate clouds, haze, fog, and rains (Demetrios et al., 2019). Historically, terrain model data is constructed from vinyl plastic, plaster, and others, and such models are represented as three-dimensional relief maps. That relief map was extensively used during the second world war for military purposes (Liu et al., 2009). By using the photogrammetry method Colonel Aimé Laussedat the French army corps of Engineers created topographic maps in 1849 (Paul et al., 2014). Moreover, the invention of the airplane in 1903 gave vital force for aerial photography to make terrain models. The development is continued here to fore by improving their techniques and accuracy of the data. The recent photogrammetry technique uses digital photogrammetry to produce accurate DTM data. However, this technique can cover a small part of the earth's surface as compared with satellite-based techniques. Interferometry synthetic aperture Radar (InSAR), Light detection and ranging (LiDAR) techniques are currently used to acquire global DEM data. InSAR technique uses two or more SAR images of the same area to extract the topography of the surface and the deformation patterns (Lu Zhong et al., 2007). It measures signal phase change between two images that were acquired from the same area at different times (A CLS Group Company, 2020). Or it uses two antennas in the same distance and

platform at the same time to record signal phase change. It is an active system and used for different applications; monitoring of wetland water level (Kim Jin Woo, 2013), monitoring landslide (Herrera et al., 2014), ice flow measurement, tectonic deformation, DEM generation (Zhou et al., 2005), etc. LiDAR technology is a method to measure the distance of the object on the earth's surface by using light, which transmits the pulse of light to the object and is recorded by the reflected lights (Liu Xiaoye, 2011). The difference between these two techniques is, RADAR uses radio waves to record data from the ground surface, while LiDAR uses laser light rather than radio waves. Some selected DEM product for this study is one of the InSAR products; SRTM uses two SAR systems X-band and C-bands interferometric radar (Yang et al., 2011) whereas, PALSAR DEM both 12.5 m and 30 m resolution uses L-band SAR (Japan Aerospace Exploration Agency, 2008). Whatever, those selected open access DEM data like ASTER GDEM, SRTM, and others exhibit a vertical error (Gallien et al., 2011). Because their quality depends on several factors; types of topography and vegetation (Lane et al., 1998), the method used for data collection, DEM resolution, DEM grid type, and DEM generation methods (Zhang et al., 2005), sensor and terrain types, algorithm (Hebeler et al., 2009). However, some applications require high accuracy DEM data; the vertical accuracy data used for the design of roads and Engineering applications requires less than 0.5 m, the vertical accuracy required for hydrology or flood risk modeling is less than 0.2 m and urban modeling requires less than 0.15 m accuracy data (Joachim et al., 2011). Therefore, assessing the accuracy of DEM data is indispensable for different applications, it verifies the reliability of the DEM data.

Accuracy assessment was investigated in previous studies (Abdulkareem et al,, 2020; Abili et al.,2021; Elkhrachy, 2018). The way of investigation of accuracy assessment is assessed by comparison between DEM and reference data. The reference data is different from one study to another like, GPS point data (Kwanchai et al., 2016; Abili et al., 2021), topographic map (Ismail Elkhrachy, 2018), LiDAR data (Fahad et al., 2019), photogrammetric DEM (Hareya et al., 2020) and etc. It is depending on existing data and location of the study. GPS point data is measured by high precision instruments and others reference data should be at least one order better than the data to be evaluated. In the study of (Ismail Elkhrachy, 2018) 30 RTK-GPS point data are collected by using dual frequency GNSS instrument. The obtained accuracy for horizontal accuracy is 10mm+ppm and the vertical accuracy is 15mm+1ppm. Which it is enough accuracy

for assessing the accuracy of DEM. Hailu (Hailu Zewde Abili, 2021) uses reference DEM which processed from contour data and it validated by DGPS data and the accuracy is 1.2m RMSE.

Different platforms are used to carry sensor for the DEM creation data, one is ground-based, which the relevant point data is collected by total station or GPS receiver; it is a close range to the objects and collect accurate data, the second is aerial-based like UAV or drone, aircraft, and helicopter; it captures digital aerial photographs from low, medium or high altitudes, their altitude depends on applications. And the third one is satellite-based, which is spaceborne and covers a wide area (Ismail Elkhrachy, 2018) and it consumes a short time as compared with the other methods. In developing countries like Ethiopia DEM accuracy assessment is rarely applied, some of them are applied around Mekelle city (Hareya et al., 2020), Adama city (Hailu Zewde Abili, 2021), and others. They all are tried to assess the conventional global DEM data like SRTM, ASTER-GDEM, ALOS, and Tan-DEM. However, the recent global high-resolution data (ALOS-PALSAR) is not assessed in Ethiopia. Therefore, this study was tried to assess high-resolution PALSAR (12.5 m and 30 m) data and common global DEM data. Additionally, bias correction was applied for the selected DEM data. The selected open access DEM data are; shuttle radar topographic mission (SRTM DEM) 1 arc-second (30m), advanced Spaceborne thermal emission, and reflection radiometer global DEM (ASTER GDEM) 1 arc second (Ismail Elkhrachy, 2018) ALOS-PALSAR with 12.5 m and 30 m resolution.

GPS point data (GCP and RTK-GPS) and photogrammetric DEM were used as reference data because the checkpoint is guarantees stability for error estimates (A. Cuartero et al., 2004).

1.2 Statement of the problem

Acquiring high-quality DEM data is a critical issue for the different applications. Because many sources of the factors influence the quality of DEM data like DEM generation techniques (LiDAR, InSAR, photogrammetric, ground-based or conventional techniques) (Zhang et al., 2005), selected interpolation method, resolution of the data, terrain complexity, and vegetation in target area (Lane et al., 1998), the budget which allocate to the project, available technology, and other different factors are affecting the quality of the data. Their all results influence the accuracy of DEM data and the results perhaps shift the location, wrong output, and others anomalies. Currently, many global open-access DEM data are available; Shuttle Radar Topographic Mission (SRTM), Advanced Spaceborne Thermal Emission, and Reflection Radiometer Global Digital

Elevation Model (ASTER GDEM), Advanced Land Observing Satellite/Phased Array type L-band Synthetic Aperture Radar (ALOS/PALSAR) and others. And they all are affected by the mentioned factors. However, Engineering and non-Engineering applications like road design, flood risk modeling, urban modeling require highly accurate DEM data. Therefore, to coincide the applications requiring accuracy and the DEM data accuracy, assessing the accuracy and correcting the bias for the DEM data is an important issue. Different approaches are used to assess the accuracy of DEM data, most of the studies are tried to assess in conventional methods (Sandip et al., 2013), Geostatistical method, visual assessment method (Fahad Salim Alahmadi, 2019). And by using the mentioned approach different countries were tried to assess the DEM accuracy. In Tunisia and Algeria (Athmania et al., 2014), India (Sandip et al., 2013), Indonesia (Suwandana et al., 2012) Saudi Arabia (Ismail Elkhrachy, 2018), and many others. In our country Ethiopia, some of the studies are applied, around Mekelle city (Hareya et al., 2020), in Adama city (Hailu Zewde Abili, 2021), and others. However, all of them are tried to assess common global DEM data like ASTER, SRTM, ALOS, and tan-x DEM which have 1-arc second and less resolution; and the latest released high resolution (12.5m) global DEM is not assessed in Ethiopia. High-resolution DEM like PALSAR is more important for engineering and non-engineering applications. Therefore, this study is assessing the accuracy and bias correction for four free sources of DEM data in vertical (SRTM, ASTER, ALOS-PALSAR (12.5m and 30m)) resolution by using photogrammetric DEM, GCP data, and RTK-GPS reference data in Eastern Ethiopia, Dire Dawa city.

1.3 Objective of the study

1.3.1 Main objective

The main objective for this study is the vertical accuracy assessment and bias correction for four global DEMs by using photogrammetric DEM, GCP, and RTK-GPS reference data: a case study in and around Dire Dawa city.

1.3.2 Specific objective

- ✓ To evaluate the vertical accuracy of DEM data using point-based and pixel-based data
- ✓ To evaluate the vertical accuracy of DEM using terrain classification and land use land cover point data
- ✓ To make bias corrections for evaluated data

1.4 Research questions

- Which DEM data is low accurate from the assessed free global DEM data?
- Which DEM data is highly accurate from the assessed free global DEM data?
- Which DEM data accuracy is less improved after bias correction?
- Which DEM data accuracy is more improved after bias correction?

1.5 Scope of the study

This study is focused on the vertical accuracy assessment and bias correction for four open sources global DEM data (SRTM, ASTER-GDEM, ALOS-PALSAR (12.5 m and 30 m spatial resolution)) in and around Diredawa city. The least-square method is used to compute linear transformation parameters based on multiple linear regression in the bias correction part. Horizontal accuracy assessment is not applied, because global DEM data is affected in vertical errors rather than horizontal errors. Reference datum for horizontal is WGS84 and for vertical is EGM2008 geoid model.

1.6 Significance of the study

This study is important to know the characteristics of selected DEM data and improve the quality of the DEM, it plays a vital role to enhance the accuracy of the global DEM data and it gives full accurate information for the selected DEM data, which is used to decide DEM data from the selected data. Different engineering and non-engineering applications require high accuracy DEM data. So, to realize data quality in the study area, this study is indispensable for different applications.

1.7 Organization of the thesis

This thesis was structured in five chapters and summarized as follows:

Chapter one describes the background of DEM data, the statement of the problem, the objective of the study, research question, the scope of the study, and significance of the study, whereas Chapter Two describes review literature which includes a background of DEM data, global DEM data, accuracy assessment methods, accuracy standard, reference datum and, bias correction methods. And Chapter Three: deals with the study area, methodology of the study, used materials, and data analysis. Then Chapter Four presents the results of the study and discussion, and the last Chapter Five describes the conclusion and recommendation of the study.

Chapter Two

2. Literature Review

2.1 Introduction

Digital elevation model (DEM) is a digital representation of ground surface with or without any features (bare land) in 3D (Ismail Elkhrachy, 2018). Irregular distributed points are forming a non-overlapping triangle, which is connected to each other and shows the figure of the earth, which is called triangulated irregular network (TIN) (Joachim et al., 2011). Some web definitions classify DTM as a 3D TIN and DEM is considered as regular spaced GRID. There is no clear and universally agreed distinction among digital surface model (DSM), digital elevation model (DEM), and digital terrain model (DTM). Some common tenets are described in the following ways. DEM comprises two things, elevation data does not include building height, forest height, and any features height in DTM. Whereas, the elevation data include building height, forest height, or any features height (man-made and natural) in DSM (Li Zhilin et al., 2007). Both DSM and DTM data are their advantages, for road design, hydrology (Joachim et al., 2011) mapping, mining engineering, land planning and geology (Aktaruzzamane t al., 2009) and others, use DTM, however, the DSM is used for 3D building change detection, analysis, visualization and variety of planning (INNOTER Geospatial Agency, 2020). Those mentioned applications are requiring highly accurate DEM products, but different factors are affecting the accuracy of DEM data; algorithm types, terrain type, grid spacing (Kwanchai et al., 2016), resampling techniques, and DEM resolution (Tang-guo et al., 2001) are affecting the accuracy of the DEM data. So, assessing the accuracy and bias correction in vertical for global free DEM data is important to increase the reliability of the data. In this study, the term DEM is used as DTM. There are different sources to make DEM data, generally, the following three techniques are basic ones.

2.2 Digital elevation data

2.2.1 Ground survey techniques

This method uses theodolite instruments to measure the angles in horizontal and vertical planes. And triangulation methods create dense triangles with the observation points at each apex and this created mesh of triangles represent the terrain of the measured point location landscape (Nelson et al., 2009). This technique requires highly skilled chief surveyors and experienced

persons, later EDM (electronic distance measurement), total stations (combination of theodolite and EDM), GPS (GNSS) instruments have improved the accuracy of this technique. The recent instruments measures easting, northing, and elevation of the points then digital modeling makes terrain representation data (TIN, contour, or DEM by interpolation techniques). The main advantage of this method is highly accurate terrain representation data was acquired, nevertheless, it is complex, expensive, and covers small areas. This method is used for dams, roads, bridges, etc. applications.

2.2.2 Existing topographic map

If there is no existing DEM data, there is a method to obtain DEM data from an existing topographic map by the following approach

i. Digitizing of the topographic map (manually)

The operator digitizes the existing topographic map or aerial photo from the analog map into a digital form. All the existing features like water bodies (rivers, coastlines, and lakes), contours, spot height, intersecting features (road, railway, cliffs, and others) (Nelson et al.,2009) are digitized. But there is also a semi-automated and automated method from analog into a digital form (Peter et al., 1998).

ii. Automated digitizing (cartographic map)

It is a process of extracting features from the map semi-automated by using the software. Then it is edited and corrected by the analyst, it is a vector form data.

2.2.3 Remote sensing data

This method is different from the mentioned sources, it covers a large area. And it uses two types of platforms: aerial-based or satellite-based. The resulting images from those platforms are aerial photography, radar image, and LiDAR image.

i. Photogrammetric land surface model

Aerial photography has high accuracy and resolution which it takes from an airborne platform (Nelson et al., 2009). By using GCP data and survey point photography, aerial photography is geo-referenced digitally; a single photo shows the terrain but it does not provide the elevation data. So, overlapping photographs to each other (55%-65% overlap) shows a 3D representation

of the earth's surface by using photogrammetric principles. Then Orthorectification is applied to acquire accurate data and the resulting map is orthophoto. Vertical photography is required for this process, low oblique or high oblique aerial photography is not possible to create a highly accurate orthophoto. One advantage of this method is the standard approach and covers large areas as compared with ground survey techniques. However, there are several drawbacks; systematic errors occur for elevation if the camera has the distortion, and the clarity of the aerial photography is affected by snow cover and frequent cloud cover (Ravibabu et al., 2008).

ii. LiDAR (Light detection and ranging)

This technique uses airborne laser scanning and it is an active system. The sensor transmits its signal to the ground (in near-infrared red) and records reflected light. The time delay between the transmission and reflection is recorded, and it is used to determine the distance between the sensor and the ground. 5000-10,000 points are collected for each second and the expected accuracy in the vertical plane is 15cm (Huising et al., 1998) and in the horizontal plane is 50-100cm (Grunwald, Sabine, 2005). IMU (Inertia measuring unit) measures every movement of the platform and a very sophisticated GPS unit records several signals from satellite (Carter et al., 2012). High-density sampling points and high accurate vertical data are some of the advantages of this technique. Elevation data are collected repeatedly, the first elevation (Z_1) is the first return signal and the last one (Z_n) is the last return signal. The last return signal is recorded the time from the ground surface. In other words, the LiDAR technique can record both ground surface and vegetation surface above the ground. One of the drawbacks of this technique, it is difficult to handle dense data. However, it is superior in accuracy as compared with RADAR and topographic map techniques. Unlike RADAR, LiDAR data cannot penetrate clouds, dense haze, and fog (Cartere t al., 2012).

iii. RADAR

This system sensor is mounted on either airborne or satellite-based (Nelsonet al., 2009). Satellite-based radar systems cover the whole or part of the world. It can penetrate clouds and dense haze because it uses radio waves. DEM data acquired from radar images using the following techniques, the same scene is recorded two or more times in a radar system at a different position then signal phase change is recorded and it gives DEM data. Comparing radar data with topographic maps, radar data contains a lot of errors; mountain or tall towers are mislocated and

which leads to height error and geometric error. Some of the global DEM data selected for this study is one of the InSAR products. The marriage between the SAR and InSAR is, SAR is releasing a signal and that signal contains amplitude and phase information then InSAR exploits the phase difference between two SAR images of the same scene then the phase difference creates elevation data. The following are some of the Remote-sensing based global DEM data.

2.3 Global Digital elevation model (DEM) data

Shuttle Radar Topographic Mission **(SRTM)**: -this is a free DEM data source and global coverage. And acquired from the United States geological survey (USGS) (https://earthexplorer.usgs.gov/). The vertical and horizontal accuracy for SRTM at 90% confidence interval is 16 m to evaluate in linear error and 20 m to circular error (Jarvis et al., 2004). It produces 1-arc second (~30 m) and 3-arc second (~90 m) spatial resolution. It is produced by using two single-pass interferometers in C-band and X-band systems (Yang et al., 2011). Joint forces of NASA (National Aeronautics and Space Administration), NGA (National Geospatial-Intelligence Agency), Italian and German space agencies participated (Farr et al., 2015). SRTM for the first time launched on a space shuttle in February 2000 in version-1 (Yang et al., 2011). This study uses SRTM version-3 DEM which is a revised version and has moderate resolution 1-arc second (~30 m resolution).

Advanced Spaceborne Thermal Emission and Reflection Radiometer Global Digital Elevation Model **(ASTER GDEM):** - this was established by both the ministry of economy, trade and industry (METI) of Japan and the National Aeronautics Space Administration (NASA). It was launched in 1999 on NASA terra spacecraft (Ismail Elkhrachy, 2018). And it has produced 30m spatial resolution data since 2009, and version 2 was released in 2011 and the absolute vertical accuracy at 90 % confidence interval is 20m (Kwanchai et al., 2016) and 30m at 95 % confidence interval. It covers large areas of the world (83°N and 83°S) (ASTER GDEM Validation Team, 2009), which covers 99 % of the world's landmass. Version-3 ASTER GDEM data was applied for this study. Which is an improved version of the DEM data and includes significant improvements like additional stereo pairs (Jet propulsion laboratory, 2020).

Advanced Land Observing Satellite/Phased Array type L-band Synthetic Aperture Radar (**ALOS/PALSAR**)

ALOS-PALSAR is the owner of Alaska Satellite Facility Center, an L-band SAR instrument that operates onboard the ALOS satellite (Fahad et al., 2019). It is one mission instrument of ALOS for earth observation and it can change off-nadir angle covers ranging from 9.7 to 50.8 degrees according to the data ALOS Data Users Handbook (Japan Aerospace Exploration Agency, 2008). This product has a high resolution as compared with other free global DEM data and it was launched in 2006 and had been collected data until 2011. It is not limited by daylight because it is an active system and is relatively not affected by cloud cover and weather effects. To reduce radiometric and geometric distortion in high relief, radiometric terrain correction is applied which is used to produce superior products for different science applications and improve the accuracy of the DEM data (Cole et al., 2015). The ASF (Alaska Satellite Facility) prepares two DEM products, which are 12.5 m and 30 m resolution data. The product contains the following files.

Radiometric terrain corrected (RTC) GeoTIFF file, Incidence angle file (indicating the angle in radian for the pixel), shadow/layover file, GeoJEG 1km resolution data, metadata, and KMZ 30 m resolution are included in both 12.5 m resolution (RT1 product) and 30m resolution (RT2 product) RTC packaged data. RTC GeoTIFF file is used for different applications. Most DEM products are geoid based and it requires correction before using for different applications. However, in PALSAR DEM correction was applied and the orthometric height is converted to the ellipsoidal height by using ASF Map-ready software. According to Topographic correction guideline of the ALOS-PALSAR study (Das et al., 2015), SRTM and ASTER DEM data produce orthometric height while the ALOS-PALSAR DEM data produce ellipsoidal height. During ALOS-PALSAR DEM processing time five global DEM products were used (NED13 with 10m resolution, SRTMGL1 30m resolution, SRTMUL-1 30m resolution, NED1 and NED2 30m and 60m resolution). Those NED and SRTM were mosaicked and clipped in DEM available area and resampled in 12.5m resolution. That means it is not the original resolution of the DEM. Many NASA-provided DEMs is used the EGM96 geoid model but it is converted to ellipsoidal height in the PALSAR DEM product.

2.4 Vertical and horizontal datum

The referenced geoid model for the DEM data and reference data must be the same. The horizontal position reference datum for ASTER and SRTM DEM data is WGS84 ellipsoid and for vertical datum, it is EGM96 (Earth Gravitational Model 96) (Xiaoping et al., 2015; Hareya et

al., 2020). However, the horizontal reference datum for the ALOS/PALSAR is WGS84 and the vertical datum is referenced by ellipsoidal height by using WGS84 ellipsoid. So, to match the vertical reference datum for all global DEM and reference DEM data, the latest EGM2008 geoid model was used for this study for vertical reference datum. Referenced EGM96 geoid height and ellipsoidal height were converted to EGM2008. MATLAB R2016b and Alltrans EGM2008 calculator were used for geoid calculations. There are three versions of the EGM: - EGM84, EGM96, and EGM2008. EGM84 is the oldest and has low accuracy as compared with the latest geoid model. EGM96 is published by both the National Geospatial-intelligence Agency (NGA) and the National Aeronautic Space Administration (NASA) as well as Ohio University also participated, it is used as the geoid reference in the WGS84 (world geodetic system). The degree and order of EGM96 are 360. But, in EGM2008 degree and order increases up to 2159 and 2190 (Roh et al., 2014). The SRTM, ASTER, and other NASA-provided DEM data use the EGM96 geoid model as the reference.

The applied Geoid model for this study is EGM2008, EGM96 is transformed to the ellipsoidal height and again the EGM2008 geoid model is subtracted from the ellipsoidal height. Because EGM2008 is improved in accuracy and additional newer data is added. The EGM96 geoid model used as a reference for the vertical datum in the ASTER, SRTM, was transformed to the improved EGM2008 and PALSAR (12.5 m and 30 m resolution) ellipsoidal height is subtracted by geoid height EGM2008 geoid model.

The Ethiopian Geospatial information agency (EGIA) uses the Clarke 1880 (Adindan) ellipsoid for horizontal datum, so to transform the photogrammetric DEM and GCP data which gained from Ethiopia Geospatial information Agency (EGIA) and Dire Dawa Land Administration and management bureau is transformed to WGS84 ellipsoid by using the following parameters.

Dx = −162 m, Dy = −12 m, Dz = 206 m, and the vertical datum is referenced by the EGM96 geoid model was transformed to the latest EGM2008 geoid models. EGM2008 is a modified and improved spherical harmonics coefficient which is determined by National Geospatial-Intelligence Agency (NGA). According to NGA transform EGM96 to EGM2008 the following method is important (Hareya et al., 2020).

1. Computing the geoid height of the reference geoid model, SRTM and ASTER GDEM use the EGM96 geoid model.

2. Add the geoid height value (EGM96) and orthometric height value to get the ellipsoidal height.

3. Subtract the geoid height referenced by the EGM2008 geoid model from an ellipsoidal height of WGS84 to get the orthometric height presented in Figure 2.1.

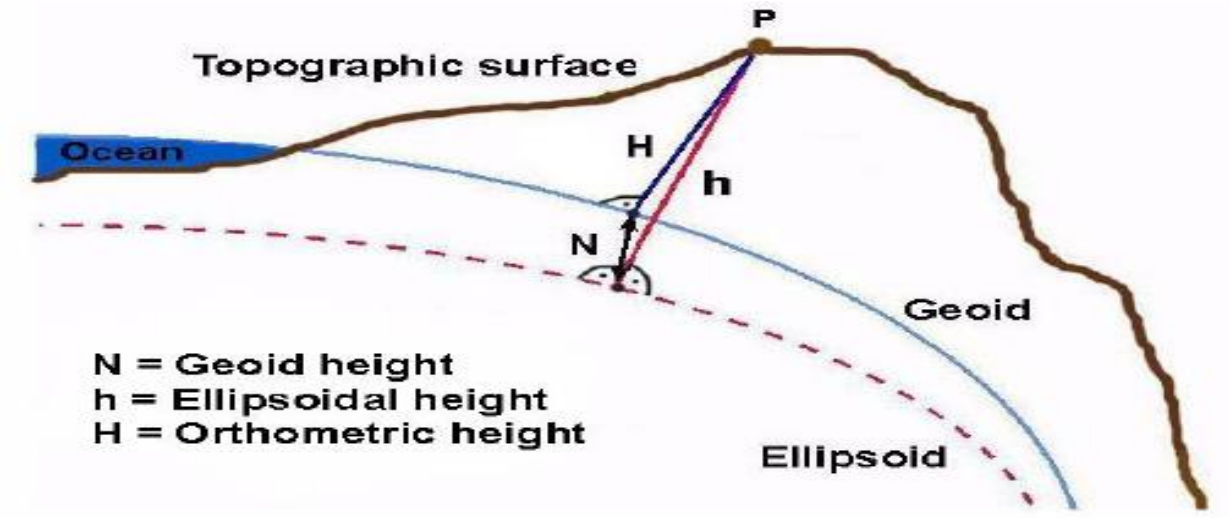

Figure 2.1 The difference between Orthometric height, ellipsoidal height, and geoid height

Source: (Evaluation of recent global geopotential models based on GPS/leveling data over Afyonkarahisar (Turkey) (Ylmaz et al., 2010)).

2.4.1 Types of vertical height

Global position system (GPS) or Global navigation Satellite System (GNSS) point data measure ellipsoidal height, however, the reference data used for assessing global DEM is orthometric height. There are three types of height system, the first is the ellipsoidal height which uses the reference ellipsoid as Geodetic height and as a datum, and the result is ellipsoidal height; the second one is a classic system which uses the geoid as a datum and gives orthometric height and the last one is Molodenski system, this uses Quasi-geoid as a datum and gives normal height (Santos et al., 2019). Geoid and quasi-geoid are the same in ocean surface but different in meter level over mountain area. The classical system is the winner of all because it is best approximated to the mean sea level (MSL) except within high rugged mountains, it considers the influence of gravity and ocean current (free from the tidal system). Although, mean sea level and geoid are not the same because geoid is an equipotential surface but the mean sea level is a non-equipotential surface due to inconsistent datum points (Amos et al., 2009). All the global free

DEM data provided in NASA is the orthometric height with EGM96 geoid model reference. But GPS gives ellipsoidal height (height above the ellipsoid), so there is a deviation between the Orthometric and ellipsoidal height also called Geoid undulation or geoid height. To get the orthometric height we subtract the geoid height from the ellipsoidal height. The following equation shows the relation between ellipsoidal height, geoid height (undulation), and Orthometric height.

$$N = h - H, \quad (2.1)$$

where N is geoid undulation or geoid height; h is ellipsoidal height and H is orthometric height. Currently, the combination of the remote sensing satellite with navigation satellite and geoid gives the high-resolution DEM products (Hareya et al., 2020). And high-resolution DEM data is used for different high accuracy requiring applications in road design, urban modeling (Joachim et al., 2011), flood modeling (Hasina et al., 2017), geomorphology (Bartłomiej Szypuła, 2019), and others.

2.5 Global positioning system (GPS)

Global positioning system is a satellite-based navigation system that was developed by the US department of defense (DoD) for military purposes later the civilian was used for different applications like timing information, weather condition, positioning systems, and for several applications (Klusberg A, 1990). It is a one-way ranging system, which the users only can receive the satellite signals, the transmitted signal (microwave radio signal) contains carrier frequencies waves (L1 and L2 frequency), codes (P-code and C/A code, M-code (military code), and L1C (civil)) and navigation messages; L1 and L2 generated their frequencies at 1575.42 MHz and 1227.60 MHz and their wavelength is approximately 19cm and 24.4cm. Then GPS, the receiver which is connected to the GPS antenna gives us the location data from the received signal and navigation message in the technique of resection by built-in software. There are 24 operational satellites in 6 orbital planes, each orbital contains four satellites. At least four satellites are needed to provide information for position or location and any information (El-Rabbany, 2002). Three of them are used for x, y, and z information, and the rest is used for time information. If the number of satellites increases the precision also increases simultaneously. There are three main GPS components; space segment, control segments, and user segments. A space segment is a GPS satellite that is found in space, control segment is used for tracking the

GPS satellite, predicting the location, studying the behavior of the atomic clock which is attached on the satellite board, and other multi-tasks. The user segments include civilian and military users. To keep military services, the US Department of Defense (DoD) provides two levels of positioning and timing services; PPS (precise positioning service) and SPS (standard positioning service). PPS is highly precise and encrypted by P(Y) code and is only used for authorized users. SPS is accessible for all users and the accuracy is less as compared with PPS. C/A code modulated on to L1 frequency and P-code modulated on both L1 and L2 frequencies until December 2005. However, currently, L1 can transmit C/A, P(Y), M-code (military code), and the new L1C signal (Ávila et al.,2021). The GPS data is affected by different errors and the origin of the error is from three sources; one is satellite errors include orbital error, satellite clock error, and others; dual-frequency is used to reduce this error. The second one is originated in the receiver; includes multipath error which is reduced by choke ring antenna, antenna center variation, this error is canceled by if the antenna is oriented by the same direction, receiver clock errors, etc. and the third is signal propagation error, ionospheric and tropospheric layers of the atmosphere, This error is reduced by combining L1 and L2 frequencies but tropospheric delay not reduced by combining L1 and L2 it depends on temperature, humidity, and pressure so to reduce this error collecting data in clear sky day. The collected RTK data for this study was collected in clear sky days. Satellite geometry is considered for this study during data collection time and it is in a very good position. PDOP (precision dilution of position) is in a very good position because it shows the contribution of 3-D position accuracy. To measure the range between satellite and receiver, there are two approaches; the first is pseudo-range measurement and it is presented in the following equation (Thomas Herring, 2012).

$$P_k^p = (t_k - t^p) * c \tag{2.2}$$

where P_k^p is pseudo-range between the satellite and the receiver; t_k is receiver time (signal received time in the receiver), t^p is transmitted time from the satellite, and c is the speed of light

The second technique is carrier phase measurements which measure the distance between satellite and receiver in the following equation.

$$\phi = f\Delta t \tag{2.3}$$

where ϕ is phase and f is the frequency

And the core part of the GPS is GPS positioning mode and it is performed in two ways; the first one is point positioning and the second is relative positioning. The point position system employs one satellite receiver that measures pseudo-range codes to determine the point of the user when the four or more satellites are tracked by the receiver. The GPS point positioning mode has low accuracy and it requires low accuracy requiring applications (Shaw et al., 2000). The second is relative positioning which employs two GPS receivers simultaneously tracking four or more satellites to obtain high accuracy data from a few meters to centimeter-level. And data can be made either post-processing or in real-time. And both base receiver and rover receiver track the same satellite at the same time. The number of satellites must be four or more. There are four types of relative positioning modes;

a) **Static GPS surveying**: -it is one of the relative techniques and it depends on carrier-phase measurement (Hofmann-Wellenhof et al., 2012). Two or more receivers track four or more common satellites simultaneously. Base receiver setup on a known point and rover receiver set at unknown points (Survey department Minister of Development Brunei Darussalam, 2017). The observation time is more than 30. This technique is most accurate in carrier phase measurements and the expected accuracy is 5mm+1 ppm. After collecting the data PC software was used to download and post-process the data.

b) **Fast (rapid static) surveying**: -this technique is similar to the static method, which is a carrier phase measurement; base and rover receiver track four or more satellites simultaneously. This method is suitable when a survey involves more unknown points around 15km. The duration for collecting data is 2-10 mins and a post-process is required. Accuracy is expected from this method decimeter to sub-meter level.

c) **Stop-and-go surveying**: - this technique is also a carrier phased relative positioning technique. It is a suitable method if more unknown points are available around 10-15km. Requiring time for data collection is 30 seconds per stop. Centimeter level accuracy is obtained if four or more satellites are simultaneously tracked at both base and rover receiver. The Rover receiver is moved from one point to another without being switched off.

d) **RTK-GPS:** - this method is are also carrier phase-based relative positioning technique. And two or more receivers track four or more common satellites simultaneously. It is suitable if many unknown points are available around 10-15 km and the obtained data is in real-time,

but the latter methods are post-processing. In this method, the base receiver is set up on a stationary precise known coordinate point and the radio link is connected to the base and rover receiver. The base receiver coordinates and measurement data are transferred to the rover receiver through the radio link and the rover receiver combines the base measurement data and rover measurement data to obtain the coordinates data of the rover receiver point location. The process is done by built-in software in the rover receiver. The expected positional accuracy is 2-5 cm. The duration of time for data collection is very short. On-the-fly (OTF) ambiguity resolution is used to determine the initial ambiguity parameters instantaneously. The collected data for this study is RTK-GPS/GNSS in TRIMBLE R8 GNSS/R6/5800 instrument. According to the product specification (Trimble Engineering and construction group, 2003), the instrument is a dual-frequency GPS receiver. The position of the UHF (ultra-high frequency) radio antenna further increases the accuracy. High precision multiple correlates for L1 and L2 pseudo-range measurements and very low noise with L1 and L2 carrier phase measurements with <1mm. The radio link is used to transfer the base receiver information to the rover receiver at a 9600 baud rate (which means the serial port is transferring a maximum of 9600 bits per second). The radio link is essential for the RTK-GPS survey and real-time DGPS (differential GPS). Real-time DGPS transfers at 200kbps. PDL (positional data Link) radio is used for the data collection. Additionally, the car battery was used during data collection to extend the operation of the base receiver and radio link. TSC2 Trimble controller was used during data collection presented in Figure 2.2.

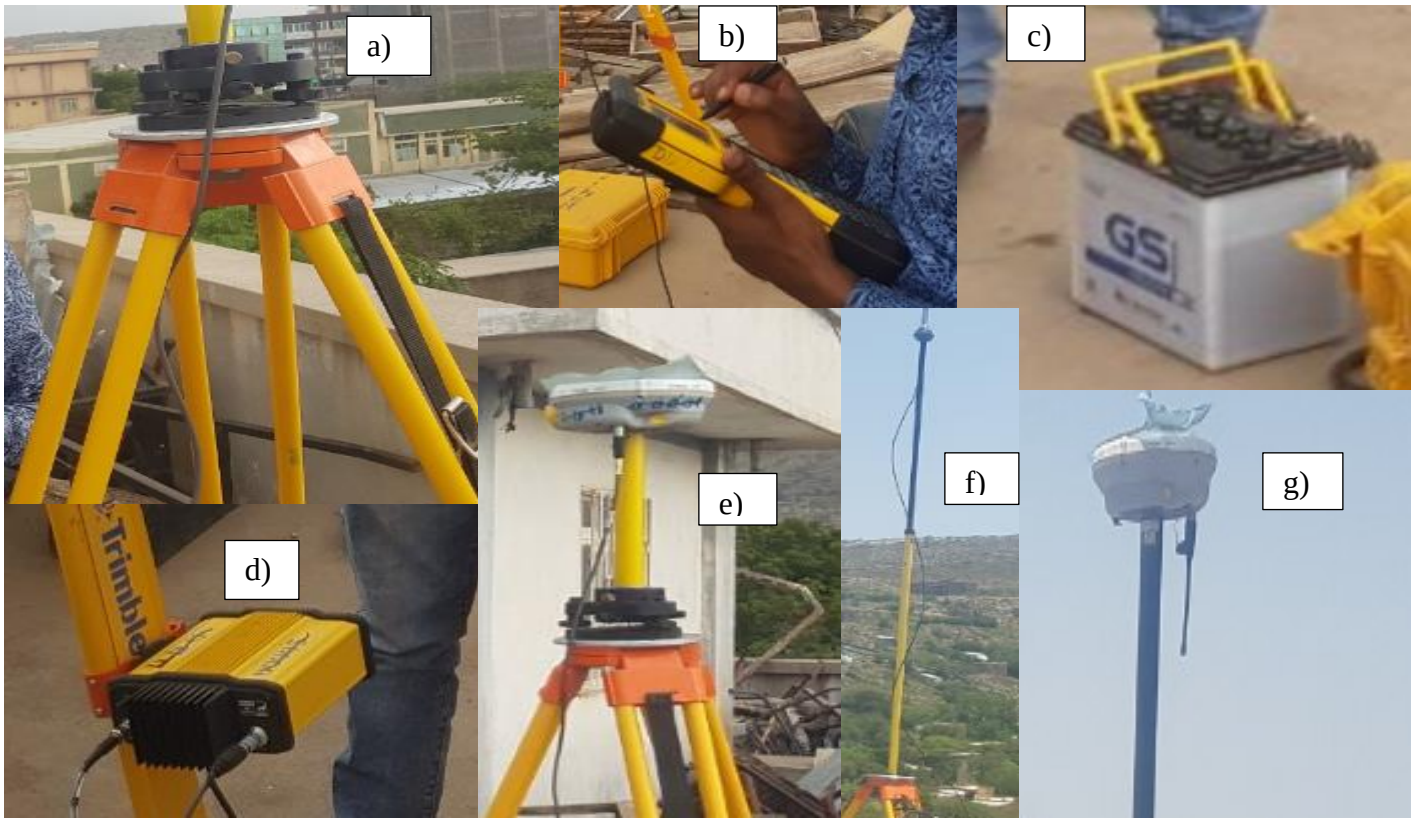

Figure 2.2 Instruments used for RTK data collection

Plate: a) Tripod b) Trimble controller c) Car battery d) Radio Link e) Base receiver f) GPS-Antenna, and g) Rover receiver

2.6 Accuracy Assessment

Accuracy is one of the factors for the data sets, vertical accuracy in DEM means quality elevation data in DEM products. The vertical accuracy is directed related to the discrepancies of elevation data that are obtained from global DEM, against the reference greater accurate elevation data in the same location. Vertical accuracy assessment is the process of measuring the accuracy of DEM data against reference data by using some statistical measurement and other assessing methods. Nevertheless, horizontal accuracy is very important and influences vertical accuracy (ASPRS Lidar Committee (PAD), 2004). However, it is not usual to inform the horizontal accuracy in the case of DEM products. The difference between a value in a data set and a truth or modeled value is called Error. Modeled value is used as a reference and it must be more accurate than a data value. According to the vertical accuracy report in LiDAR (ASPRS Lidar Committee (PAD), 2004), reference data is at least three times more accurate than the observing data. It is impossible to measure true value in continuous data (Ravibabu et al., 2008),

but relatively accurate data is collected from the grid data comparison with sample points. Well distributed sample point data and densely sampled points are important to determine the DEM accuracy and the difference between the DEM and control point elevation (reference data) values can be calculated. Thus, the error is calculated by RMSE (Eq. 2.7), standard deviation (Eq. 2.5). There is no clear standard method for DEM accuracy assessment with an integral vision (Mesa-Mingorance et al., 2020). However, many methods are used to assess the positional accuracy of the DEM data such as NMAS (National Map Accuracy Standard), ASPRS (American Society for Photogrammetry and Remote Sensing), NDEP (National Digital Elevation Program), and NSSDA (National Standard for Spatial Data Accuracy). Lower mean error and the standard deviation are considered as highly accurate data, however, RMSE also determines the accuracy of the elevation data in different standard guidelines (Mesa-Mingoranceet al., 2020). The following equation is given us the discrepancies between the observing elevation data and the reference data.

1. Elevation error, $Z_{diff} = Z_{DEM} - Z_{ref}$ (2.4)

where Z_{diff} is the elevation value difference between reference and free DEM value

Z_{DEM} is free DEM elevation data and Z_{ref} reference point data

2. Mean error, ME = $\frac{\sum_{i=1}^{n} z_{diff}}{n}$ (2.5)

where, n is the total number of the reference points (observation)

3. Standard deviation error $STD_{err} = \sqrt{\frac{\sum_{i=1}^{n}(Z_{diff} - ME)^2}{n-1}}$ (2.6)

4. Root mean square error (RMSE) = $\sqrt{\frac{\sum_{i=1}^{N}(Z_{DEM} - Z_{ref})^2}{n}}$ (2.7)

where, Z_{DEM} =extracted height from global DEM, Z_{ref} =Observed height in reference DEM

n = total number of observations

5. Linear error at 90 confidence level, LE at 90 =1.6449*RMSE (2.8)
6. Linear error at 95 confidence level, LE at 95 =1.960*RMSE (2.9)

2.6.1 Sample size for accuracy assessment

The sample size is very important because it is related to the representativeness of samples and relevant to achieving precision for DEM data in statistical approaches. Most accuracy standards like NMAS, NSSDA recommends a minimum of 20 Control points is recommended for sample in positional accuracy assessment for each land cover type (FGDC, 1998). FEMA (Federal Emergency and Management Agency) (FEMA, 2003) also advises 20 control points to assess accuracy for each land cover and 100 control points are used in the study area if it has five land cover types. Also, the latest ASPRS 2015 guideline (ASPRS, 2015) recommends 20 control points for each land cover type.

2.6.2 Terrain classification for Accuracy Assessment

Different critical aspects influence the accuracy of the DEM data: vegetation cover, different producers and technologies used to data capture, and topographic variation of the study area. Topographic variation or sloped terrain is highly affecting the quality of the DEM data. Most studies concluded that high slope areas have greater uncertainty than moderating and flat areas (Tang-guo et al., 2001; Mesa et al., 2020).

2.6.3 Mathematical Models for accuracy assessment

Interpolation techniques play an important role in DEM accuracy assessment. The elevation of the DEM is extracted by using interpolation techniques. Common interpolation techniques are the nearest neighbor, bilinear interpolation, and cubic convolution. The nearest neighbor is suitable for categorical data like land use land classification data and others. Bilinear interpolation calculates the value of a pixel by using four surrounding pixels and this technique is suitable for continuous data. Bi-Cubic convolution uses 16 surrounding pixels to calculate the value of the unknown pixel and this technique is also suitable for continuous data if sink or peak is occurring in the data.

2.6.4 Functional quality for accuracy assessment

Maybe the perspective of data quality depends on the applications of the DEM. Drainage networks and watersheds are important for hydrological applications (Saffet Erdoğan, 2010). Slope and aspect are using different civil engineering applications. There are also other parameters to determine functional quality like visibility, the orientation of the data.

2.7 Bias correction

To reduce systematic and random errors, correcting biases is important. There are different approaches to reduce the error of global DEM. Some studies are tried to improve the accuracy of DEM data by fusion of different DEM (Manoj et al., 2008; Amin et al., 2014; Tian et al., 2018) and the obtained DEM data are precise. A different algorithm is also used to improve the accuracy of the DEM data like multi-look iteration for InSAR DEM (Gao et al., 2017). Others study like, (Kwanchai et al., 2016) use linear transformation to reduce the error produced in global DEM. A matrix that represents a linear transformation of the project plane is called a homogenous transformation matrix and when constant value is zero in x and y direction and different from zero in Z direction is called affine transformation. To reduce the residual of DEM data, bias correction is applied in affine transformation for this study, in the following equation (Kwanchai et al., 2016).

$$Z=f(x,y,w) \quad (2.10)$$

$$Z=a.x+b.y+c.w+z_o \quad (2.11)$$

where, Z is observation data, x and y are the coordinates of the estimation data and a,b,c,z_o are the transformation parameters. W is estimation value. The observation point is run first value until to n, therefore $z=z_1, z_2, z_3 \ldots z_n$, $x= x_1,x_2,x_3 \ldots x_n$ $y= y_1,y_2,y_3 \ldots y_n$ $z= z_1,z_2,z_3 \ldots z_n$ and $w= w_1,w_2,w_3 \ldots w_n$

$$Z_1=a.x_1+b.y_1+c.w_1+z_o \quad (2.11a)$$

$$Z_2=a.x_2+b.y_2+c.w_2+z_o \quad (2.11b)$$

$$Z_3=a.x_3+b.y_3+c.w_3+z_o \quad (2.11c)$$

…..

$$Z_n=a.x_n+b.y_n+c.w_n+z_o \quad (2.11d)$$

To sum up the equation of the first point until n, it is written in the following form

$$\sum_{i=1}^{n} z_i = \sum_{i=1}^{n}(a.x_i + b.y_i + c.w_i + z_o) \quad (2.12)$$

Write least square method based on the sum of square error

$$E = \sum_{i=1}^{n}(a.x_i + b.y_i + c.w_i + z_o - z_i)^2 \quad (2.13)$$

Minimize sum square error by ordinary least square methods (partial differentiation)

$\frac{\partial E}{\partial a}$ =0, $\frac{\partial E}{\partial b}$ =0, $\frac{\partial E}{\partial c}$ =0 and $\frac{\partial E}{\partial z_0}$ =0

$$\frac{\partial E}{\partial a} = (x_i)*[\sum_{i=1}^{n} a.x_i + b.yi + c.wi + Z_o - Z_i]=0 \quad (2.14a)$$

$$\frac{\partial E}{\partial b} = (y_i)*[\sum_{i=1}^{n} a.x_i + b.yi + c.wi + Z_o - Z_i]=0 \quad (2.14\ b)$$

$$\frac{\partial E}{\partial c} = (w_i)*[\sum_{i=1}^{n} a.x_i + b.yi + c.wi + Z_o - Z_i]=0 \quad (2.14\ c)$$

$$\frac{\partial E}{\partial z_o} = (1)*[\sum_{i=1}^{n} a.x_i + b.yi + c.wi + Z_o - Z_i]=0 \quad (2.14\ d)$$

And write in matrix form, AX=L (2.15)

$$A = \begin{bmatrix} \sum_{i=1}^{n} x_i . x_i & \sum_{i=1}^{n} x_i . y_i & \sum_{i=1}^{n} x_i . w_i & \sum_{i=1}^{n} x_i \\ \sum_{i=1}^{n} x_i . y_i & \sum_{i=1}^{n} y_i . y_i & \sum_{i=1}^{n} y_i . w_i & \sum_{i=1}^{n} y_i \\ \sum_{i=1}^{n} x_i . w_i & \sum_{i=1}^{n} y_i . w_i & \sum_{i=1}^{n} w_i . w_i & \sum_{i=1}^{n} w_i \\ \sum_{i=1}^{n} x_i & \sum_{i=1}^{n} y_i & \sum_{i=1}^{n} w_i & n \end{bmatrix} \quad L = \begin{bmatrix} \sum_{i=1}^{n} z_i . x_i \\ \sum_{i=1}^{n} z_i . y_i \\ \sum_{i=1}^{n} z_i . w_i \\ \sum_{i=1}^{n} z_i \end{bmatrix} \quad X = \begin{bmatrix} a \\ b \\ c \\ Z_o \end{bmatrix} \quad (2.15a)$$

The value of X is calculated in the following equation (CHharlesD Ghilani, 2010)

$$X=\left[\left(A^T * A\right)^{-1}(A^T * L)\right] \quad (2.16)$$

2.8 Accuracy standards

The National Map Accuracy Standards (NMAS) set accuracy standards based solely on the scale and contour interval of printed maps in 1947. And the National Standard for Spatial Data Accuracy (NSSDA, 1988) established a technique for assessing horizontal and vertical accuracy at 95 percent confidence levels, but no accuracy standards were set. It employs RMSE multipliers, which are based on the premise that all errors are distributed regularly. However, this technique is incorrect for LiDAR data in vegetated terrain (ASPRS, 2015).

The ASPRS accuracy standard for large scale maps (1990), the ASPRS guidelines, and vertical accuracy reporting for LiDAR data (2004) have all been replaced by the newly issued ASPRS 2015 positional accuracy standards for Digital Geospatial Data. This standard uses RMSE error for accuracy assessment for non-vegetated terrain in the NSSDA concept and it follows normal distribution at a 95% confidence level.

$$\text{Accuracy} = 1.96 * \text{RMSE} \qquad (2.17)$$

The standard recommends that the value of mean error be less than the value of RMSE by 25 %. A total number of static 3D checkpoints for elevation data 20 checkpoints is recommended for <500 km^2 area (ASPRS, 2015). The following (Table 2.1) describes recommended point number for accuracy check-in ASPRS 2015 (ASPRS, 2015).The National standard for spatial data (NSSDA) was formed by the Federal Geographic control subcommittee (FGCS) also uses root mean square (RMSE) at a 95 % confidence level. 95 % confidence level means data will have an error concerning the true ground position that is equal to or less than the reported accuracy value (FGDC, 1998). This standard also recommends a minimum of 20 checkpoints shall be tested in the area of interest. Ethiopia Geospatial Information Agency (EGIA), former Ethiopia Mapping Agency (EMA), Information Network Security Agency (INSA) and other regional states Urban Land development experts organized the Urban legal cadaster standard in 2015 for Ethiopia (FDRE Ministry of Urban Development, 2015). The standard recommends less than 30 cm RMSE error for horizontal and 45 cm error for vertical in aerial photography. Table 2.1 present the checkpoints of accuracy standards.

Table 2.1Recommended checkpoints in ASPRS accuracy standards

Project area (km^2)	Number of static vertical checkpoints
<500	20
501−750	20
751−1000	25
1001−1250	30
1251−1500	35
1501−1750	40
1751−2000	45
2001−2250	50
2251−2500	55

(Source: New ASPRS Positional Accuracy Standards for Digital Geospatial data 2015 (ASPRS, 2015) .

The area of interest increase, number of accuracy checkpoints are must be increased. Well distributed accurate checkpoint is important to reflect the accuracy of assessing data. NSSDA also recommends that the checkpoints data is independent of being tested data and well distributed across the project area.

Chapter Three

3. Materials and Methods

3.1 Study area

Dire Dawa city is the second-largest city next to Addis Ababa and is located in the eastern part of Ethiopia, it is surrounded by the Oromia region on the Northern, southern, western sides, and the Somalia region on the Eastern sides. The road distance from Addis Ababa to Dire Dawa is 515 km and 311 km from Djibouti (Abdi Ibrahim, 2018). The study area covers latitude of 9° 33′45″–9° 38′38″ N and longitude of 41°46′7″–41°53′57″ E, and with an elevation between 1087 and 1474 m based on the photogrammetric DEM data. It covers 94.75 km^2, which it includes in and around the city of Diredawa (Figure 3.1). The selected study area is based on ground control point data.

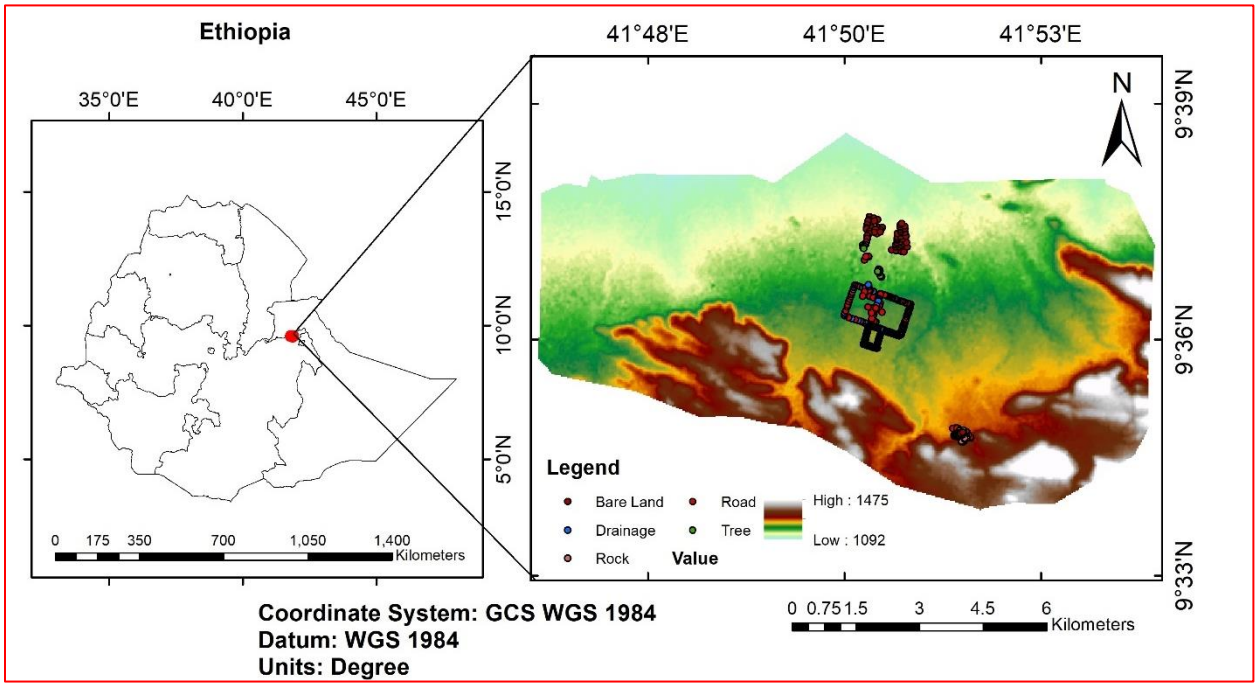

Figure 3.1 Location map of the study area

3.2 Used software's and Instruments

The following (Table 3.1) present used software's for this study and its specifications

Table 3.1 List of software's and its specifications

Software	Version	Production company	Function
ArcGIS	10.7.1	Environmental system research institute (ESRI)	✓ Extract elevation point data from DEM data ✓ To display output of DEM data ✓ Transform the horizontal datum from one to another and others
Microsoft office	2019	Microsoft	✓ To organize thesis document (Word) ✓ To compute statistical measurement (Excel)
MATLAB	R2016b	MathWorks	✓ To compute the geoid height of the EGM96 geoid model ✓ To compute linear transformation parameters for bias correction
Alltrans EGM2008 calculator	1.2	Hans-Gerd Duenck-Kerst	✓ To compute the geoid height of the EGM2008 geoid model

TRIMBLE R8GNSS/R6/5800 instrument

This instrument was used to collect the RTK coordinate points in the study area. According to the product specification (Trimble Engineering and construction group, 2003), the instrument is a dual-frequency GPS receiver. The position of the UHF (ultra-high frequency) radio antenna further increases the accuracy. High precision multiple correlators for L1 and L2 pseudo-range measurements and very low noise with L1 and L2 carrier phase measurements with <1mm. Additional supportive materials were also used during data collection (Tripod, radio antenna, car battery, Trimble controller TSC2, PDL radio link).

3.3 Data source and its description

3.3.1 Global DEM data

i. SRTM data

This is open access near-global DEM data which it downloads from (https://earthexplorer.usgs.gov/ website and is owned by NIMA later NGA and NASA, and also Italian and German space agencies have participated. SRTM was first launched in February 2000 (NGA and NASA, 2015). It uses two SAR images on both X and C-band components in single-interferometry. It covers the surface of the earth from 56ºS to 60ºN. Which means 80% of the earth's total landmass is covered in the data. According to the SRTMv3 user guideline (NGA and NASA, 2015), the earlier version of SRTM data (version-3) includes additional topographic data from ASTER-GDEM, GMTED2010, and NED data to fill the void in DEM data. Selected SRTM dem data for this study is version3, approximately 30m spatial resolution data. The referenced horizontal datum and vertical datum are the WGS84 and EGM96 geoid model. The mission objective accuracy of the SRTM is expected less than 16m at 90% confidence level (Farr et al., 2007), which is 19.1m accuracy at 95 % confidence interval. It was released in January/2015.

ii. ASTER-GDEM

ASTER G DEM is a global DEM and downloaded from https://search.earthdata.nasa.gov/search. It was produced by both the Minister of Economy, Trade, and Industry of Japan (METI) and NASA during 1999 from optical stereo data, but it has been freely available since 2009 (ASTER GDEM Validation Team, 2009) . The ASTER-GDEM v3 validation report describes the accuracy value of Z is 12.1m of standard deviation (Japan's Ministry of Economy, Trade, and Industry (METI) et al., 2019) and it covers 83ºN and 83ºS. It is packaged in 1ºx1º tiles and a totally 22, 912 tiles are included in version-3 GDEM. The selected DEM used for this study is version-3, 30 m spatial resolution DEM data. There are some improvements in version-3 rather than version-2, some of the bad lines and outliers are removed, 1.5 million cloud-free scene data is increased to 1.8 million, the river is separated from lakes and water body detection size is minimized from 1km^2 to 0.2 km^2 in version-3 and others significant improvements are applied (NASA et al., 2019). It was released in June/2019 (NASA et al., 2019). Referenced horizontal and vertical datum is WGS84 and EGM96 geoid model. Most of the time NASA provided DEM data like SRTM, ASTER-GDEM uses WGS84 and EGM96 for horizontal and vertical datum.

iii. ALOS-PALSAR

This is high-resolution global DEM data as compared with SRTM and ASTER. It was downloaded from the Alaska satellite facility website (https://search.asf.alaska.edu/) and produced by a collaboration of the Ministry of the Economy, Trade, and Industry (METI) and Japan Aerospace Exploration Agency (JAXA) (Japan Aerospace Exploration Agency, 2008). It is one of the remote sensing data from ALOS instruments and launched in January 2006 and data was collected until April 2011 (Cole et al., 2015). During data collection time solar illumination is not applied because it is an active system. Radiometric terrain correction was applied in the latest released ALOS-PALSAR data, it corrects radiometric and geometric distortion (Alaska satellite Facility, 2014). When in Radiometric terrain correction (RTC) time SRTM and NED DEM data were used and it easily presents in GeoTIFF format. GeoTIFF data format is compatible with different software like ArcGIS, QGIS, etc. Two DEM products are available in 12.5 m and 30 m spatial resolution and referenced in ellipsoidal height. Both 12.5m and 30m spatial resolution data were used for this study. ALOS-PALSAR is presented in WGS84 for horizontal datum and ellipsoidal height (WGS84) for vertical datum.

3.3.2 Reference data

i. Ground Control point (GCP) data

The reference ground control point data is used to validate the selected open access DEM data. The data was produced and adjusted by EMA (Ethiopia Mapping Agency) later Ethiopia Geospatial Information Institute (EGIA. The horizontal and vertical datum is Adindan and EGM96. Which is highly accurate and used as reference data for cadastral surveys in Dire Dawa land management. Totally 121 GCP data has been used in this study and it was acquired from Diredawa land administration and management bureau.

ii. Photogrammetric DEM

The photogrammetric DEM was acquired from Ethiopia Geospatial Information Agency (EGIA) and it was produced in 2016. It is referenced by Adindan and EGM96 for horizontal and vertical datum. It was prepared from 15x15 cm spatial resolution aerial photographs. The elevation of the building, trees, and other features were removed and edited manually using photogrammetric techniques. During preparation time interior orientation, exterior orientation, and movement of

the platform were considered. In this study end product photogrammetric DEM 10x10m, spatial resolution data was used. The accuracy of this data is checked by GCP data.

iii. **RTK-GPS (Real-Time kinematic)**

RTK-GPS point data was collected using TRIMBLE R8 GNSS/R6/5800 instrument to assess land use land cover accuracy assessment. It is more described in the next section.

The following (Table 3.2) shows a summarized description for reference and assessing DEM data.

Table 3.2 Sources of the data and its description

Data name	Source	Data types	Spatial Resolution	Datum H.	Datum V.
GCP data	Dire Dawa Land Administration and Management	Point data	-	Adindan	EGM96
RTK data	Primary sources	Point data	-	WGS84 ellipsoid	Ellipsoidal height (WGS84)
Photogram metric DEM	Ethiopia Geospatial Information Agency (EGIA)	Raster data	10x10m	Adindan	EGM96
SRTMv3	(https://earthexplorer.usgs.gov/)	Raster data	1 arc-second ~30x30m	WGS84 ellipsoid	EGM96
ASTER_GDEM	(https://search.earthdata.nasa.gov/search)	Raster data	1 arc-second ~30x30m	WGS84 ellipsoid	EGM96
ALOS-PALSAR	(https://search.asf.alaska.edu/)	Raster data	Both 12.5m and 30m	WGS84 ellipsoid	Ellipsoidal height (WGS84)

3.4 Data Processing, methods, and Analysis

3.4.1 Transforming different horizontal datum to the same datum

Fortunately, the horizontal datum of global DEMs data is the same, however GCP and photogrammetric DEM data were referenced by Adindan (Clarke 1880 ellipsoid) horizontal datum and it is transformed to WGS84 datum using Ethiopia Geospatial Information Agency (EGIA) transformation parameters (FDRE Ministry of Urban Development, 2015), X=-162 m, Y=-12 m and Z=+206 m; the rotation (Rx, Ry, Rz) and the scale factor is to be considered 0. ArcGIS 10.7.1 was used to apply this transformation by using the 'Create custom Geographic transformation' tool and the 'Project Raster' tool was used to transform the data in the above-given parameters.

3.4.2 Extracting point elevation data from DEM data

To assess the accuracy of global DEM data; extracted point elevation data is important. ArcGIS is used to extract the elevation point data from the global DEM data by using the 'Extract multi values to points' tool and exported to Microsoft Excel to compute statistical measurement.

3.4.3 Transforming different vertical datum to the same datum

The vertical datum of SRTM and ASTER-GDEM is referenced by the EGM96 geoid model which means it extracts orthometric height value from the DEM data while ALOS-PALSAR both 12.5 m and 30 m spatial resolution was referenced by ellipsoidal height in vertical datum. The reference vertical datum for the ground control point (GCP) is also the EGM96 geoid model. Therefore, to assess the open-access global DEM data accuracy, the reference for vertical datum must have coincided with each other. Referenced vertical datum applied for this study is EGM2008; SRTM and ASTER-GDEM data vertical datum (EGM96) was transformed to EGM2008 geoid model, and ALOS-PALSAR DEM product (12.5 m and 30 m) ellipsoidal height is also converted to EGM2008 geoid model to get the same orthometric height. Vertical datum for Ground control point (GCP) and photogrammetric DEM data was also transformed to the EGM2008 geoid model, the procedure is the same as an SRTM and ASTER-GDEM. To transform the EGM96 to the EGM2008 the following procedures were used.

i. Compute EGM96 geoid height by using MATLAB software. MATLAB R2016b software requires only latitude and longitude data as an input and gives geoid height for input point data by using the 'geoidheight' inbuilt function. The EGM96 geoid

model has 15' grid spacing (Sandip et al., 2013) and degree and order extend up to 360 only (Pavlis et al., 2012).

ii. Add EGM96 geoid height and orthometric height to get the ellipsoidal height (WGS84)

iii. Compute EGM2008 geoid height by using the Alltrans EGM2008 calculator and subtract geoid height from ellipsoidal height to obtain orthometric height referenced by EGM2008. The internal database for the Alltrans EGM2008 calculator is 10' grid space data but the external database is downloaded from the NGA website in 1' grid spacing.

3.4.4 Checking the reference control point data and DEM data accuracy

Ensuring the accuracy of the reference data is important. Reference data should be three times more accurate than the assessing value. The accurate GCP data that was obtained from Dire Dawa land administration and management bureau, which is collected by Ethiopia Geospatial Information Agency expert in 2013, and is second-order GCP data. And accuracy of the photogrammetric DEM data is checked by GCP data using statistical measurement (root mean square error).

3.4.5 RTK GPS data

Totally, four hundred ninety-one (491) RTK GPS point data were collected from different land covers in the study area (Road line, Bare land, Rock area, trees, Drainage pattern). And it is listed in abbreviation; Road line (RD), Drainage pattern (DR), Bare Land (BL), Rock area (RC), and tree (TR). 211 sample data were collected from road lines, 99 from drainage patterns, 58 from rock areas, 58 from trees, and 65 from bare land. For accuracy check purposes, one GCP point data is measured in RTK data (GCP data, X=811506.729 m, Y=1063681.614 m, and Z=1160.5046 m and RTK-GPS data are, X=811506.708 m, Y=1063681.591 m, and Z=1160.5353 m). The deviation shows that δx = 2.1 cm, δy = 2.3 cm, and δz = 3.1 cm, they show the cm accuracy level, which is good accuracy for accuracy assessment. TRIMBLE R8 GNSS/R6/5800 dual-frequency and supportive instruments were used for the data collection (Figure 3.2), during data collection satellite geometry position PDOP (position dilution of precision) and GDOP (Geometric Dilution of precision) is to be considered. Data is collected for

five consecutive days (August 10-14/2021 G.C). The duration time for data collection is 30-45 sec. for each point. Which

Figure 3.2 Connecting radio link with base and rover receiver

3.4.6 Vertical accuracy assessment (using point-wise measurement)

i. Accuracy assessment using statistical analysis (in original resolution raster data)

The vertical accuracy of all global DEMs data was calculated, which are minimum error, maximum error, mean error, standard deviation, and root mean square error (RMSE). The elevation error value is positive means; the elevation value is exceeded the reference point data; while the elevation error is negative means; the elevation value is under the reference point data. Statistical measurement was computed between global DEM and GCP, RTK, and photogrammetric DEM (the mathematical part is more described in the literature review part).

ii. Accuracy assessment using statistical analysis (in equal pixel size)

To match the pixel size, resampling was applied using the 'Resample' tool in ArcGIS. ALOS-PALSAR 12.5 m resolution and photogrammetric DEM 10m resolution data are down sampled to 30m spatial resolution. Resample is used to calculate a new pixel value by using the existing

original pixel value (Baboo et al., 2010). There are four resampling techniques in ArcGIS software; nearest neighbor, bilinear interpolation, cubic convolution, and majority. The nearest neighbor is the fastest and suitable for the discrete data; it uses four nearest pixels to calculate new pixels. When the majority algorithm is also used for discrete data like land use classification and determines the new value of the cell based on the most popular values in the filter window. Bilinear interpolation technique is determining the new pixel value by using a weighted distance average of the nearest four pixels and used for the continuous data. Whereas cubic convolution determines the new pixel by using 16 nearest original pixels. This technique is less distorted as compared with the neighbor resampling technique but their drawback is, it requires more time for processing. Cubic convolution technique was used for this study for both PALSAR DEM and photogrammetric DEM data.

iii. Accuracy assessment using scatter plot diagram and histogram of the elevation errors

To visualize the error of global DEM, scatter plot and histogram elevation error diagram was plotted between the global DEM and GCP data and RTK-GPS. The value that fits the line is precise data and away from the line is considered a high error value. This technique is used to easily identify the error by visualization. A Scatter plot is used to identify the correlation of reference DEM data and assess DEM data. The following equation shows how to calculate the correlation coefficient of both data.

$$R^2 = \left(\frac{n(\sum Z_{ref}Z_{DEM}) - \sum Z_{ref} \sum Z_{DEM}}{\sqrt{[n\sum {Z_{ref}}^2 - (\sum Z_{ref})^2][n\sum {Z_{DEM}}^2 - (\sum Z_{DEM})^2]}}\right)^2 \quad (3.1)$$

where n is a total number of observation points, Z_{ref} is the reference point elevation data, Z_{DEM} is the elevation data of global DEM data, R^2 is the correlation coefficient value.

iv. Accuracy assessment by using different land use and land cover

Totally, 491 RTK-GPS data were collected from five different land cover areas; Road line, bare land, drainage patterns, sparse trees, and rock area data. Among the collected points were 211 from the road lines, 99 from the drainage pattern, 58 rock areas, 58 sparse tree area, and 65 from bare lands. Statistical analysis was applied between global DEM and land use land cover point data.

3.4.7 Vertical accuracy assessment (using pixel-based measurement)

i. Accuracy assessment by using photogrammetric DEM data

Random points data are extracted from the photogrammetric DEM data and global DEM data. Then statistical measurement was computed by using those random extracted points using the 'create random points' tool in ArcGIS 10.7.1 software. ALOS-PALSAR 12.5 m spatial resolution and Photogrammetric DEM is down sampled to 30m when we using extraction. 10,000 random sample points are extracted from photogrammetric DEM and global DEM data. Then statistical measurement was computed between photogrammetric DEM and global DEM data. And, DEM data was produced for those extracted random points data using Topo to Raster interpolation. Topo to Raster interpolation is based on the ANUDEM algorithm developed by 1998. This interpolation technique is specifically designed to create correct DEM data for hydrological purposes and it uses an iterative finite-difference interpolation technique for interpolation. This method is the best interpolation method for the elevation, which produces a high surface with fewer input data. |The deviation map of reference photogrammetric DEM data and global DEM was created to visualize the difference between the reference DEM and global DEM data.

ii. Accuracy assessment by using profile graph

To identify the accuracy of the global DEM data in terrain classification, the terrain is segmented into three classes, which it is flat, moderate, and steep slopes. And which the accuracy of classified terrain is assessed by photogrammetric DEM data. 500 random point is extracted from both global DEM slope data and photogrammetric DEM slope data to assess the accuracy of the data.

3.5 Bias correction

The quality of the DEM data depends on the accuracy of the data. Large shifts in global DEM data may be due to inaccurate GCP data used by DEM production companies (Manoj et al., 2008). Bias correction was applied for four global DEM data. The linear transformation approach was used to correct the bias of DEM data by using shift the DEM, using MATLAB 2016b software, which is used to compute the parameters of linear transformation. Script of MATLAB code is attached in appendix part. The least-square method was used to calculate the

linear transformation parameters using the inverse matrix technique. The following equation shows the bias correction approach (it is more described in the Literature review part).

$$Z=a.x+b.y+c.w+z_o \quad (3.2)$$

where a, b, c and Zo are parameters of a linear transformation, x and y are estimated coordinates, w is estimation data

The value of linear transformation parameter value is solved by using matrix

$$AX=L \quad (3.3)$$

The following chart shows (Figure 3.3) the whole methodology of the study.

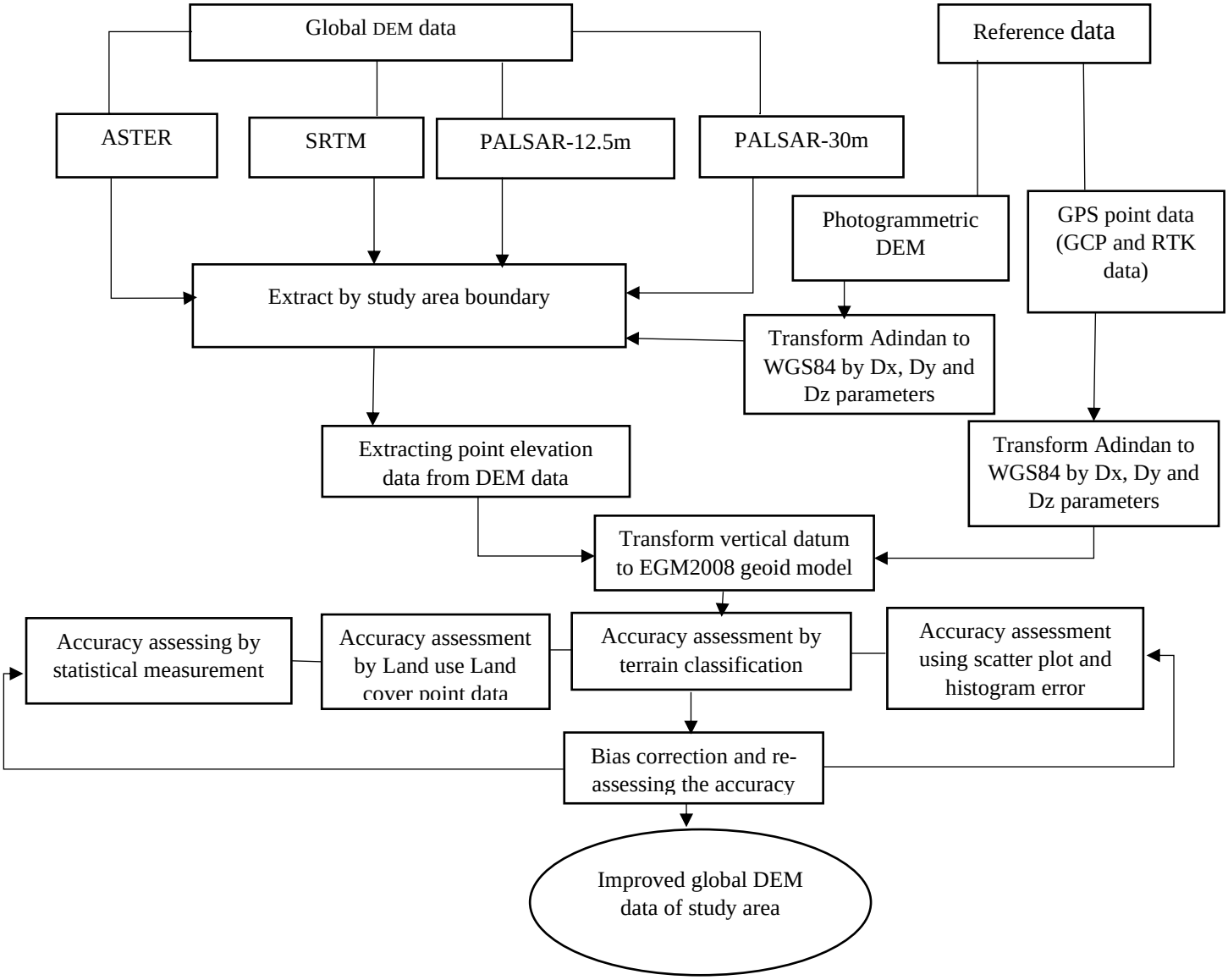

Figure 3.3 The flow charts of the methodology

Chapter Four

4. Results and Discussion

4.1 Reference data

4.1.1 GCP (Ground control point) data

The vertical datum is transformed to the EGM2008 latest geoid model. The deviation between EGM96 and EGM2008 is expected 0.5-1.0 m (Ismail Elkhrachy, 2018), the average difference between EGM1996 and EGM2008 is 15 cm in the study area. Totally, 121 (Ground Control Point) GCP was used for this study. The following table shows the sample value of transferring EGM96 to EGM2008. The whole GCP data which transformed to EGM2008 (Table 4.1) and all data transformation is attached in the appendix part.

Table 4.1 Transforming vertical datum GCP data EGM96 geoid model to EGM2008

Lat (^{O})	Long (^{O})	Orth.Height (EGM96) (m)	EGM96 (m)	EGM2008 (m)	Ellipsoidalh (m)	diff (EGM96-08) (m)	OrthoH(08) (m)
9.633663	41.779626	1102.887	−13.032	−12.878	1089.855	−0.1543	1102.733
9.63401	41.805571	1101.505	−13.055	−12.906	1088.450	−0.1494	1101.356
9.633104	41.815666	1112.143	−13.063	−12.915	1099.080	−0.1479	1111.995
9.632844	41.88893	1111.371	−13.132	−12.96	1098.240	−0.1715	1111.200
9.622816	41.897571	1148.497	−13.127	−12.948	1135.370	−0.1791	1148.318
9.623464	41.889471	1139.365	−13.120	−12.948	1126.246	−0.1715	1139.194
9.62478	41.870099	1143.307	−13.102	−12.944	1130.205	−0.1577	1143.149
9.632868	41.870546	1171.876	−13.114	−12.954	1158.762	−0.1596	1171.716
9.632733	41.85096	1115.976	−13.095	−12.943	1102.881	−0.1517	1115.824

Legend: Lat and Long are Latitude and longitude of the GCP point data, ortho.Height(EGM96) is orthometric height which referenced by the EGM96 geoid model, EGM96 is geoid height which is computed for given latitude and longitude in the EGM96 geoid model, diff (EGM96-08) is the deviation between EGM96 and EGM2008, OrthoH(08) is the orthometric height which referenced by EGM2008 geoid model.

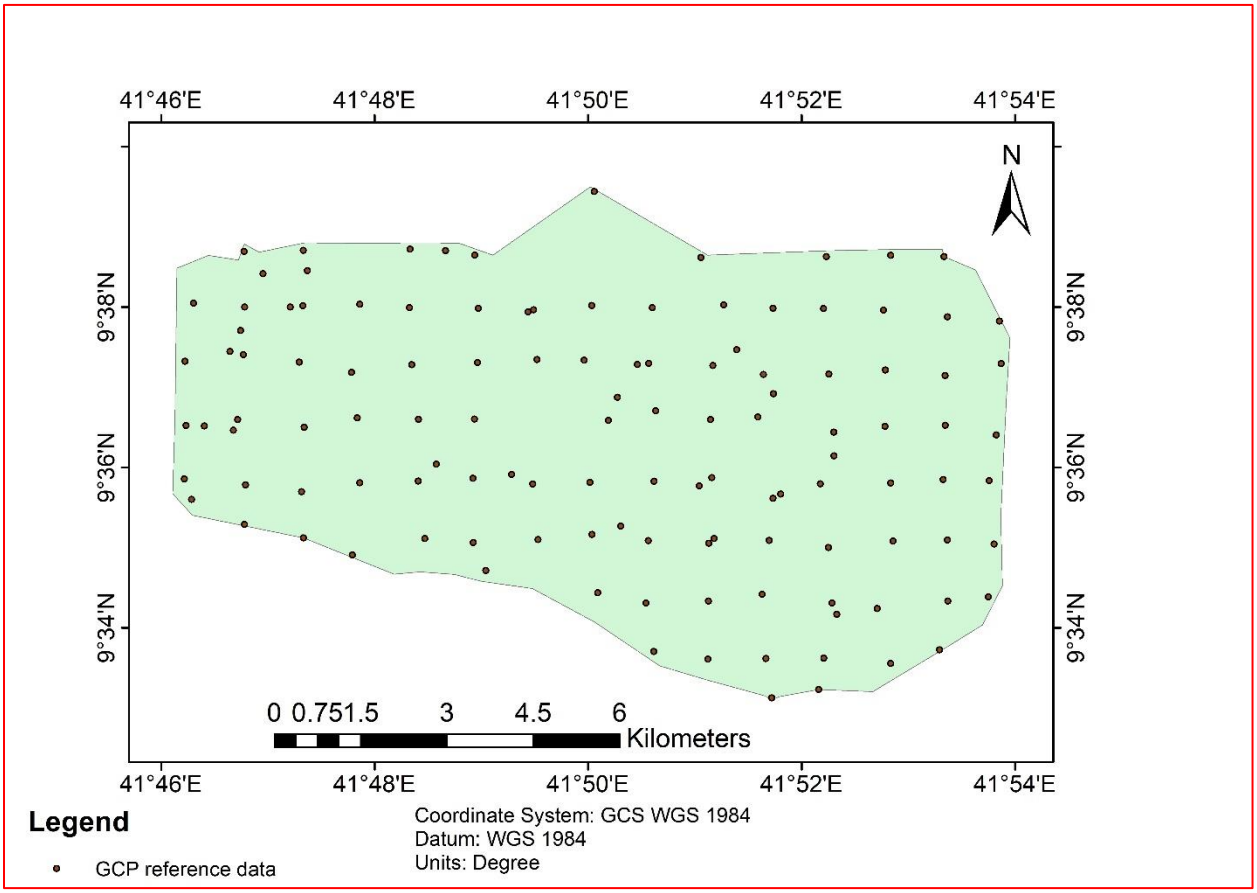

Figure 4.1 GCP reference data in the study area

4.1.2 RTK GPS data

RTK-GPS data is collected from different land use and land covers (Bare lands (BL), rock areas (RC), drainage patterns (DR), trees (TR), and road lines (RL)). Total four hundred ninety-one (491) point data was collected from those land use and land covers. The deviation between GCP and RTK GPS data (2~3 cm) error is ignored. The following (Table 4.2) and (Figure 4.2) shows the sample data for the collected data.

Table 4.2 RTK GPS Sample data which collected from the study area

Easting (m)	Northing (m)	Elevation (m)	Desc_
813877.213	1060289.359	1234.843	RD
813874.073	1060270.935	1235.42	RD
813858.712	1060232.773	1242.453	RD
813857.896	1060232.264	1242.749	RC
813929.438	1060242.415	1235.303	RD
813945.922	1060224.706	1235.554	DR
813945.153	1060223.100	1236.244	RC
813555.698	1060410.098	1227.501	RD
813648.487	1060409.077	1229.226	RD
813731.702	1060361.246	1230.737	RD
813727.489	1060359.437	1230.905	RD
813739.389	1060354.754	1231.909	TR
813723.063	1060365.717	1230.872	TR
813722.662	1060273.241	1231.944	BL
813741.368	1060288.487	1232.548	BL

X, Y are the coordinates of the data; Z is elevation data which is referenced in EGM2008 vertical datum, RD is point data which is collected from road places, RC is rock area, DR =drainage pattern, TR =trees, and BL = Bare Land.

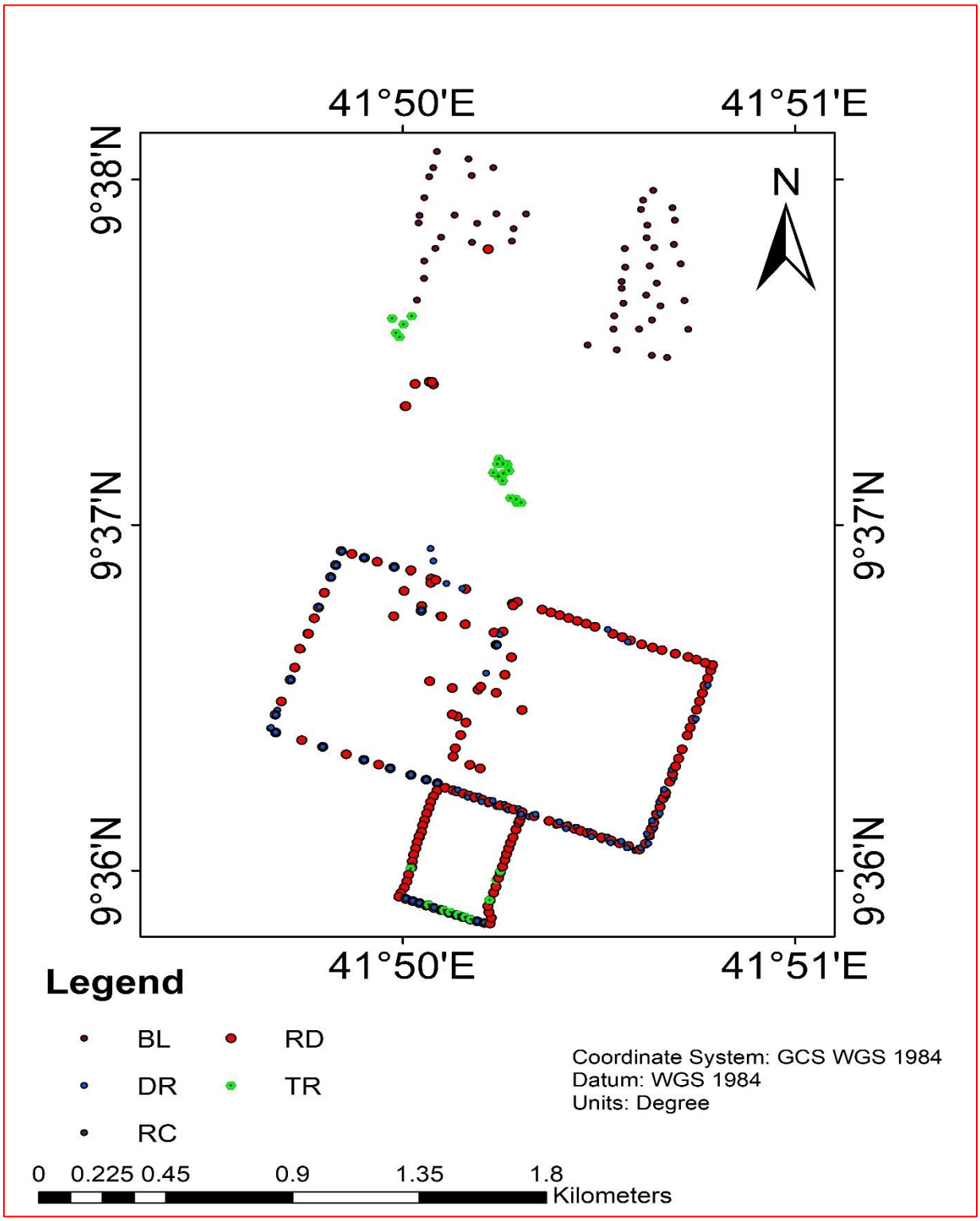

Figure 4.2 RTK GNSS reference point data of BL-bare land, RD-road line, DR-drainage pattern, TR-tree, and RC- rock area

4.1.3 Photogrammetric DEM data

Table 4.3 Statistical analysis for the photogrammetric DEM using GCP reference data

Statistical measured value	In 10 m spatial resolution	In 30 m spatial resolution
Mean error	−0.31	−0.50
Standard Deviation	1.34	1.52
RMSE	1.37	1.59
LE at 90%	2.25	2.62
LE at 95%	2.69	3.12

Accuracy assessment between GCP data and photogrammetric DEM was applied to check the deviation of the photogrammetric DEM from the GCP data in both 10 m and 30 m spatial resolution (Table 4.3). There is not high difference value between the two spatial resolutions, the RMSE difference is only 0.22 m and the mean difference is 0.193 m in both 10 m and 30 m spatial resolution data. The following (Figure 4.3) present the elevation of study area in photogrammetric data.

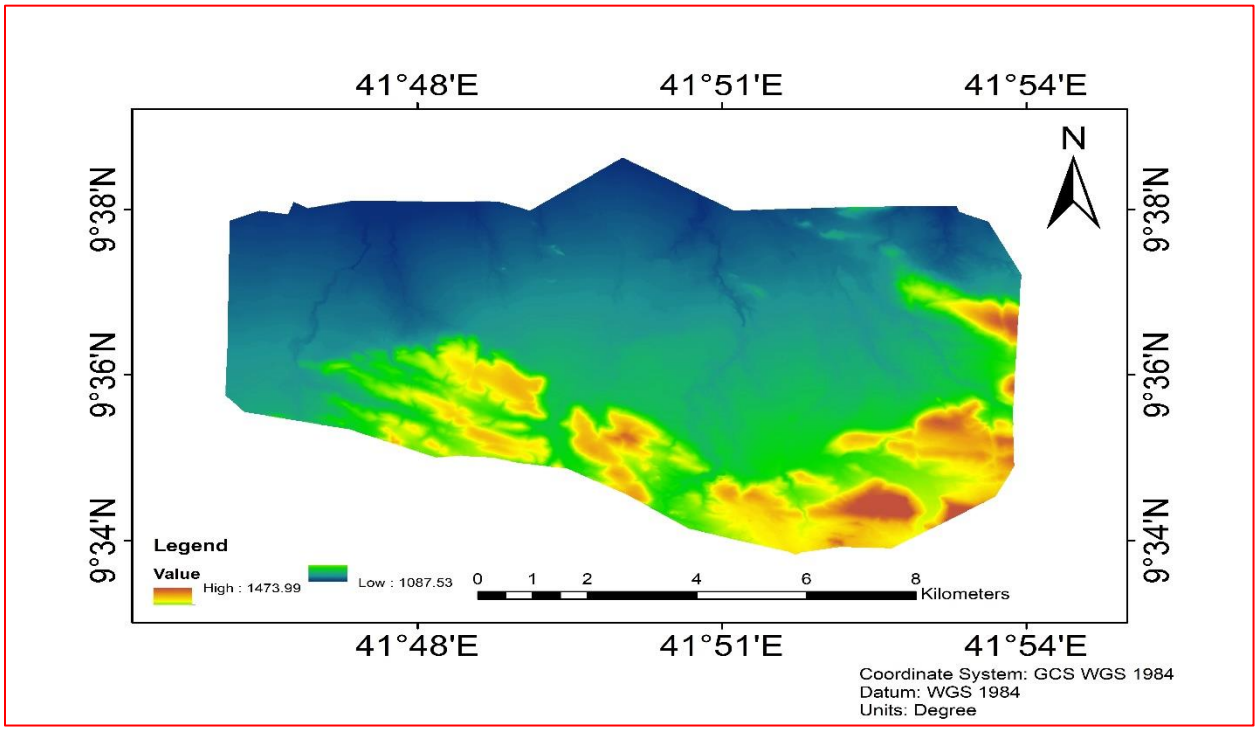

Figure 4.3 Photogrammetric DEM

4.2 Vertical Accuracy assessment (using point measurement)

4.2.1 Statistical measurement for four global DEM

Statistical analysis was applied for four global DEM data in original point-grid size. The (Table 4.4) shows the statistical measurement for four global DEMs by using GCP reference data and the second one (Table 45) shows the statistical measurement for global DEM using RTK GPS reference data.

Table 4.4 Statistical analysis for four global DEM using GCP data reference

DEM	Min. error (m)	Max. error (m)	ME (m)	STDEV (m)	RMSE (m)	LE (m) at 90%	LE (m) at 95%
SRTM	−19.13	7.28	0.76	3.62	3.68	6.06	7.22
ASTER_GDEM	−42.76	9.20	−5.19	7.22	8.87	14.58	17.38
PALSAR1	−16.63	10.23	0.04	4.60	4.58	7.53	8.97
PALSAR2	−22.23	15.02	×0.44	5.60	5.58	9.18	10.94

Table 4.5 Statistical analysis for four global DEM using RTK GPS reference data

DEM	Min. error (m)	Max. error (m)	ME (m)	STDEV (m)	RMSE (m)	LE (m) at 90%	LE (m) at 95%
SRTM	−23.03	9.99	2.10	3.93	4.45	7.32	8.72
ASTER-GDEM	−26.35	5.29	−5.21	5.30	7.43	12.22	14.56
PALSAR1	−23.54	8.75	0.93	4.59	4.68	7.70	9.17
PALSAR2	−24.38	7.45	0.36	5.35	5.36	8.81	10.50

Min. error =minimum error, Max. error = Maximum error, ME =mean error, STDEV = standard deviation, RMSE = root mean square error, LE at 90 % = Linear error at 90 % confidence interval and LE at 95 % = Linear error at 95 % confidence interval, PALSAR1 is 12.5 m spatial resolution ALOS-PALSAR DEM, PALSAR2 is 30 m spatial resolution ALOS-PALSAR DEM.

The value of RMSE for the SRTM is 3.68m in GCP reference data and the value in RTK-GPS reference data is 4.45m which increases by 0.77 m. The value of RMSE for ASTER DEM is 8.87 m and 7. 43 m in GCP and RTK GPS reference data reference, which decreases by 1.79 m in RTK-GPS reference data and it is the lowest accuracy value among the selected global DEM. Whereas, the RMSE value of the PALSAR1 is 4.58 m and 4.68 m in GCP and RTK-GPS

reference, and in 30m spatial resolution the RMSE value of PALSAR DEM is 5.58m and 5.36m in GCP and RTK-GPS reference data. The RMSE difference of PALSAR1 DEM data in both GCP and RTK-GPS data is 0.10 m and for PALSAR2 the difference is 0.22. Both tables showed that the accuracy of SRTM is high and the accuracy of ASTER-GDEM is low among the selected DEM data.

4.2.2 Statistical measurement for four global DEM in equal pixel size

The spatial resolution of SRTM, ASTER-GDEM, and ALOS PALSAR 30 m are approximately equal while the second ALOS-PALSAR DEM has 12.5 m spatial resolution. To match the pixel size of ALOS-PALSAR12.5 m DEM, it is down sampled to 30 m in (Table 4.6).

Table 4.6 Statistical measurement for resampled ALOS-PALSAR DEM in GCP and RTK reference data

DEM	Min. error (m)	Max. error (m)	ME (m)	STDEV (m)	RMSE (m)	LE at 90% (m)	LE at 95% (m)
PALSAR(G)	-17.830	10.338	-0.0005	4.715	4.696	7.724	9.204
PALSAR(R)	-23.691	8.505	0.915	4.615	4.478	7.366	8.777

PALSAR(G): statistical analysis was computed using GCP reference data.

PALSAR(R): statistical analysis computed using RTK GPS reference data.

There is not too difference between original pixel size DEM data and resampled DEM data; the RMSE for original pixel size is 4.58 m and the resampled DEM data is 4.70 m, the difference in two values is only 0.12 m in GCP reference data. And in RTK-GPS reference data the difference is 0.68 m.

4.2.3 Accuracy assessment using scatter plot diagram and histogram errors

Quantile-quantile (Q-Q) plot is used for visual examination and scatter plot (Kwanchai et al., 2016).

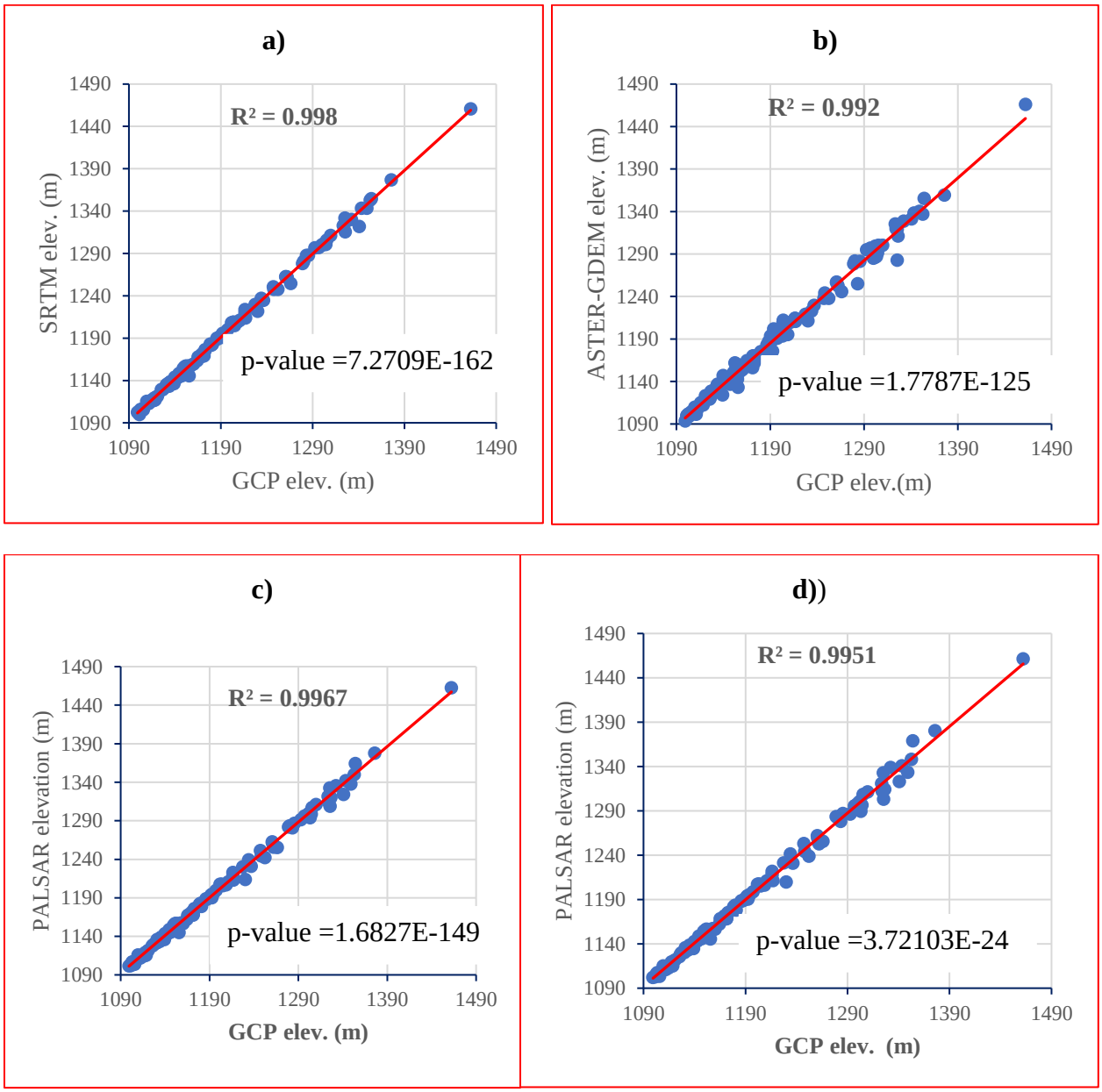

Figure 4.4 Scatter plots of GCP elevation data and a) SRTM DEM b) ASTER-GDEM c) ALOS-PALSAR (12.5 m) D) ALOS-PALSAR (30 m) DEM elevation data

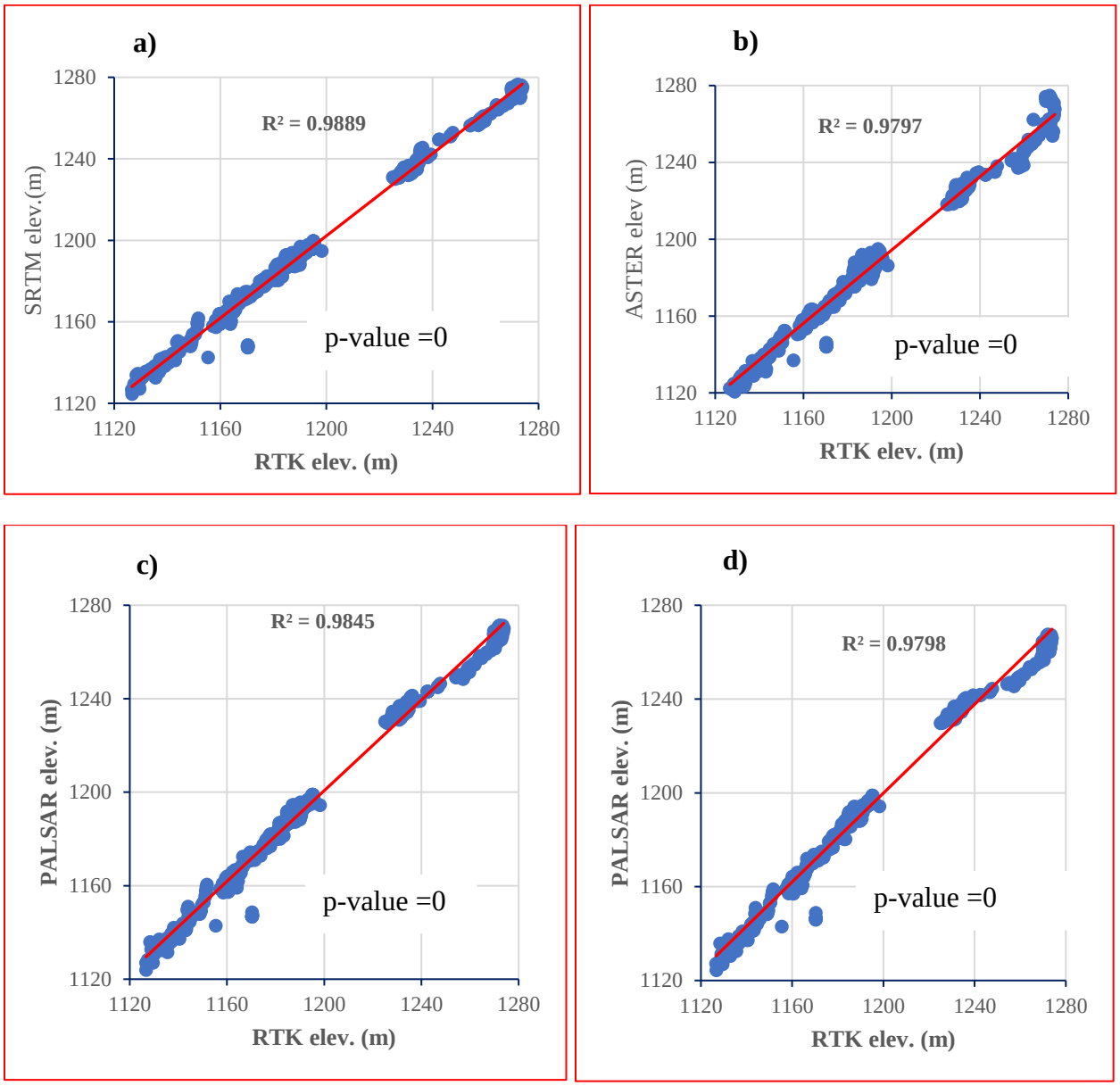

Figure 4.5 Scatter plots of RTK elevation data and a) SRTM DEM b) ASTER-GDEM c) ALOS-PALSAR (12.5m) D) ALOS-PALSAR (30m) DEM elevation data

Perfect fit the red lines indicate a strong correlation between two data. The correlation coefficient value is displayed for each global DEM data and reference data (GCP or RTK GPS) in the above (Figure 4.4). All global DEM data correlation coefficient values are good, which they show greater than 0.9. The value of correlation varies between 0 and 1, 0 indicates no relationship between two values and 1 indicates strong relations between two values. Among the DEM data, in (Figure 4.4) the SRTM DEM value has a strong correlation and greatest of all (0.998 and

0.989 in both GCP and RTK GPS reference data (Figure 4.4 and Figure 4.5). However, ASTER-GDEM is less correlation coefficient value among the selected global DEM data value, it is 0.992 and 0.980 for GCP and RTK GPS reference data. The computed value of the p-value is closed to zero in GCP reference data (Figure 4.4 and it is zero in RTK-GPS reference data (Figure 4.5). if the value of the p-value is less than 0.05, it is statistically significant correlation. Unless the value is not statistically significant correlation. The value of p-value in all global DEM shows less than 0.05, therefore it can conclude that data is statistically significant correlation.

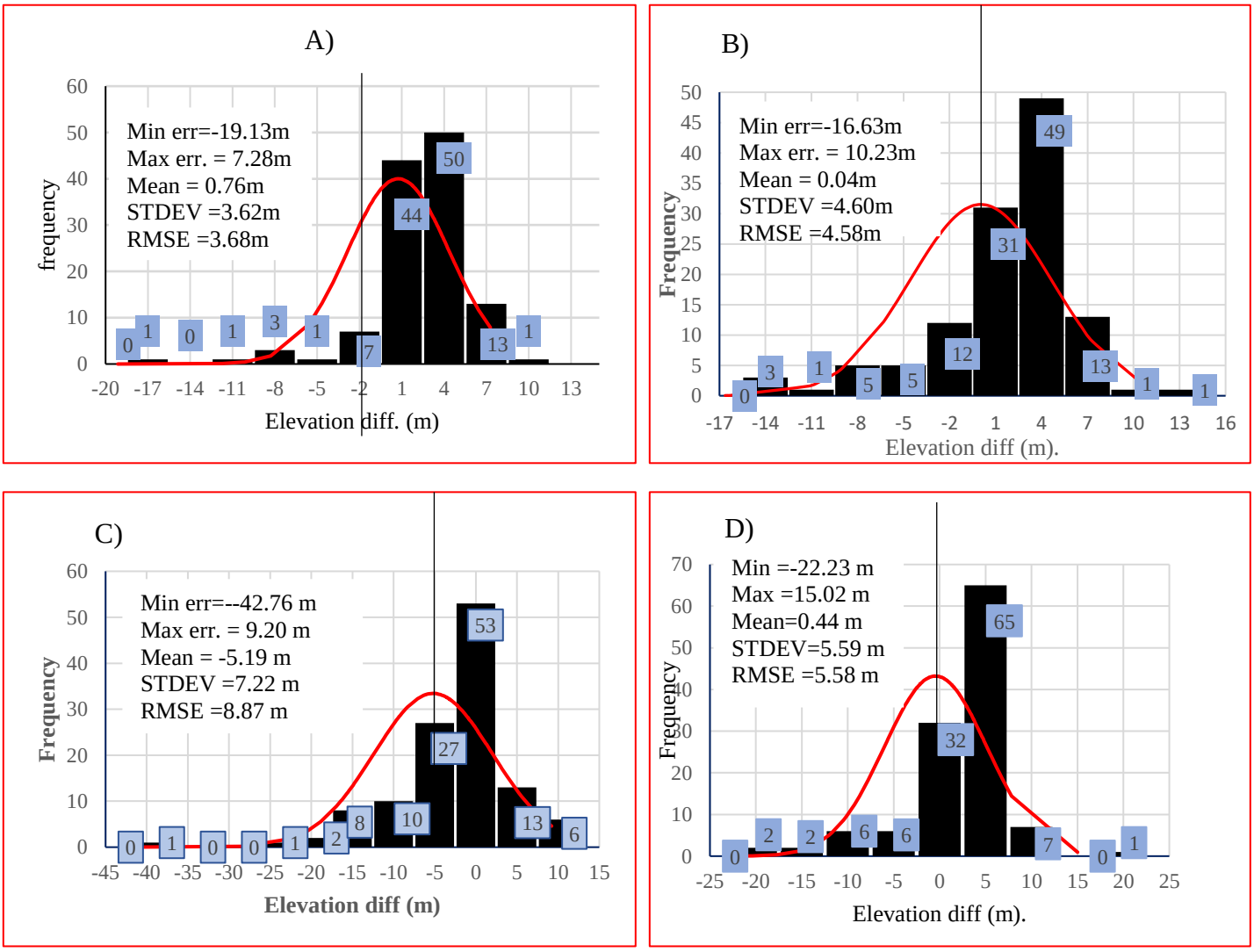

Figure 4.6 Histograms with normality curve between GCP and a) SRTM-DEM b) ALOS-PALSAR (12.5 m) c) ASTER-GDEM d) ALOS-PALSAR (30 m)

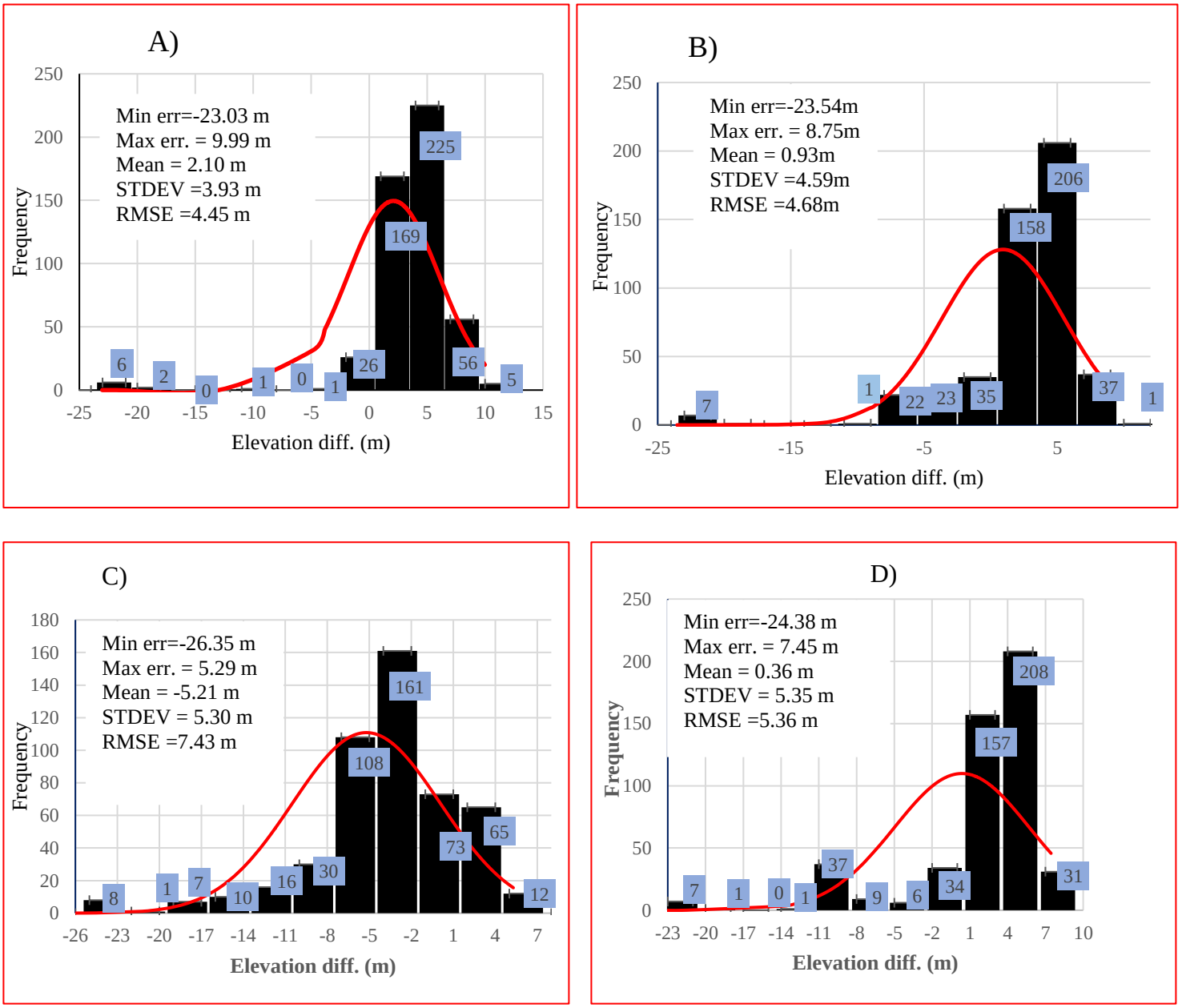

Figure 4.7 Histograms with normality curve between RTK-GPS and **a**) SRTM-DEM **b**) ALOS-PALSAR (12.5 m) **c**) ASTER-GDEM **d**) ALOS-PALSAR (30 m)

Histograms errors show frequencies in the elevation error; it is used to visual impression, in GCP reference data (Figure 4.6) the highest accumulated error value for SRTM is between 2.5 m and 5.5 m, which means the highest amount of elevation error data is stored between 2.5 m and 5.5 m. For ASTER-GDEM the highest frequency value is between -2.5m and 2.5m, for ALOS-PALSAR (12.5m) the value is between 2.5 m and 5.5 m, and for ALOS-PALSAR (30 m) the

value is between 2.5 and 7.5. whereas, for RTK GPS reference data and the global DEM value (Figure 4.7) the highest error frequencies in SRTM is stored between 2.5 and 7.5 m, for ASTER-GDEM the value is between -4.5 and -1.5 m, for ALOS-PALSAR (12.5 m) the highest value is between 2.5 m and 7.5 m, and for PALSAR2 the highest error value is accumulated between 4 m and 6 m, respectively.

4.2.4 Accuracy assessment by using different land use and land cover

Statistical measurement was computed for each land use land cover data using RTK-GPS reference data. The sample data was collected from five different land use and land cover areas (road alignment (RD), trees (TR), drainage pattern (DR), rock area (RC), and bare land (BL)). And the following (Table 4.7) present the statistical measurement for land use land cover point data

Table 4.7 Statistical measurement of different land use and land covers between RTK-GPS and global DEM data, unit is (m)

DEM	LULC type	Min err.	Max err.	Mean err.	STDEV	RMSE	LE at 90%	LE at 95%
SRTM	RD	−23.03	8.38	1.74	5.30	5.56	9.15	10.90
	DR	−1.49	9.32	3.00	2.07	3.64	5.99	7.13
	BL	−3.09	6.64	1.76	2.35	2.92	4.81	5.73
	RC	−3.25	9.24	1.33	2.54	2.85	4.69	5.59
	TR	−3.46	9.99	3.03	2.45	3.88	6.39	7.61
ASTER	RD	−26.35	3.83	−4.22	5.39	6.84	11.24	13.40
	DR	−8.41	5.29	−2.56	3.42	4.26	7.00	8.35
	BL	−12.06	−0.22	−6.22	2.29	6.62	10.89	12.97
	RC	−21.25	4.27	−11.60	6.21	10.05	16.54	19.70
	TR	−11.96	1.09	−5.82	3.37	6.71	11.03	13.15
PALSAR1 (12.5m)	RD	−23.54	6.96	1.19	5.30	5.42	8.91	10.62
	DR	−2.03	7.46	2.75	2.04	3.42	5.63	6.71
	BL	−4.10	7.54	1.42	2.57	2.92	4.80	5.72
	RC	−8.89	5.05	−5.32	2.95	6.07	9.98	11.89
	TR	−3.77	8.75	2.57	2.33	5.73	9.43	11.23
PALSAR2 (30m)	RD	−24.38	6.85	1.05	5.38	5.47	9.00	10.72
	DR	−2.63	7.05	2.68	2.00	3.34	5.49	6.54
	BL	−3.39	7.45	1.31	2.43	2.74	4.51	5.38
	RC	−13.74	4.28	−9.11	3.70	9.82	16.15	19.25
	TR	−4.04	7.17	2.33	2.18	3.18	5.23	6.23

Legend: RD =road data, DR =drainage pattern, BL = Bare land data, RC =rock area and TR =sparse tree area, LULC is land use land cover type

Min err. =Mean error, Min err. = minimum error, Max err. = maximum error, STDEV =standard deviation and RMSE =root mean square error, PALSAR1 is 12.5m spatial resolution PALSAR DEM and PALSAR2 is 30m spatial resolution PALSAR DEM

The RMSE of road line data in SRTM DEM occurs with high error and less error occurred in rock area data. While the ASTER-GDEM data showed a higher error in the rock area and low error in drainage patterns. In PALSAR1 the accuracy is high in bare land area and low in rock area. And the PALSAR1 DEM data showed high accuracy in bare land area and low accuracy in rock area. Yet again, the PALSAR2 data also shows less accuracy in rock area and high accuracy in bare land area. All the results indicate that most global DEM shows averagely high accuracy in bare land area and less accuracy in rock area except SRTM DEM data.

4.2.5 Accuracy Assessment in classified elevation data

To identify the frequency of elevation error, elevation data is classified into three classes; low elevation, medium elevation, and high elevation data. The following (Table 4.8) is describing the elevation classes and their RMSE value.

Table 4.8 Statistical measurement for classified elevation data

DEM	Elevation class (m)	Classes	RMSE (m)	Sample point
SRTM	1099-1150	Low elevation	2.64	41
	1151-1210	Medium elevation	3.22	39
	1211-1463	High elevation	4.82	41
ASTER-GEM	1099-1150	Low elevation	4.76	41
	1151-1210	Medium elevation	7.80	39
	1211-1463	High elevation	12.30	41
ALOS-PALSAR1	1099-1150	Low elevation	2.66	41
	1151-1210	Medium elevation	3.09	39
	1211-1463	High elevation	6.76	41
ALOS-PALSAR2	1099-1150	Low elevation	2.53	41
	1151-1210	Medium elevation	2.94	39
	1211-1463	High elevation	8.79	41

All of the elevation class values have the lowest RMSE value in the low elevation class and the highest RMSE value in the high elevation class, the value of RMSE for SRTM, ALOS-

PALSAR1, and ALOS-PALSAR2 are closest to each other in the low elevation class but the deviation is increasing from medium class to high elevation class. ASTER-GDEM elevation value shows low accuracy both in low and high slope elevation classes. Among the slope values, the accuracy of ALOS-PALSAR (30m) is the winner in the low elevation class and the accuracy of SRTM DEM is better in the high elevation class. Generally, the accuracy of the elevation class is better for three global DEMs (SRTM, PALSAR1, and PALSAR2) in the low class and less accuracy for ASTER-GDEM and PALSAR2 in the high elevation class (Figure 4.8).

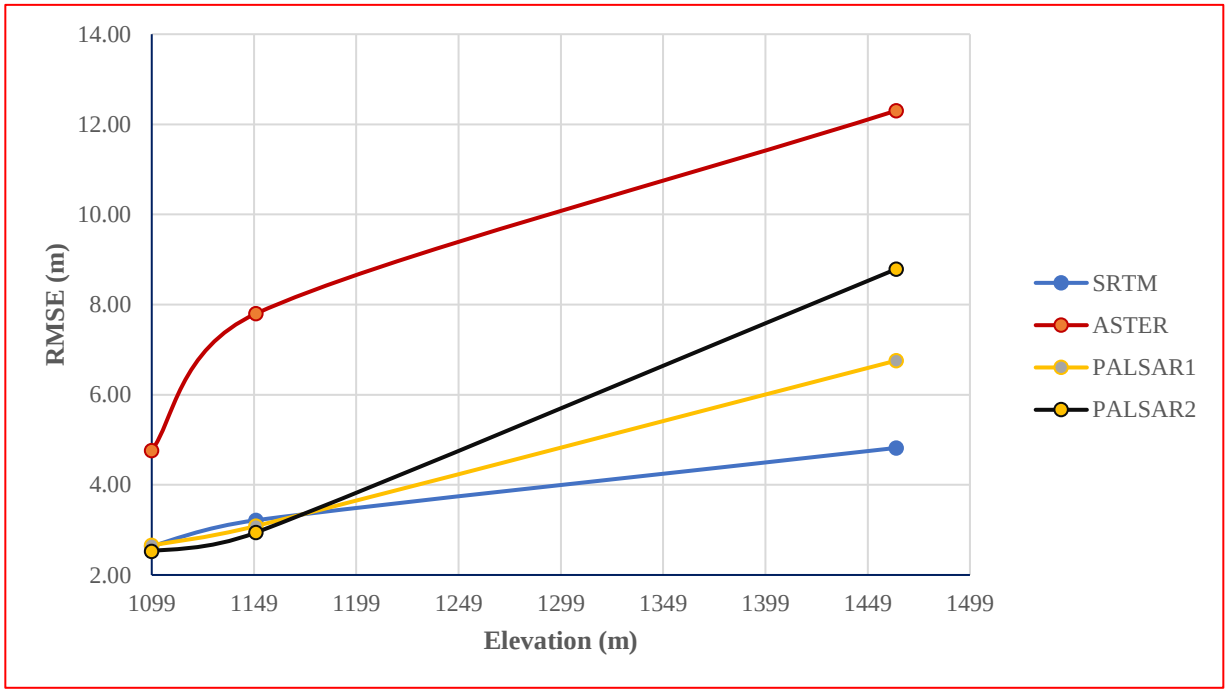

Figure 4.8 RMSE value for classified elevation data using GCP reference data

Table 4.9 Statistical measurement for classified elevation data (RTK-GPS reference data)

DEM	Elevation class (m)	Classes	RMSE (m)	Sample point
SRTM	1099−1150	Low elevation	2.57	67
	1151−1210	Medium elevation	5.02	307
	1211−1463	High elevation	3.65	117
ASTER-GDEM	1099−1150	Low elevation	6.02	67
	1151−1210	Medium elevation	6.13	307
	1211−1463	High elevation	10.61	117

ALOS-PALSAR1	1099−1150	Low elevation	2.35	67
	1151−1210	Medium elevation	4.94	307
	1211−1463	High elevation	4.96	117
ALOS-PALSAR2	1099−1150	Low elevation	2.20	67
	1151−1210	Medium elevation	4.95	307
	1211−1463	High elevation	7.31	117

The vertical error of three global DEM data (SRTM, PALSAR1, and PALSAR2) is closest to each other in the low elevation class and ASTER-GDEM data have a high error in both low elevation area and high elevation area (Table 4.9). The value of SRTM data shows better accuracy in the high elevation class and ASTER-GDEM shows less accuracy in the high elevation class. Generally, the accuracy of Low elevation classes showed better accuracy and the high elevation class is showed less accuracy (in RTK-GPS reference data).

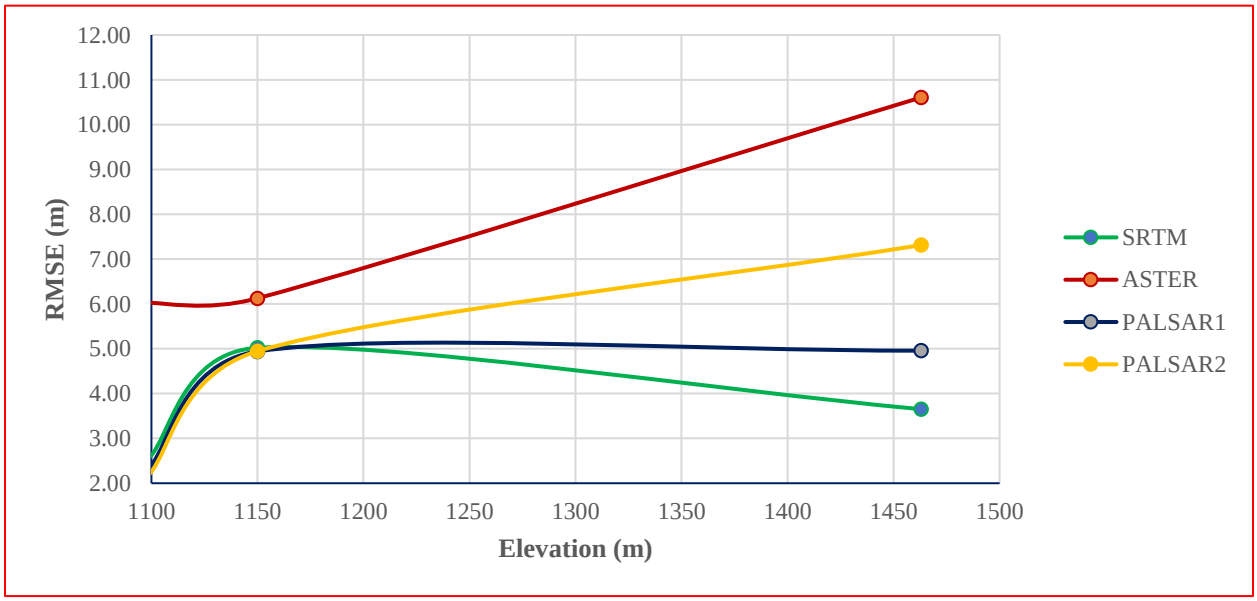

Figure 4.9 RMSE value for classified elevation data using RTK-GPS reference data

4.3 Vertical accuracy assessment using pixel-based

4.3.1 Accuracy assessment using photogrammetric DEM data

Photogrammetric DEM was used for reference data, and random points are created from both reference data and global DEM data. Then the statistical measurement is computed for selected random points in (Table 4.10). B65oth Reference data and ALOS-PALSAR 12.5m were down-

sampled to 30 m. 10,000 sample random points are extracted from both reference and global DEM data.

Table 4.10 Random point data statistics measurement by using photogrammetric DEM reference (m)

DEM	Min err.	Max err	STDEV	RMSE	LE at 90%	LE at 95%
SRTM	−14.62	39.59	2.74	3.41	5.61	6.68
ASTER	−58.60	28.18	5.87	7.05	11.59	13.81
PALSAR1	−25.64	42.30	4.36	4.58	7.53	8.98
PALSAR2	−35.50	43.19	5.22	5.34	8.78	10.46

The value of RMSE between global DEM and photogrammetric DEM results is approximately the same RMSE result with GCP reference data. For SRTM-DEM the difference is 0.21 m, for ASTER-GDEM the difference is 1.82 m, for PALSAR 12.5m-DEM the difference is 0.003 and for PALSAR 30 m the difference is 0.243 m respectively. The accuracy of the SRTM value is high and the ASTER-GDEM is low in the above table.

Based on random point data, DEM is created based on topo to raster interpolation technique then a deviation map is produced to visualize the difference of all global DEM from the reference data in equal pixel size (Figure 4.10). A raster calculator is used to show the difference of the global data from the reference.

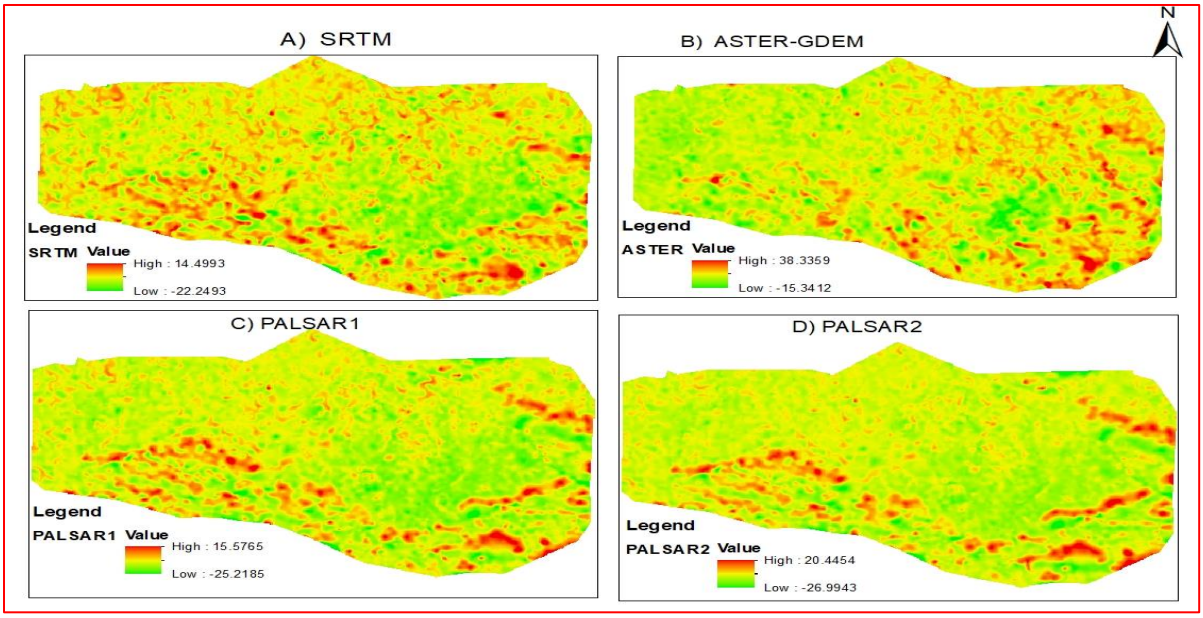

Figure 4.10 : Deviation map of photogrammetric DEM and A) SRTM B) ASTER-GDEM c) ALOS-PALSAR (1) D) ALOS-PALSAR (2)

The deviation map of global DEM and photogrammetric DEM reference was plotted, the maximum value in deviation map among four global DEM is ASTER GDEM data, which is 38.336m and the smallest minimum value in deviation map is PALSAR2, -26.99m. The minimum and maximum values for SRTM are 14.49m and -22.49m, for ASTER-GDEM it is -15.34m and 38.3359m, for PALSAR1 the value is -25. 22m and 15.58m and for PALSAR2 is -26.99 and 20.45m respectively. (Table 4.10) is also showing the statistical measurement of the global DEM data using photogrammetric DEM reference data; RMSE of the global DEM SRTM, ASTER-GDEM, PALSAR1 and PALSAR2 is 3.41m, 7.05m, 4.58m and 5.34m. The RMSE value of SRTM showed high accuracy and ASTER-GDEM showed less accuracy. Statistical measurements of the data are approximately the same result as GCP reference data statistical measurements.

4.3.2 Accuracy assessment using profile graph

Photogrammetric DEM data and Global DEM data profile graph was plotted, which it contains from low elevation up to high elevation areas.

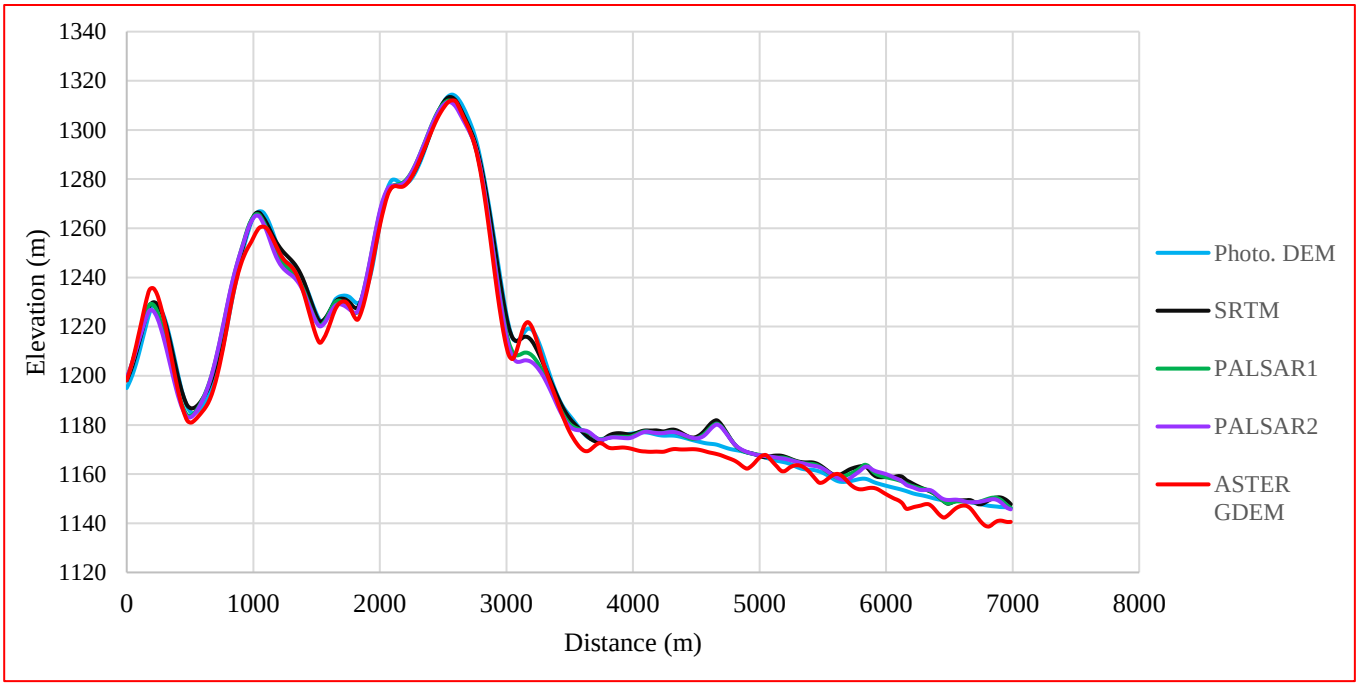

Figure 4.11 Profile graph of Photogrammetric DEM and global DEM

Legend: PALSAR1 =ALOS-PALSAR 12.5m spatial resolution and PALSAR2 is for 30m spatial resolution.

The above (Figure 4.11) shows the profile graph of reference data (photogrammetric DEM) and global DEM data. The graph shows the line of 7000m distance. which the line is randomly created in ArcGIS and the above figure is displayed profile graph for the created line. The graph indicates that the ASTER-GDEM profile graph has some deviation from the reference line (photogrammetric DEM) and other Global DEM. The rest of the profile graphs are closer to the photogrammetric DEM; in high elevation data there are no more deviation between photogrammetric DEM and global DEM, it is closer to each other but ASTER-GDEM is increasing the deviation in low elevation areas. ALOS-PALSAR-2 (30m spatial resolution) DEM data and ALOS-PALSAR (12.5m spatial resolution) is closer to each other in both high and low elevation area. Therefore, based on graph visualization the ASTER GDEM is less accurate as compared with other global DEM based on photogrammetric DEM reference profile line.

4.3.3 Accuracy assessment using slope classes

In this study, the slope is classified into 3 classes which are flat, moderate, and steep slope; resampled photogrammetric DEM slope data was used as a reference for assessing the slope map of the global DEM data. Slope data extracted from the photogrammetric DEM slope map and global DEM slope map is used to compute the RMSE of the data. To compute the statistical measurement 500 sample point is extracted from both global DEM slope data and photogrammetric DEM slope data.

Table 4.11 Statistical measurement for classified slope data

DEM	Slope class	RMSE (Degree)	Sample point
SRTM	0−1.5	0.80	189
	1.5-5	0.81	158
	>5	1.36	153
ASTER-GDEM	0−1.5	2.38	189
	1.5−5	3.53	158
	>5	12.26	153
ALOS-PALSAR1	0−1.5	0.74	189
	1.5−5	1.19	158
	>5	2.32	153
ALOS-PALSAR2	0−1.5	1.36	189
	1.5−5	2.67	158
	>5	11.79	153

The (Table 4.11) result shows the lowest RMSE value in a flat area and the highest RMSE value in a steep slope, the value of RMSE for SRTM, ALOS-PALSAR1, and ALOS-PALSAR2 are closest to each other in low slope value (flat area) but the deviation is increasing from moderate slope value to steep slope (high slope value). ASTER-GDEM slope value shows low accuracy both in low and high slope values. Among the slope values, the accuracy of ALOS-PALSAR (30m) is the winner in the flat areas and the accuracy of SRTM DEM is better in the high slope (steep-slope) area. Generally, the accuracy of the slope value is better for three global DEMs (SRTM, PALSAR1, and PALSAR2) in low slope value (flat area) and less accuracy for ASTER-GDEM and PALSAR2 in high slope value (steep slope area). The (Figure 4.12) describe the accuracy of terrain classification for four global DEM.

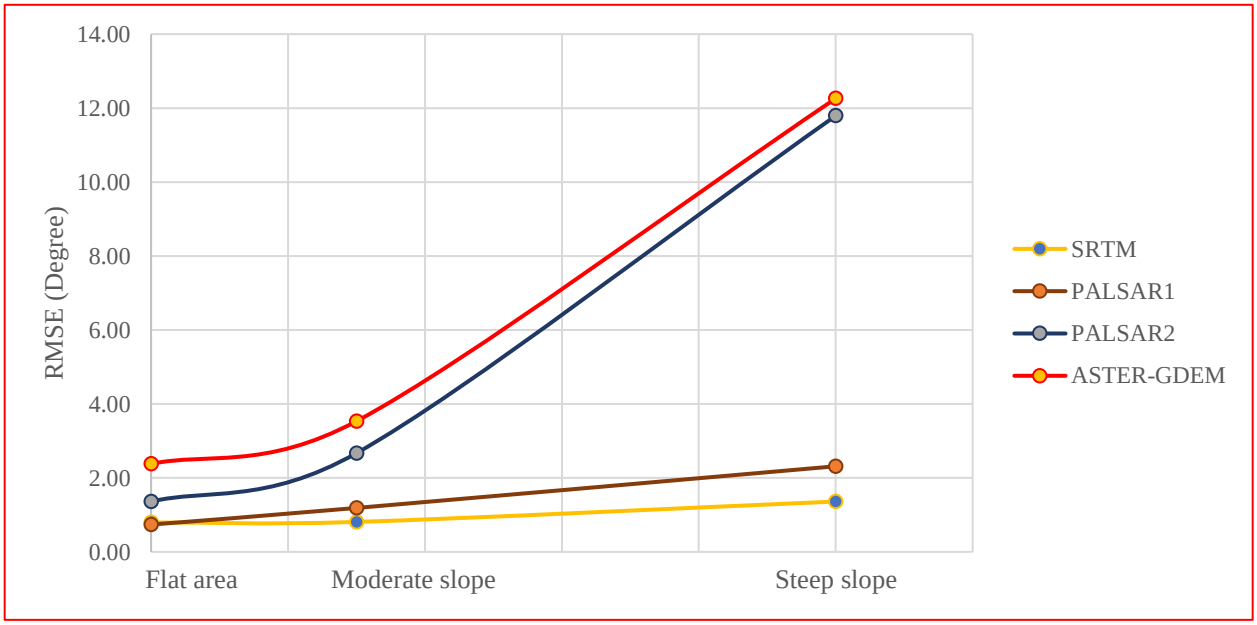

Figure 4.12 Slope classification of global DEM data in photogrammetric DEM reference data

4.4 Bias correction

The linear transformation method was applied in this study to eliminate the deviation between the reference data and global DEM data. Linear transformation parameters (a, b, c, and Z_o) are calculated and shown in the following (Table 4.12).

Table 4.12 Linear transformation parameters for bias correction in different DEM based on multiple linear regression

DEM data	a	b	c	Zo
SRTM	-6.62580E-05	2.42646E-04	1.01976	-228.6473
ASTER	4.49022E-04	3.08526E-05	1.01144	-405.5846
PALSAR1	5.48676E-05	4.21960E-04	1.02442	-522.3854
PALSAR2	8.51139E-05	-4.04306E-04	1.00716	352.5807

a,b,c and Zo are parameters of the linear transformation

The parameter of SRTM value is negative while three DEMs value is positive, *b* parameter is negative in PALSAR2 DEM data and positive value in rest of DEM data. The parameter of Z_o is also negative in PALSAR2 DEM data and positive in three DEMs data. And the parameter of *c* value is close to each other. Statical measurement is recalculated after the bias correction. The following (Table 4.13) shows the statistical measurement of DEM data before and after bias correction.

Table 4.13 Statistical measurement value of DEM value before and after bias correction (in GCP reference data)

	SRTM (m)		ASTER (m)		PALSAR1 (m)		PALSAR2 (m)	
	Before	After	Before	After	Before	After	Before	After
Min err	−19.13	−6.98	−42.76	−34.40	−16.63	−16.05	−22.23	−20.22
Max err	7.28	17.70	9.2	15.07	10.23	12.59	15.02	18.75
Mean err	0.76	1.50E−04	−5.19	−9.15E-04	0.04	7.08E−04	−0.44	9.20E−02
STDEV	3.62	3.45	7.22	6.87	4.6	4.37	5.61	5.41
RMSE	3.68	3.44	8.87	6.84	4.58	4.35	5.58	5.46
LE at 90%	6.06	5.65	14.58	11.25	7.53	7.15	9.18	8.82
LE at 95%	7.22	6.73	17.38	13.40	8.97	8.52	10.94	10.51

Legend: Min err =Minimum error, Max err =Maximum error, Mean err = Mean error, STDEV =standard deviation, RMSE =root mean square, LE =linear error at 90 % and 95 %

The table results show the statistical measurement of DEM data before and after bias correction. The compared value of RMSE after bias correction for SRTM DEM is improved by 6.7 %, while the accuracy of the ASTER-GDEM is improved by 22.9 % and the accuracy of PALSAR1 and PALSAR2 DEM are improved by 5.1 % and 2.2 %, respectively.

The statistical measurement of four global DEM and RTK-GPS reference data are also computed after bias correction (Table 4.14), and the accuracy of SRTM-DEM is improved by 7.3%, whereas the ASTER-GDEM has improved accuracy by 30.7 %, and PALSAR1 and PALSAR2 data have improved the accuracy by 2.3 % and 1 %. The modified DEM data mean error is close to zero. Both table results indicate (Table 4.13 and Table 4.14), that the accuracy of the global DEM data is improved after correcting the bias for all the DEM data.

Table 4.14 Statistical measurement value for improved global DEM (in RTK-GPS reference data)

	SRTM (m)		ASTER (m)		PALSAR1 (m)		PALSAR2 (m)	
	Before	After	Before	After	Before	After	Before	After
Min err	−23.03	−24.50	−26.35	−21.60	−23.54	−24.25	−24.38	−24.87
Max err	9.99	8.66	5.29	11.40	8.75	8.18	7.45	7.75
Mean err	2.10	1.04	-5.21	0.28	0.93	0.58	0.36	1.01
STDEV	3.93	4.00	5.30	5.15	4.59	4.53	5.35	5.23
RMSE	4.45	4.13	7.43	5.15	4.68	4.57	5.36	5.32
LE at 90%	7.33	6.79	12.22	8.47	7.69	7.51	8.81	8.75
LE at 95%	8.73	8.09	14.56	10.10	9.16	8.95	10.50	10.43

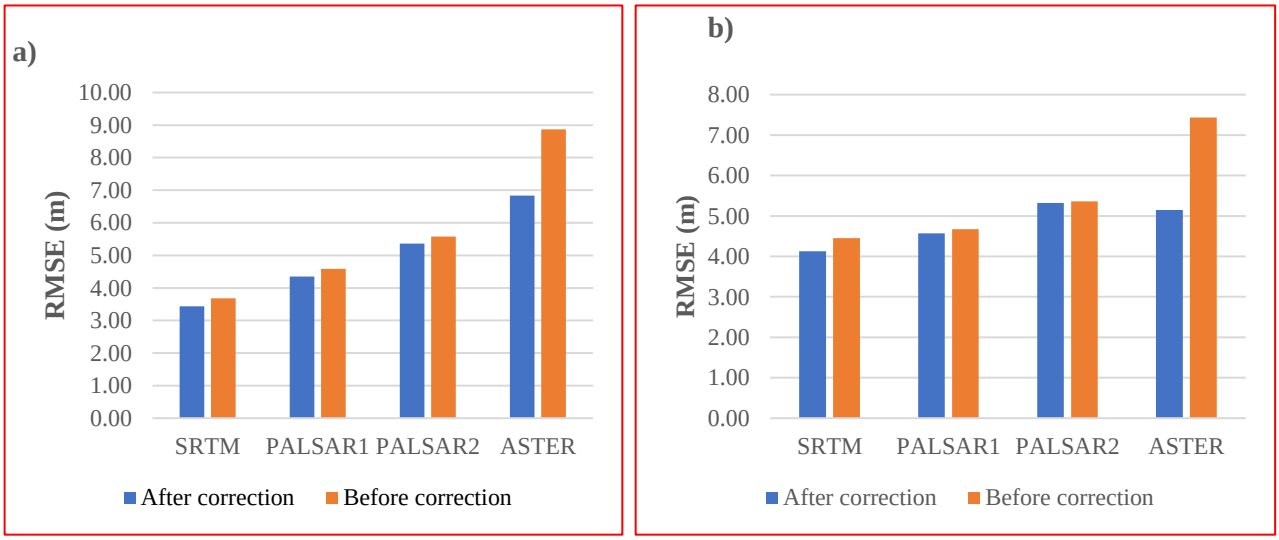

Figure 4.13 RMSE value before and after bias correction a) GCP reference and b) RTK-GPS reference

The chart (Figure 4.13) describes the RMSE value of global DEM data before and after bias correction, the accuracy of ASTER DEM was highly improved after bias correction. While the accuracy of PALSAR1 and PALSAR2 were less improved after bias correction.

Additionally, land use land cover data cover statistical measurement was recalculated after bias correction, the SRTM-DEM has improved the accuracy by 13.6 %, 22.4 %, 7.2 %, 2.7 %, and 19.5 % for bare land, drainage pattern, rock area, road line, and tree areas. While the ASTER_GDEM accuracy improved by 61.7 %, 22.1 %, 17.9 %, and 57.8 % for bare land (BL), rock area (RC), road pattern (RD), and trees; however, drainage pattern did not improve accuracy. ALOS-PALSAR1 improved the accuracy by 3.1%, 8.4%, 4.6%, and 43.9% for bare land (BL), drainage pattern (DR), and trees. Road line accuracy has not changed the accuracy in PALSAR1 DEM. PALSAR2 has increased the accuracy only by 20.4% for rock area.

The results of all data indicate that the accuracy of the global DEM after bias correction was improved. The accuracy ASTER-GDEM and SRTM-DEM were highly improved after bias correction. And the accuracy of PALSAR1 and PALSAR2 was less improved after bias correction.

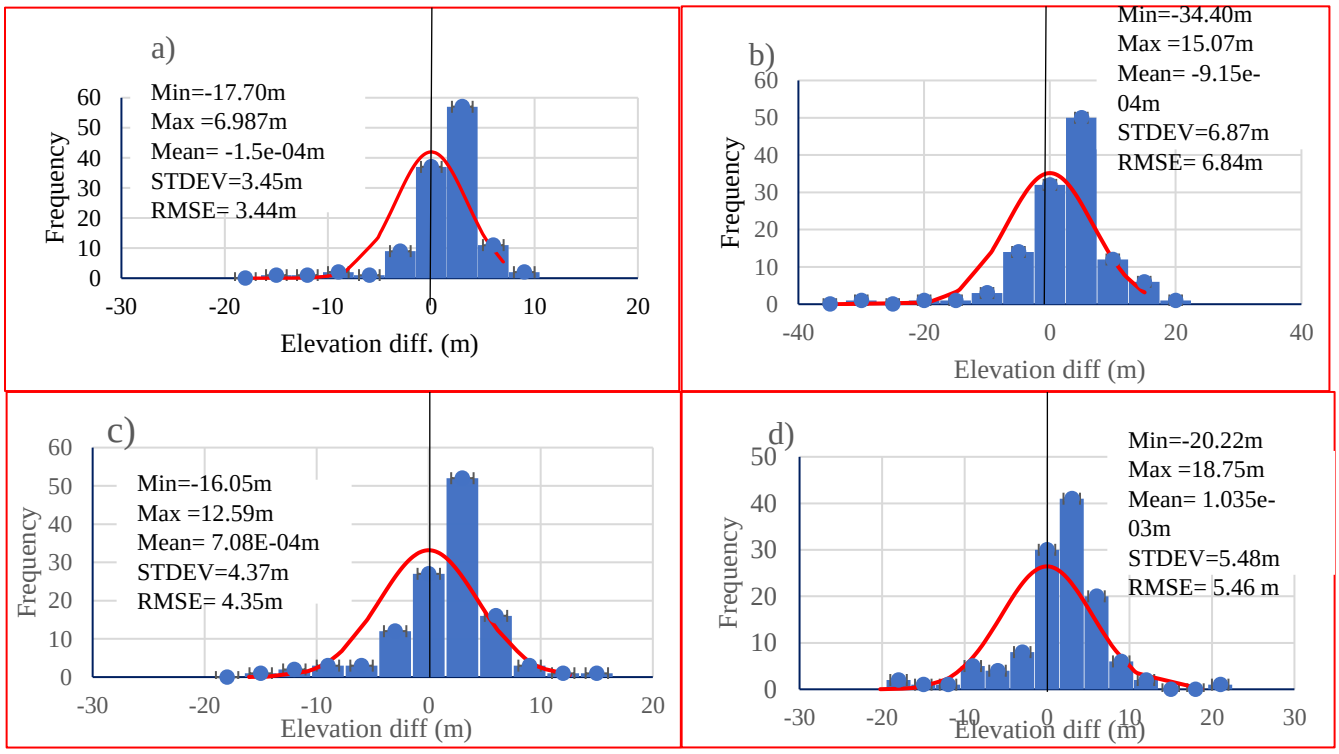

Figure 4.14 Histograms of elevation errors and normal distribution curve after bias correction in GCP reference data

The (Figure 4.14) present the histogram of modified DEM elevation error, the mean value of elevation error after bias correction is close to zero. RMSE value for ASTER-GDEM, SRTM, PALSAR1, and PALSAR2 data is decreased highly after bias correction, which shows the improvement of accuracy in DEM data after bias correction.

4.5 Discussion

The accuracy of SRTM, ASTER, ALOS-PALSAR1, and ALOS-PALSAR2 were assessed using Ground Control Point (GCP), RTK-GPS, and photogrammetric DEM reference data. Next bias correction was applied for all DEM data based on linear transformation parameters. The accuracy of SRTM version3 data showed better performance as compared with its product specification (19.1 m) at a 95% confidence interval (Farr et al., 2007), the vertical accuracy for SRTM data is showed 7.22 m at a 95% confidence interval. This shows the vertical accuracy of SRTM in the study area has proven to be more than two times higher than the SRTM product specification, using GCP reference data. Yet again, the accuracy of ASTER-GDEM v3 also showed high accuracy as compared with its user guide (Japan's Ministry of Economy, Trade, and Industry (METI) et al., 2019), the expected accuracy of the ASTER-GDEM v3 user guide is 12.1 m standard deviation. Which our result showed better accuracy (7.22 m standard deviation) as compared with the product specification. Which is 67 % improved than the product specification. The quality of PALSAR DEM data is directly related to DEM which was used in radiometric terrain correction processes (SRTM and NED DEM) (Alaska satellite Facility, 2014). Our finding is showed that the accuracy of SRTM and PALSAR1 were confirmed better performance than ASTER-GDEM and PALSAR2. While, the accuracy of ASTER-GDEM is lowest among the DEM data, this may be caused by the topographic variation or poor accuracy optical data. InSAR product DEM data is better in accuracy as compared as optical image, because radar system can penetrate clouds, fogs, and rains during data collection. The finding of this study showed some improvements in SRTM and less improvement in ASTER-GDEM as compared with other studies. Ismail Elkhrachy in Najiran city, Saudi Arabia (Ismail Elkhrachy, 2018) studied the accuracy of ASTER and SRTM using GPS elevation reference data and the result is 11.64 m and 9.94 m vertical accuracy for SRTM and ASTER at 95% confidence interval after the removal of blunders and systematic errors, this shows the accuracy of SRTM in this study gives the better performance, and the accuracy of ASTER-GDEM in our finding showed the less accuracy as compared with the above study. This perhaps the cause of variation of topography in

the study area. Fahad S. Alhmadi assesses the accuracy of ALOS-PALSAR 12.5 m spatial resolution using Airborne LiDAR point reference data in Almadinah Almunawarah city (Saudi Arabia) (Fahad et., 2019) and his value of RMSE is 8.01 m. This showed less accuracy as compared with our study in both PALSAR1 and PALSAR2. Other studies were also applied in different places at relative topics, Athmania uses GNSS elevation point to assesses the accuracy of three global DEM data (ASTER GDEM2,C SRTM v4.1 and GDEMTED2010) over two different localities in Tunisia and Algeria (Athmania et al., 2014), for site 1 the value of RMSE for ASTER-GDEM is 5.3 m and for SRTM the value is 3.6 m, which it has high accuracy as compared with this study in both SRTM and ASTER-GDEM data. For site2 the result shows 8.3m for SR|TM and 9.8m for ASTER-GDEM data. which the accuracy of site2 RMSE result is less as compared with site1 and this study. Hareya (Hareya et al, 2020) also assess the accuracy of global DEM (SRTM, ASTER, TDX) using RTK-GNSS point reference data in Mekelle town (Ethiopia), the study shows that the value of RMSE for SRTM is 4.68 m and 7.24 m in 30 m v3and 90m v4.1 spatial resolution data. The RMSE value of ASTER-GDEM is 14.77 m, both the accuracy of ASTER-GDEM and SRTM data shows less accuracy as compared with this study. The study of Hailu for SRTM and ASTER-GDEM is 4.63 m and 11.8 m value of RMSE for in his study area (Adama town (Ethiopia) (Hailu et al., 2021)) using DGPS reference data. This also shows less accuracy as compared with this study. Their all results tendency is showed SRTM as a better accuracy than ASTER-GDEM data, but the value of RMSE is varies from one place to another, this may be the amount of reference data, terrain characteristics of study area and features in target area is the reason for the variation.

The accuracy of DEM data is also assessed in different land use land cover areas, a study area is mostly covered by Bare land, Rock area, Road line, drainage pattern, and sparse trees. The accuracy of the rock area is less in ASTER, PALSAR1, and PALSAR2, however, the accuracy of the road line and the tree is low in SRTM data. This may be because the penetration of vegetation canopy in the C-band is not fully capable (SRTM data). The elevation of the Rock area is high in the study area, this perhaps the cause for high error in ASTER, PALSAR1, and PALSAR2 data. Hareya Birhane (Hareya et al., 2020) study was agreed with this study by some land use land cover data.

On the other hand, the accuracy of global DEM is assessed by slope classification using photogrammetric DEM reference data; the result showed that the accuracy of all global DEM has

low accuracy in steep slope areas and high accuracy in flat and moderate slope. Different studies are agreed in this study and their tendency indicates that the accuracy of flat area is more accurate than the complicated terrain (Tang-guo et al., 2001; Hareya et al., 2020). Tang-guo in his study (Tang-guo et al., 2001) concluded that the accuracy of DEM is drastically affect in terrain complexity. However, Zhou (Zhou et al., 2006) conclude in his study, the accuracy of flat areas is low as compared with steep slopes. This may be caused by the behavior of data capture techniques in vegetation areas.

Lastly, bias correction was applied for the selected DEM data to reduce the residual of the data, linear transformation parameters based on multiple regression approach is used to reduce the residual of the DEM data, then statistical measurements and other assessments were re-computed using GCP and RTK-GPS reference data. The accuracy of SRTM after bias correction is highly improved in the Kwanchai (Kwanchai et al., 2016) study (7.66 %), which is 0.96 % greater than this study. However, the accuracy of ASTER-GDEM after bias correction in this study showed better improvement, which is 14.4 % greater than the kwanchai's study (Kwanchai et al., 2016). This may be depended on environmental conditions. (Abdulkareem *et al.* 2020) study was improved accuracy by 40.8 % in SRTM and 74% in ASTER GDEM. Which is the highest bias improvement from the above one and the other is one shows less improvement after bias correction.

Chapter Five

5. Conclusion and Recommendations

5.1 Conclusion

The accuracy of DEM data is a critical issue for different applications and it is ensured by assessing the accuracy of the data. This study is focused on the vertical accuracy assessment of four global open-access DEM data (SRTM, ASTER-GDEM, PALSAR1, and PALSAR2) and bias correction, a case study in and around Dire Dawa city, Ethiopia. Totally, 121 ground control point (GCP) data, 491 RTK-GPS point data, and photogrammetric DEM of study area data were used for reference data. To match the reference datum of selected global DEM and reference data, the vertical datum is transformed to the latest geoid model (EGM2008) and the horizontal datum is transformed to WGS84. Then accuracy is assessed by point-based vertical accuracy. Based on result it can be concluded that the accuracy of SRTM showed better accuracy among the DEM data and PALSAR1 is followed by SRTM. While, the accuracy of ASTER GDEM showed less accuracy among the DEM data. To identify the accuracy in land use land cover data, accuracy was assessed using land use land cover point data which cover the study area (Bare land, road line, drainage pattern, rock area, and trees) using RTK-GPS reference data. The result accuracy of rock area was showed less for all DEM data except in SRTM data and the accuracy of the bare land area averagely showed better accuracy in all DEM data. To differentiate the accuracy of terrain difference, the segmented terrain classes accuracy shows. The accuracy of DEM data in the flat areas showed better, and the accuracy of a steep slope in all global DEM data showed less accuracy using photogrammetric DEM reference data.

Finally, bias correction was applied to reduce the residual of DEM data, based on linear transformation parameters. The accuracy of SRTM, ASTER-GDEM, PALSAR1, and PALSAR2 have improved the accuracy by using GCP reference data. The results indicate that the accuracy of the DEM data is highly improved after bias correction in ASTER-GDEM and less improved in PALSAR1 and PALSAR2 data.

5.2 Recommendations

This study revealed the accuracy of four global DEM data based on different assessing methods. Thus, the following recommendations are hereby presented:

- ✓ SRTM DEM data showed better accuracy among the selected data, so it is recommended that different DEM users should use SRTM DEM data for better accuracy.
- ✓ PALSAR1 is another alternative DEM data for a high-resolution requiring application and ASTER-GDEM is not recommended to use in high accuracy requiring applications at Dire Dawa city and around.
- ✓ Future researchers should give great attention to bias correction and terrain characteristics.

References

Paul R. Wolf, Bon A. Dewitt, Benjamin E. Wilkinson, 2014. *Elements of Photogrammetry with Applications in GIS.* Newyork: McGraw-Hill Education.

A CLS GROUP COMPANY, 2020. *InSAR AT A GLANCE.* [Online]
Available at: https://site.tre-altamira.com/insar/
[Accessed April 2021].

A. Cuartero a, A.M. Felicísimo a, F.J. Ariza, 2004. Accuracy of DEM Genaration from Terra-Aster Stereo Data. *International Archives of the Photogrammetry, Remote Sensing and Spatial Information Sciences - ISPRS Archives,* 35(B2), pp. 559-563.

Abdi Ibrahim, 2018. *Vertical Accuracy Assessment of open Source Digital Elevation Model using GPS Point And Reference DEM Over Ethiopia A Case study In Addis Ababa And Dire Dawa,* Addis Ababa and Dire Dawa: Addis Ababa University.

Abdulkareem, Imzahim Zina Walid Samuel and Qassim K. Abdullah,, 2020. Accuracy Assessment of Digital Elevation Models Produced From Different. *Engineering and Technology Journal,* 38(11), pp. 1580-1592..

Agency, F. E. a. M., 2003. *Guide line and specifications for flood hazard mapping partners; Appendix A: Guidance for Aerial Mapping and Surveying,* Washington DC: Federal Emergency and Mnagement Agency.

Aguilar F.J., Agüera F., Aguilar M.A., Carvajal F, 2005. Effects of terrain morphology, sampling density, and interpolation methods on grid dem accuracy. *Photogrammetric Engineering and Remote sensing* .

Aktaruzzaman, M. and Schmidt, T, 2009. Detailed Digital Surface Model (DSM) Generation and Automatic object detection to facilitate modelling of Urban flooding.. *ISPRS Workshop, Hannover,* 8(4), pp. 1-7.

Alaska satellite Facility, 2014. *ASF radimetric correction.* [Online]
Available at: https://asf.alaska.edu/data-sets/derived-data-sets/alos-palsar-rtc/alos-palsar-radiometric-terrain-correction/
[Accessed 10 11 2021].

Amin, Maher M., Saadia M. El-Fatiry, and ENG Nasr Mohammady Saba., 2014. Improving Accuracy and Increasing Resolution of the World and Local DEMs though data fusion. *ERJ–Faculty of Engineering,* Issue 20, pp. 101-120.

Amos MJ, Featherstone WE, 2009. Unification of New Zealand's local vertical datums: iterative gravimetric quasigeoid computations. *Journal of Geodesy,* 83(1), pp. 57-68.

Anon., 1994. A comparative study of the accuracy of digital terrain models (DTMs) based on various data models. *ISPRS Journal ofphotogrammetry and remote sensing,* pp. 2-11.

ASPRS Lidar Committee (PAD), 2004. *Vertical Accuracy Reporting for Lidar Data*, s.l.: ASPRS.

ASPRS, 2015. *New ASPRS Positional Accuracy Standards for Digital Geospatial data,* Maryland: ASPRS.

ASTER GDEM Validation Team, 2009. *ASTER Global DEM Validation Summary report*, s.l.: USGS/EROS.

Athmania D, Achour H, 2014. External validation of the ASTER GDEM2, GMTED2010 and CGIAR-CSI-SRTM v4.1 free access digital elevation models (DEMs) in Tunisia and Algeria. *Remote sensing,* 6(5), pp. 4600-4620.

Baboo, S. Santhosh, and M. Renuka Devi, 2010. An analysis of different resampling methods in Coimbatore, District. *Global Journal of Computer Science and Technology,* 10(15), p. 61.

Bartłomiej Szypuła, 2019. Quality assessment of DEM derived from topographic maps for geomorphometric purposes. *Open Geosciences,* 1(11), pp. 843-865.

Bethesda, M., 2007. *Digital elevation model technologies and applications,* Bethesda,Maryland: American Society for Photogrammetry and Remote Sensing.

Burrough, P., 1986. *Geographical Information Systems for land resources assessment.* Oxford: Oxford University press.

Carter, J., Schmid, K., Waters, K., Betzhold, L., Hadley, B., Mataosky, R., & Halleran, J., 2012. *An introduction to LiDAR technology, data, and applications.* s.l.:NOAA Coastal Services Center.

CHharlesD Ghilani, 2010. *Adjustment Computations Spatial Data Analysis.* New Jersey: OHN WILEY & SONS, INC.

Cole, Christopher J., Michaela R. Johnson, and Garth E. Graham, 2015. Advanced Land Observing Satellite (ALOS) Phased Array Type L-Band Synthetic Aperture Radar (PALSAR) mosaic for the Kahiltna terrane, Alaska. *US Geological Survey,* Issue 3323, pp. 2007-2010.

Committee, F. G. D., 1998. *Geospatial Positioning Accuracy Standards, part 3: National standard for spatial data accuracy,* Washington, DC : Federal Geographic Data Committee Report .

A. A. A. S Company,., 2021. *GEODETICS.* [Online]
Available at: https://geodetics.com/dem-dsm-dtm-digital-elevation-models/
[Accessed 12 April 2021].

Das, Anup, Ritesh Agrawal, and Shiv Mohan, 2015. Topographic correction of ALOS-PALSAR images using InSAR-derived DEM. *Geocarto International,* 30(2), pp. 145-153.

Demetrios Gatziolis and Hans-Erik Andersen, 2008. A Guide to LIDAR Data Acquisition and Processing for the Forests of the Pacific Northwest. *US Department of Agriculture, Forest Service, Pacific Northwest Research Station,* Volume 32, p. 768.

El-Rabbany, A., 2002. *Introduction to GPS.* London: ARTECH HOUSE.

Fahad Salim Alahmadi, 2019. *Evaluation of global digital elevation model ALOS/PALSAR using aerial LiDAR.* s.l., s.n.

Farr, T.G., Rosen, P.A., Caro, E., Crippen, R., Duren, R., Hensley, S., Kobrick, M., Paller, M., Rodriguez, E., Roth, L. and Seal, D., 2007. The shuttle radar topography mission. *Reviews of geophysics,* 45(2), pp. 1-33.

Farr, T.G., Rosen, P.A., Caro, E., Crippen, R., Duren, R., Hensley, S., Kobrick, M., Paller, M., Rodriguez, E., Roth, L. and Seal, D, 2015. The Shuttle Radar Topography Mission (SRTM) Collection User Guide. *Reviews of geophysics,* 45(2), pp. 1-17.

FDRE Ministry of Urban Development, H. a. c., 2015. *Urban Legal cadastre Standard,* Addis Ababa: Ministry of Urban Development, Housing and construction.

Gallien, T. W., J. E. Schubert, and B. F. Sanders, 2011. Predicting tidal flooding of urbanized embankments: a modeling framework and data requirements. *Coastal Engineering* , 58(6), pp. 567-577.

Gao, Xiaoming, Yaolin Liu, Tao Li, and Danqin Wu, 2017. High precision DEM generation algorithm based on InSAR multi-look iteration. *Remote Sensing,* 9(7), p. 741.

Grunwald, Sabine, 2005. *Environmental soil-landscape modeling: Geographic information technologies and pedometrics.* Boca Raton, Florida: CRC Press.

Hailu Zewde Abili, 2021. Comparison of Vertical Accuracy of Open-Source Global Digital Elevation Models: A Case Study of Adama City, Ethiopia. *Turkish Journal of Computer and Mathematics Education,* 12(4), pp. 1731-1744.

Hareya Birhane Tulu B. Bedada, Berhan Gessesse and Martin Vermeer, 2020. Validation of Airborne Sensor Photogrammetric Digital Terrain and Global Digital Elevation Models around Mekelle city,Ethiopia. *Earth science,* 1(1), pp. 1-22.

Hebeler, Felix, and Ross S. Purves, 2009. The influence of elevation uncertainty on derivation of topographic indices. *Geomorphology,* 1111(1), pp. 4-16.

Herrera, G., Tomás, R., Vicente, F., Lopez-Sanchez, J. M., Mallorquí, J. J., & Mulas, J., 2010. Mapping ground movements in open pit mining areas using differential SAR interferometry [Cross ref]. *International Journal of Rock Mechanics and Mining Sciences,* 47(7), pp. 1114-1125.

Hofmann-Wellenhof, Bernhard, Herbert Lichtenegger, and James Collins, 2012. *Global positioning system: theory and practice.* Newyor: Springer Science & Business Media.

Huising, E. Jeroen, and LM Gomes Pereira, 1998. Errors and accuracy estimates of laser data acquired by various laser scanning systems for topographic applications. *ISPRS Journal of photogrammetry and remote sensing,* 53(5), pp. 245-261.

INNOTER Geospatial Agency, 2020. *INNOTER Geospatial Agency.* [Online]
Available at: https://innoter.com/en/products/spatial-data/dsm-generation/
[Accessed 1 september 2021].

Ismail Elkhrachy, 2018. Vertical accuracy assessment for SRTM and ASTER Digital Elevation Models: A case study of Najran city, Saudi Arabia. *Ain Shams Engineering Journal,* 9(4), p. 1.

J.A Ávila Rodríguez, University FAF Munich, Germany, 2021. *GPS Signal Plan.* [Online]
Available at: https://gssc.esa.int/navipedia/index.php/GPS_Signal_Plan
[Accessed 12 August 2021].

Japan Aerospace Exploration Agency, 2008. *ALOS Data Users Handbook.* [Online]
Available at: https://asf.alaska.edu/data-sets/sar-data-sets/alos-palsar/alos-palsar-documents-tools/
[Accessed May 2021].

Japan's Ministry of Economy, Trade, and Industry (METI) and National Aeronautics and Space Administration (NASA) , 2019. *ASTER Global DEM V3 User Guide,* s.l.: California Institute of Technology.

Jarvis A, Rubiano J, Nelson A, Farrow A, Mulligan M, 2004. Practical use of SRTM data in the tropics: comparisons with digital elevation models generated from cartographic data. *International Centre for Tropical, Agriculture (CIAT),* 1(1), pp. 1-36.

Jet propulsion laboratory, 2020. *ASTER Global Digital Elevation Map Announcement.* [Online]
Available at: https://asterweb.jpl.nasa.gov/gdem.asp
[Accessed 7 May 2021].

Joachim Höhle, Marketa Potuckova, 2011. *Assessment of the quality of Digital Terrain Models.* Amsterdam: European Spatial Data Research.

Kim Jin Woo, 2013. *Applications of Synthetic Aperture Radar (SAR)/SAR Interferometry (InSAR) for Monitoring of Wetland Water Level and Land Subsidence.* s.l.:Doctoral dissertaion, The Ohio State University.

Klusberg A, 1990. Comparing GLONASS and GPS. *GPS world,* 1(6), pp. 52-54.

Ku Hasina Zainurin Ku zainol Abdi, Mohd Adib Mohammed Razi, Saiiffulidan Mohd Bukari, 2017. Analysis the Accuracy of digital elevation model for flood modelling on low land areas. *IOP Conference Series: Earth and Environmental Science,* 140(1), p. 012014.

Kwanchai Pakoksung , Masataka Takagi,, 2016. Digital elevation model on acccuracy validation and bias correction in vertical. *Model. Earth System Environment,* 1-13(1), p. 2.

Kwanchai Pakoksung ,Masataka Takagi,, 2016. Digital elevation model on acccuracy validation and bias correction in vertical. *Modeling Earth Systems and Environment,* 2(1), pp. 1-13.

Lane S.N., Richards K.S., Chandler, 1998. The effect of GIS interpolation errors on the use of DEMs in geomorphology.. *Landform Monitoring, Modeling and Analysis,* p. 139–164.

Li Zhilin, Christopher Zhu, and Chris Gold,, 2004. *Digital terrain modeling: principles and methodology.* Boca Raton, Florida: CRC press.

Liu Ling and M. Tamer Özsu,, 2009. *Encyclopedia of database systems.* New York: NY.

Liu Xiaoye, 2011. Accuracy Assessment Of LiDAR Elevation Data Using Survey Marks. *Survey Review,* 43(219), pp. 80-93.

Lu, Zhong, Ohig Kwoun, and Russell Rykhus, 2007. Interferometric synthetic aperture radar (InSAR): its past, present and future.. *Photogrammetric engineering and remote sensing,* 73(3), p. 217.

Manoj Karkee, Brian L. Steward, Samsuzana Abd Aziz, 2008. Improving quality of public domain digital elevation models through data fusion. *Biosystems Engineering,* 101(3), pp. 293-305.

Mesa-Mingorance, José L., and Francisco J. Ariza-López, 2020. Accuracy assessment of digital elevation models (DEMs): A critical review of practices of the past three decades. *Remote Sensing,* 12(16), p. 2630.

Mohammad NurcholiMohammad Nurcholis Iwan Qodar Himawan, Syintianuri Intan Wijayanti,Ayu Darmaristianti, 2019. Tropical Vegetation and Land Cover Mapping Using LiDAR. *Journal of Agro Science,* 7(1), pp. 8-18.

NASA/METI/AIST/Japan Spacesystems and U.S./Japan ASTER Science Team, 2019. *ASTER Global Digital Elevation Model V003.* [Online]
Available at: https://lpdaac.usgs.gov/products/astgtmv003/
[Accessed 2 10 2021].

Nelson, A., H. I. Reuter, and P. Gessler, 2009. DEM production methods and sources. *Developments in soil science,* 33(1), pp. 65-85.

NGA and NASA, 2015. The Shuttle Radar Topography Mission (SRTM) Collection User Guide. *Reviews of geophysics,* 45(2).

Pavlis, N. K., Holmes, S. A., Kenyon, S. C., & Factor, J. K, 2012. The development and evaluation of the Earth Gravitational Model 2008 (EGM2008). *Journal of geophysical research,* B4(117).

Peter A. Burrough and Rachael A. McDonnell , 1998. *Principles of Geographic information systems.* New York: Oxford University Press .

Ravibabu, Mandla V., and Kamal Jain, 2008. Digital elevation model accuracy aspects. *Journal of Applied Sciences,* 8(1), pp. 134-139.

Roh, Kyoung-Min, and Byung-Kyu Choi., 2014. The effects of the IERS conventions (2010) on high precision orbit propagation. *Journal of Astronomy and Space Sciences,* 31(1), pp. 41-50.

Saffet Erdoğan, 2010. Modelling the spatial distribution of DEM error with geographically weighted regression. *Computers & Geosciences,* 36(1), pp. 34-43.

Sandip Mukherjee, P.K. Joshi , Samadrita Mukherjee , Aniruddha Ghosh , R.D. Garg , Anirban Mukhopadhyay , 2013. Evaluation of vertical accuracy of open source Digital Elevation Model (DEM). *International Journal of Applied Earth Observation and Geoinformation,* Volume 21, p. 205–217.

Santos Petr Vaníček and Marcelo,, 2019. What Height System Should be Used in Geomatics?. *International Journal of Earth & Environmental Sciences,* 4(160), pp. 1-8.

Shaw, M. "Sandhoo, K. andTurner, T., 2000. Modernization of the global positioning system. *GPSWorld,* 11(9), pp. 36-40.

Survey department Minister of Development Brunei Darussalam, 2017. *Regulations Of Geomatics.* [Online]
Available at:
http://www.mod.gov.bn/survey/SitePages/REGULATIONS%20OF%20GEOMATICS_GPS%20UNIT%20Latest060318.pdf
[Accessed 8 October 2021].

Suwandana, Endan, Kensuke Kawamura, Yuji Sakuno, Eko Kustiyanto, and Beni Raharjo., 2012. Evaluation of ASTER GDEM2 in Comparison with GDEM1 SRTM DEM and Topographic-Map-Derived DEM Using Inundation Area Analysis and RTK-dGPS Data. *Remote Sensing,* Volume 4, pp. 2419-2431.

Tang-guo an, Gong Jian-ya Zhiao mu-dan, Chen Zhen Jiang, 2001. Evaluation on the accuracy Digital elevation Model. *Journal of Geographical Sciences,* 11(2), pp. 209-216.

Thomas Herring, 2012. *MIT (Massachusetts Institute of Technology).* [Online]
Available at: https://ocw.mit.edu/courses/earth-atmospheric-and-planetary-sciences/12-540-principles-of-the-global-positioning-system-spring-2012/lecture-notes/MIT12_540S12_lec8.pdf
[Accessed 5 October 2021].

Tian, Yu, Shaogang Lei, Zhengfu Bian, Jie Lu, Shubi Zhang, and Jie Fang, 2018. Improving the Accuracy of Open Source Digital Elevation Models with Multi-Scale Fusion and a Slope Position-Based Linear Regression Method. *Remote sensing,* 10(12), p. 1861.

Tomás, R., Li, Z., Liu, P., Singleton, A., Hoey, T., and Cheng, X, 2014. Spatiotemporal characteristics of the Huangtupo landslide in the Three Gorges region (China) constrained by radar interferometry [Cross Ref]. *Geophysical Journal International,* 197(1), pp. 213-232.

Trimble Engineering and construction group, 2003. *Trimble 5800 GPS SySTem.* [Online]
Available at: https://kb.unavco.org/kb/article/trimble-r7-r8-user-guide-v1-00-rev-a-september-2003-165.html
[Accessed 8 October 2021].

Xiaoping Duab, Huadong Guoa, Xiangtao Fana, Junjie Zhua, Zhenzhen Yana & Qin Zhan, 2015. Vertical accuracy assessment of freely available digital elevation models over low-lying coastal plains. *International Journal of Digital Earth,* 9(3), pp. 252-271.

Yang, Liping, Xingmin Meng, and Xiaoqiang Zhang, 2011. SRTM DEM and its application advances. *International Journal of Remote Sensing,* 32(14), pp. 3875-3896.

Ylmaz, Ibrahim, Mustafa Ylmaz, and Bayram Turgut, 2010. Evaluation of recent global geopotential models based on GPS/levelling data over Afyonkarahisar (Turkey). *Scientific research and essays,* 5(5), pp. 484-493.

Zhang W., Montgomery D, 1994. Digital elevation model grid size, landscape representation, and hydrologic simulations. *Water Resources research ,* p. 1019–1028.

Zhou Chunxia, Ge Linlin, E Dongchen& Chang Hsingchung, 2005. A Case Study of Using External DEM in InSAR DEM Generation. *Geospatial Information science,* 8(1), pp. 14-18.

Zhou Qiming, Xuejun Liu and Yizhong Sun,, 2006. Terrain complexity and uncertainties in grid-based digital terrain analysis. *International Journal of Geographical Information Science,* 20(10), pp. 1137-1147.

Zhou Qiming, 2017. Digital Elevation Model and Digital Surface Model. *International Encyclopedia of Geography,* 1(1), pp. 1-17.

Appendix:

Appendix I: Transforming Ground control point (GCP) data elevation from EGM96 to EGM08

Easting (m)	Northing	OH (96)	EGM96	EGM2008	EH	(EGM96-08)	OH(08)
805083.323	1066148.602	1102.887	-13.032	-12.878	1089.855	-0.154	1102.733
807932.752	1066210.272	1101.505	-13.055	-12.906	1088.450	-0.149	1101.356
809042.495	1066119.053	1112.143	-13.063	-12.915	1099.080	-0.148	1111.995
817090.471	1066157.382	1111.371	-13.132	-12.960	1098.240	-0.172	1111.200
818049.047	1065055.358	1148.497	-13.127	-12.948	1135.370	-0.179	1148.318
817158.604	1065119.529	1139.365	-13.120	-12.948	1126.246	-0.172	1139.194
815029.314	1065247.342	1143.307	-13.102	-12.944	1130.205	-0.158	1143.149
815070.934	1066143.086	1171.876	-13.114	-12.954	1158.762	-0.160	1171.716
812919.662	1066110.099	1115.976	-13.095	-12.943	1102.881	-0.152	1115.824
814163.395	1065240.504	1135.514	-13.094	-12.941	1122.420	-0.153	1135.361
809109.024	1065200.345	1130.388	-13.050	-12.908	1117.338	-0.142	1130.246
807929.680	1065200.263	1121.145	-13.040	-12.898	1108.105	-0.142	1121.003
810057.599	1065181.141	1135.424	-13.058	-12.916	1122.366	-0.142	1135.282
807075.029	1065253.248	1111.180	-13.034	-12.890	1098.146	-0.144	1111.036
805103.234	1065190.185	1119.378	-13.018	-12.871	1106.361	-0.147	1119.232
804223.397	1065247.485	1117.540	-13.012	-12.862	1104.529	-0.150	1117.391
809104.966	1064264.155	1149.429	-13.036	-12.899	1136.393	-0.137	1149.292
810122.000	1064324.344	1151.792	-13.046	-12.908	1138.746	-0.138	1151.654
811845.940	1064252.944	1147.659	-13.060	-12.919	1134.599	-0.141	1147.518
813141.750	1064246.867	1144.601	-13.072	-12.926	1131.529	-0.146	1144.455
814008.182	1064098.464	1157.917	-13.078	-12.928	1144.839	-0.150	1157.767
815132.843	1064114.978	1155.383	-13.088	-12.932	1142.295	-0.156	1155.227
811054.193	1065264.221	1134.977	-13.067	-12.924	1121.910	-0.143	1134.834
812094.190	1065235.012	1125.539	-13.076	-12.930	1112.463	-0.146	1125.393
813318.185	1065292.666	1130.671	-13.087	-12.937	1117.584	-0.150	1130.521
808099.301	1063274.148	1230.248	-13.014	-12.879	1217.235	-0.135	1230.114
809061.192	1063287.185	1170.335	-13.022	-12.888	1157.313	-0.134	1170.201
806943.170	1064075.698	1126.243	-13.015	-12.878	1113.228	-0.137	1126.106
806047.824	1064246.039	1131.244	-13.011	-12.871	1118.233	-0.140	1131.104
804999.369	1063248.093	1153.107	-12.987	-12.850	1140.120	-0.137	1152.970
806139.669	1063124.079	1152.097	-12.995	-12.859	1139.103	-0.136	1151.962
807048.522	1063292.520	1144.601	-13.005	-12.870	1131.596	-0.135	1144.466
808103.731	1062210.381	1279.150	-12.998	-12.865	1266.152	-0.133	1279.017
809041.838	1062264.611	1343.525	-13.008	-12.874	1330.518	-0.134	1343.392
807100.665	1062174.124	1262.345	-12.989	-12.855	1249.356	-0.134	1262.211
806104.253	1062008.960	1179.951	-12.978	-12.843	1166.973	-0.135	1179.816
805141.887	1062119.380	1171.804	-12.971	-12.835	1158.833	-0.136	1171.668

804091.607	1062214.139	1165.547	-12.963	-12.826	1152.584	-0.137	1165.410
804114.876	1063135.279	1150.954	-12.978	-12.839	1137.976	-0.139	1150.815
804086.947	1064245.482	1133.865	-12.995	-12.852	1120.870	-0.143	1133.722
805086.479	1064368.968	1133.987	-13.005	-12.863	1120.982	-0.142	1133.845
806100.281	1065220.429	1114.746	-13.026	-12.881	1101.720	-0.145	1114.601
806100.926	1066174.893	1101.459	-13.041	-12.888	1088.419	-0.153	1101.307
811081.991	1067231.884	1099.526	-13.095	-12.940	1086.431	-0.155	1099.371
816175.788	1066171.647	1118.889	-13.124	-12.957	1105.765	-0.167	1118.722
816059.393	1065230.005	1164.657	-13.111	-12.947	1151.546	-0.164	1164.493
816101.659	1064193.429	1217.193	-13.098	-12.935	1204.095	-0.163	1217.030
818086.587	1064322.419	1181.066	-13.119	-12.939	1167.947	-0.180	1180.886
817898.923	1062298.208	1292.895	-13.094	-12.914	1279.801	-0.180	1292.715
813921.272	1063364.429	1173.101	-13.068	-12.919	1160.034	-0.149	1172.953
814192.438	1061960.785	1203.721	-13.053	-12.902	1190.669	-0.151	1203.571
814999.995	1062218.519	1193.774	-13.064	-12.908	1180.710	-0.156	1193.618
813109.601	1063314.564	1171.491	-13.059	-12.915	1158.432	-0.144	1171.347
812167.693	1063455.000	1169.585	-13.052	-12.912	1156.533	-0.140	1169.445
811355.618	1063284.118	1168.883	-13.043	-12.905	1155.840	-0.138	1168.745
805130.639	1061437.540	1192.730	-12.961	-12.824	1179.769	-0.137	1192.593
806144.570	1061212.839	1216.467	-12.966	-12.831	1203.501	-0.135	1216.332
806984.349	1060925.255	1340.950	-12.970	-12.834	1327.980	-0.136	1340.814
808226.240	1061222.279	1304.510	-12.986	-12.850	1291.525	-0.136	1304.375
809055.735	1061155.855	1247.358	-12.992	-12.857	1234.366	-0.135	1247.223
810165.569	1061219.399	1280.344	-13.004	-12.867	1267.340	-0.137	1280.207
810066.390	1062176.713	1197.608	-13.016	-12.881	1184.592	-0.135	1197.473
811090.447	1061315.888	1352.843	-13.014	-12.875	1339.829	-0.139	1352.704
811197.399	1060309.742	1300.079	-13.002	-12.860	1287.077	-0.142	1299.937
812057.843	1061217.005	1211.165	-13.022	-12.880	1198.143	-0.142	1211.023
812028.047	1060139.262	1227.664	-13.008	-12.863	1214.656	-0.145	1227.519
812167.774	1059302.651	1266.289	-13.000	-12.849	1253.290	-0.150	1266.139
813098.852	1059180.285	1297.146	-13.008	-12.853	1284.138	-0.155	1296.991
813097.271	1060179.642	1248.223	-13.020	-12.870	1235.203	-0.150	1248.073
814018.126	1060305.817	1252.457	-13.031	-12.877	1239.426	-0.154	1252.303
815084.017	1059211.834	1325.503	-13.030	-12.863	1312.474	-0.167	1325.337
814093.216	1059198.405	1305.529	-13.019	-12.859	1292.510	-0.160	1305.369
816233.460	1059129.473	1332.474	-13.041	-12.866	1319.433	-0.175	1332.299
815995.238	1060077.140	1283.488	-13.049	-12.880	1270.439	-0.169	1283.319
814197.867	1058521.355	1309.977	-13.012	-12.848	1296.965	-0.164	1309.813
815003.012	1058669.963	1354.335	-13.023	-12.854	1341.312	-0.169	1354.166
817070.137	1059375.611	1462.391	-13.053	-12.872	1449.338	-0.181	1462.210
817205.575	1060215.669	1285.713	-13.064	-12.885	1272.649	-0.179	1285.534
817190.891	1061268.818	1376.040	-13.075	-12.900	1362.965	-0.175	1375.865

816257.178	1061243.430	1325.745	-13.065	-12.898	1312.680	-0.167	1325.578
817898.625	1060295.285	1349.299	-13.072	-12.887	1336.227	-0.185	1349.114
817990.368	1061204.044	1324.311	-13.083	-12.900	1311.228	-0.183	1324.128
815148.476	1061123.299	1326.647	-13.052	-12.893	1313.595	-0.159	1326.488
812925.619	1062171.024	1188.622	-13.043	-12.899	1175.579	-0.144	1188.478
812147.014	1062239.149	1192.020	-13.036	-12.896	1178.984	-0.140	1191.880
811047.764	1062211.569	1193.994	-13.025	-12.888	1180.969	-0.137	1193.857
817134.377	1063248.124	1205.134	-13.097	-12.926	1192.037	-0.171	1204.963
817124.937	1064104.439	1301.870	-13.107	-12.936	1288.763	-0.171	1301.699
818010.302	1063089.270	1261.111	-13.104	-12.924	1248.007	-0.180	1260.931
817107.093	1062313.146	1208.912	-13.086	-12.914	1195.826	-0.172	1208.740
816207.981	1062246.555	1192.137	-13.076	-12.912	1179.061	-0.164	1191.973
816099.661	1063218.809	1186.046	-13.087	-12.924	1172.960	-0.163	1185.884
815224.406	1063112.064	1178.763	-13.077	-12.920	1165.686	-0.157	1178.606
814131.054	1061234.404	1216.497	-13.043	-12.891	1203.454	-0.152	1216.345
813095.954	1061180.534	1201.981	-13.032	-12.886	1188.949	-0.146	1201.835
815220.401	1060164.843	1260.857	-13.042	-12.879	1247.815	-0.163	1260.694
807977.132	1064219.035	1140.013	-13.026	-12.889	1126.987	-0.137	1139.876
810933.136	1064320.485	1149.336	-13.053	-12.914	1136.283	-0.139	1149.197
805410.839	1065768.505	1109.692	-13.029	-12.878	1096.663	-0.151	1109.541
808537.710	1066191.684	1105.896	-13.060	-12.911	1092.836	-0.149	1105.747
813549.955	1064520.494	1147.383	-13.079	-12.931	1134.304	-0.148	1147.235
805037.748	1064784.062	1127.197	-13.011	-12.867	1114.186	-0.144	1127.053
809964.277	1065143.517	1155.831	-13.056	-12.915	1142.775	-0.141	1155.690
812038.835	1064272.354	1147.912	-13.062	-12.920	1134.850	-0.142	1147.770
814185.627	1063768.788	1166.987	-13.075	-12.925	1153.912	-0.150	1166.837
809703.646	1062337.573	1234.151	-13.015	-12.880	1221.137	-0.134	1234.017
804927.223	1063060.252	1155.004	-12.983	-12.846	1142.021	-0.137	1154.867
808411.945	1062504.128	1323.642	-13.005	-12.872	1310.637	-0.133	1323.509
804218.978	1061863.863	1173.292	-12.959	-12.822	1160.333	-0.137	1173.155
804428.111	1063132.135	1152.643	-12.980	-12.842	1139.663	-0.138	1152.505
804855.403	1064419.874	1133.166	-13.004	-12.861	1120.162	-0.143	1133.023
805884.406	1065195.923	1117.102	-13.024	-12.879	1104.078	-0.145	1116.957
806171.699	1065826.510	1103.756	-13.036	-12.886	1090.720	-0.150	1103.606
814323.849	1062036.077	1203.964	-13.055	-12.904	1190.909	-0.151	1203.813
811506.729	1063681.614	1160.644	-13.049	-12.910	1147.595	-0.139	1160.505
809276.250	1060677.682	1302.330	-12.988	-12.851	1289.342	-0.137	1302.193
813138.790	1062310.773	1190.560	-13.047	-12.902	1177.513	-0.145	1190.415
811583.289	1061461.423	1236.839	-13.021	-12.881	1223.818	-0.140	1236.699
815232.811	1062703.532	1186.630	-13.072	-12.915	1173.558	-0.157	1186.473
813188.807	1061260.159	1203.581	-13.034	-12.887	1190.547	-0.147	1203.434
815300.577	1059969.322	1303.336	-13.040	-12.877	1290.296	-0.163	1303.173

Legend: Easting and Northing are coordinates of the data (WGS84), OH (96) is Orthometric height which is referenced by the EGM96 model, EGM96 is geoid height referenced by EGM96 model, EGM2008 is geoid height which is referenced by EGM2008, EH is ellipsoidal height, (EGM96-08) is a difference of both geoid models, OH(08) is Orthometric height which referenced by EGM2008 geoid model.

Appendix II. RTK-GPS data (samples)

Easting (m)	Northing (m)	Elevation (m)	Desc_
813877.213	1060289.359	1234.843	RD
813874.073	1060270.935	1235.420	RD
813858.712	1060232.773	1242.453	RD
813857.896	1060232.264	1242.749	RC
813929.438	1060242.415	1235.303	RD
813945.922	1060224.706	1235.554	DR
813945.153	1060223.100	1236.244	RC
813979.792	1060179.762	1239.400	RD
813974.375	1060203.592	1238.196	RD
813923.520	1060256.535	1234.968	RD
813887.317	1060318.430	1234.216	RD
813873.798	1060336.645	1234.126	RD
813671.683	1060409.876	1229.537	RD
813647.224	1060412.578	1229.116	RD
813615.409	1060412.136	1228.900	RD
813555.698	1060410.098	1227.501	RD
813648.487	1060409.077	1229.226	RD
813731.702	1060361.246	1230.737	RD
813727.489	1060359.437	1230.905	RD
813739.389	1060354.754	1231.909	TR
813723.063	1060365.717	1230.872	TR
813724.564	1060365.757	1230.909	TR
813726.632	1060365.722	1230.892	TR
813719.792	1060361.897	1230.846	TR
813804.457	1060367.361	1233.269	TR
813858.303	1060232.737	1242.471	RC
813858.319	1060232.719	1242.467	RC
813852.960	1060222.701	1246.657	RC
813848.870	1060220.661	1246.830	RC
813844.963	1060218.546	1246.707	RC
813843.326	1060210.675	1247.717	RC
813849.352	1060203.356	1254.256	RC

813850.180	1060200.377	1255.422	RC
813848.321	1060188.070	1259.734	RC
813853.087	1060190.264	1260.099	RC
813857.892	1060197.178	1258.880	RC
813861.790	1060201.354	1258.807	RC
813863.626	1060208.188	1257.075	RC
813871.071	1060210.790	1257.870	RC
813875.514	1060208.573	1259.286	RC
813881.083	1060214.758	1258.233	RC
813881.678	1060211.977	1259.775	RC
813869.024	1060209.695	1257.684	RC
813871.114	1060216.356	1257.212	RC
813874.393	1060217.561	1257.198	RC
813868.061	1060206.908	1258.054	RC
813861.590	1060201.438	1258.813	RC
813856.242	1060198.847	1258.799	RC
813858.613	1060196.078	1259.165	RC
813852.692	1060190.401	1260.250	RC
813851.621	1060184.996	1261.626	RC
813855.424	1060181.479	1263.593	RC
813855.077	1060177.032	1265.196	RC
813852.135	1060177.524	1264.840	RC
813856.908	1060172.242	1266.785	RC
813852.729	1060171.231	1266.702	RC
813852.490	1060165.914	1268.520	RC
813849.352	1060158.776	1268.977	RC
813856.476	1060160.240	1269.436	RC
813859.711	1060165.332	1269.217	RC
813865.626	1060164.668	1270.229	RC
813869.586	1060163.518	1271.703	RC
813873.623	1060165.636	1272.566	RC
813879.311	1060166.824	1273.239	RC
813879.708	1060171.793	1272.929	RC
813832.012	1060129.737	1269.955	RC
813825.021	1060119.986	1269.761	RC
813820.565	1060112.018	1269.830	RC
813817.128	1060103.318	1271.618	RC
813804.812	1060095.726	1272.192	RC
813792.802	1060092.739	1273.515	RC
813788.285	1060096.472	1273.340	RC
813782.148	1060094.301	1273.900	RC
813774.290	1060097.690	1273.703	RC

813768.623	1060097.319	1273.433	RC
813759.447	1060101.473	1272.023	RC
813764.400	1060107.226	1271.754	RC
813759.648	1060114.189	1270.355	RC
813771.819	1060110.055	1271.135	RC
813831.678	1060153.285	1264.190	RC
813840.943	1060175.686	1261.928	RC
813812.044	1060300.030	1233.992	BL
813790.641	1060264.678	1233.882	BL
813780.732	1060260.313	1233.674	TR
813753.280	1060237.262	1233.094	BL
813734.013	1060229.991	1232.693	BL
813716.273	1060231.240	1232.466	BL
813701.737	1060244.407	1231.739	BL
813686.928	1060262.593	1231.397	BL
813690.212	1060285.575	1231.072	BL
813671.575	1060288.914	1231.179	BL
813665.393	1060304.156	1230.983	BL
813644.526	1060285.936	1231.572	BL
813624.411	1060265.412	1231.820	TR
813610.287	1060274.370	1231.640	TR
813605.209	1060283.796	1230.835	TR
813593.865	1060269.123	1227.560	TR
813591.709	1060257.980	1227.091	TR
813592.473	1060246.570	1226.391	TR
813595.714	1060240.214	1226.060	TR
813585.951	1060240.073	1225.960	TR
813594.931	1060230.557	1225.315	TR
813595.455	1060224.636	1225.104	TR
813603.401	1060238.838	1226.463	TR
813622.938	1060229.617	1227.869	TR
813636.913	1060233.770	1228.120	TR
813639.357	1060252.740	1230.721	TR
813648.340	1060240.442	1230.884	TR
813656.984	1060226.349	1231.930	TR

Legend: RD =Road line, TR =Trees, BL =Bare land, RC = Rock areas, DR =Drainage pattern

Appendix III. Bias correction script in MATLAB software

```
AA=load('Bias correction3.txt');
U=AA(:,1); %coordinate estimation of the X
V=AA(:,2); %coordinate estimation  of the Y
W=AA(:,4); %elevation  for SRTM
W2=AA(:,5);%elevation  for ASTER
W3=AA(:,6);%elevation  PALSAR1
W4=AA(:,7);%elevation  PALSAR2
Z=AA(:,3); %elevation  for GCP data
%%%%computing the summation the value
SUU=transpose (U)*U; %square of the reference x and its sumation
SUV=transpose(U)*V; %the multiplication of the X and Y and its sumation
SUW=transpose(U)*W; %for SRTM
SUW2=transpose(U)*W2; %%for ASTER
SUW3=transpose(U)*W3; % for PALSAR1
SUW4=transpose(U)*W4; % for PALSAR2
SVV=transpose(V)*V; %square  Y and its sumation
SVW=transpose(V)*W; %for SRTM
SVW2=transpose(V)*W2; %for ASTER
SVW3=transpose(V)*W3; %for PALSAR1
SVW4=transpose(V)*W4; % for PALSAR2
SWW=transpose(W)*W; %for SRTM
SWW2=transpose(W2)*W2;%for ASTER
SWW3=transpose(W3)*W3;%for PALSAR1
SWW4=transpose(W4)*W4;%for PALSAR2
SOU=sum(U); %summation of the value U
SOV=sum(V); %summation of the value V
SOW=sum(W); %summation of the value W for SRTM
SOW2=sum(W2); %summation of the value W for ASTER
SOW3=sum(W3); %summation of the value W for PALSAR1
SOW4=sum(W4); %summation of the value W for PALSAR2
SZU=transpose(Z)*U; %the multiplication of the observation Z and reference X
and its summation
SZV=transpose(Z)*V; %the multiplication of the observation Z and reference Y
and its sumation
SZW=transpose(Z)*W; %for SRTM
SZW2=transpose(Z)*W2; %for ASTER
SZW3=transpose(Z)*W3; %for PALSAR1
SZW4=transpose(Z)*W4; %for PALSAR2
SOZ=sum(Z);%summation of the value Z
UU  =79653842135510.2000; %which is equal to SUU=transpose (U)*U;
UV  =104358356137709.0000; %which is equal to SUV=transpose (U)*V;
UW  =117827428415.1680;%which is equal to SUW=transpose (U)*W; for SRTM
VV  =136729826145347.0000;%which is equal to SVV=transpose (V)*V;
VW  =154339102691.1310;%which is equal to SVW=transpose (V)*W;for SRTM
WW  =174945668.8491;%which is equal to SUU=transpose (W)*W; for SRTM
SU  =98172585.350;%which is equal to SOU=sum(U);
SV  =128624445.152;%%which is equal to SOV=sum(V);
SW  =145205.130;%%which is equal to SOU=sum(U);for SRTM
ZU  =117753163870.995;%which is equal to SZU=transpose (Z)*U;
ZV  =154241487212.912;%which is equal to SZV=transpose (Z)*V;for SRTM
ZW  =174844484.977;%which is equal to SZW=transpose (Z)*W;for SRTM
SZ  =145113.421;%which is equal to  SOZ=sum(Z);;
N=121; %which is total number of observations
 %%% for ASTER
UW2 =117242753891.7870; %which is equal to SUW2=transpose (U)*W2;
```

```
VW2 =153574512897.5990; %which is equal to SVW2=transpose (W2)*W2;
WW2 =173207985.8483; %which is equal to SWW2=transpose (W2)*W2;
SW2 =144485.6400; %which is equal to SOW2=sum(W2);
ZW2 =173971708.4852; %which is equal to SZW2=transpose (Z)*W2;
%for ALOS-PALSAR 12.5m spatial resolution
UW3 =117756507346.7890; %which is equal to SUW3=transpose (U)*W3;
VW3 =154246562320.8610; %which is equal to SVW3=transpose (W3)*W3;
WW3 =174731205.4382; %which is equal to SWW3=transpose (W3)*W3;
SW3 =145118.0500; %%which is equal to SOW3=sum(W3);
ZW3 =174736806.9135; %which is equal to SZW3=transpose (Z)*W3;
%for ALOS-PALSAR 30m spatial resolution
UW4 =117709319142.3020; %which is equal to SUW4=transpose (U)*W4;
VW4 =154184913529.8580; %%which is equal to SVW4=transpose (W4)*W4;
WW4 =174587810.0594; %%which is equal to SWW4=transpose (W4)*W4;
SW4 =145060.0500; %%%which is equal to SOW4=sum(W4);
ZW4 =174664492.8636; %which is equal to SZW4=transpose (Z)*W4;
%%num2str() is used to convert scientific notation to decimal value
A= [UU,UV,UW,SU;UV,VV,VW,SV;UW,VW,WW,SW;SU,SV,SW,N]; %matrix of A
L=[ZU;ZV;ZW;SZ]; %matrix of L
B=transpose(A)*A; %multiplication of A transpose and A
D=transpose(A)*L; %multiplication of A transpose and L
C=B\D; %parameters of the value (a,b,c and Zo)
%%%for ASTER
A2= [UU,UV,UW2,SU;UV,VV,VW2,SV;UW2,VW2,WW2,SW2;SU,SV,SW2,N];%matrix of A
L2=[ZU;ZV;ZW2;SZ];%matrix of L
B2=transpose(A2)*A2;%multiplication of A2 transpose and A2
D2=transpose(A2)*L2; %multiplication of A2 transpose and L2
C2=B2\D2; %parameters of the value (a,b,c and Zo)
%for ALOS-PALSAR 12.5m spatial resolution
A3= [UU,UV,UW3,SU;UV,VV,VW3,SV;UW3,VW3,WW3,SW3;SU,SV,SW3,N];%matrix of A3
L3=[ZU;ZV;ZW3;SZ];%matrix of L3
B3=transpose(A3)*A3;%multiplication of A3 transpose and A3
D3=transpose(A3)*L3;%multiplication of A2 transpose and L2
C3=B3\D3;% parameters of the value (a,b,c and Zo)
%for ALOS-PALSAR 30m spatial resolution
A4= [UU,UV,UW4,SU;UV,VV,VW4,SV;UW4,VW4,WW4,SW4;SU,SV,SW4,N];%matrix of A3
L4=[ZU;ZV;ZW4;SZ];%matrix of L3
B4=transpose(A4)*A4;%multiplication of A4 transpose and A4
D4=transpose(A4)*L4;%multiplication of A4 transpose and L4
C4=B4\D4; % parameters of the value (a,b,c and Zo)

%%The Value of a, b, c, and Zo
```

```
>> num2str(C)          the value of SRTM

ans =

-6.6258e-05      the value of a
0.000242646      the value of b
   1.019759      the value of c
  -228.6473      the value of Zo
```

```
                the value of ASTER-GDEM
>> num2str(C2)

ans =

0.0004490221    the value of a
3.085259e-05    the value of b
    1.011443    the value of c
   -405.5846    the value of Zo
```

```
>> num2str(C3)    The value of PALSAR1

ans =

5.486757e-05      the value of a
0.0004219602      the value of b
    1.024416      the value of c
   -522.3854      the value of Zo

>> num2str(C4)    the value of PALSAR2

ans =

  8.51139e-05     the value of a
-0.0004043064     the value of b
     1.007163     the value of c
     352.5807     the value of Zo
```